Assessing the Feasibility of San Salvatore Dam Removal on the Trebbia River: A Study of River Restoration Through Hydrodynamic and Morphodynamic Simulation

Thesis by
Shishir Kumar Acharya (s298619)

In partial fulfillment of the
Requirements for the Degree of
Master of Science in Civil Engineering

Supervisor: Prof. Carlo Vincenzo Camporeale
Co-Supervisor: Dr. Luca Salerno

POLITECNICO DI TORINO
Turin, Italy
April 2024

Thesis Certificate

This is to undertake that the thesis titled ***Assessing the Feasibility of San Salvatore Dam Removal on the Trebbia River: A Study of River Restoration Through Hydrodynamic and Morphodynamic Simulation*** submitted to the Department of Environment, Land and Infrastructure Engineering, Politecnico di Torino, for the award of Master of Science in Civil Engineering, is a bona fide record of the research work done by me under the supervision of Prof. Carlo Camporeale, and Dr. Luca Salerno. The contents of this thesis, in full or in parts, have not been submitted to any other Institute or University for the award of any degree or diploma.

Signature of the Author:_____

Shishir Kumar Acharya

Certified by:_____

Prof.Carlo Vincenzo Camporeale Dr. Luca Salerno

Accepted by:_____

Abstract

Dam removal has garnered significant attention as an alternative option for river restoration over several years. To that end, the Open Rivers Programme has proposed an innovative initiative in Italy to restore the Trebbia River by demolishing the obsolete San Salvatore Dam. This thesis delves into a comprehensive assessment, including both one dimensional and two-dimensional hydrodynamic modeling, alongside 1D morphodynamic numerical simulations, to evaluate the feasibility of removing such a dam and its potential impact on the downstream due to the impounded sediments transport.

This thesis includes a thorough set of studies, starting with the acquisition of point clouds aided by unmanned Aerial Vehicles (UAVs) and continuing with post-processing using CLOUDCOMPARE to generate a high-resolution Digital Terrain Model. The grain size distribution near the dam section was determined using the BASEGRAIN software. The primary goal of the thesis was to evaluate the volume of sediment transport and the possible geomorphic and flood inundation impacts to the downstream and the response of time scale of sediment transport to reach nonlinear adjustment towards equilibrium of the geomorphic evolution of riverbed. For the same reason, the 1D hydrodynamic model in HECRAS was developed to calculate the discharge that initiates sediment transport in this specific case that contains the bypass connecting upstream and downstream of dam section. The discharge calculated was then integrated to see the geomorphic evolution of riverbed and sediment transport volume through 1D morphodynamic simulations using MATLAB software. Finally, the results obtained from 1D morphodynamic simulations were used for 2D hydrodynamic modeling in HECRAS to observe the spatial inundation map and flow depth before and after dam removal.

It was found from the analysis that the volume of sediment transport downstream of the dam after removal was low and the results showed no significant changes in spatial flood mapping and the flow depth after the sediment transport. However, it still requires the detailed quantification of the amount of sediment that could be deposited in the pools and riffles present downstream the dam and the ecological response after post-dam removal. The results strongly indicate minimal impacts to the downstream due to the sediment transport after dam removal. This evidence robustly bolsters the decision to proceed with the San Salvatore dam removal project for river restoration proposed by the Open rivers Programme.

Acknowledgements

I would like to express my utmost gratitude to all who have helped and supported me during this process. I am truly grateful to express my heartfelt appreciation to my advisor, Professor Carlo Vincenzo Camporeale, for his invaluable guidance and constant encouragement during my masters degree and thesis work. I have been fortunate to have a advisor whose guidance provided me a valuable insights consistent with my long-term career goals. Without his unwavering support, I could not have completed this work.
I would also like to extend my gratitude to my co-supervisor Dr. Luca salerno for his invaluable guidance throughout this journey. His support, advice on writing and research, and encouragement to prioritize my dissertation have been instrumental in my academic progress.
I am grateful to the Civil and Environmental Engineering Department of Politecnico Di Torino for generously providing the resources and equipment necessary for surveys and data acquisition. Furthermore, I extend my appreciation to Dr. Mellisa Latella, my colleague Juan and PhD student Alessandro for their invaluable assistance during the field visit and data collection process.
The Free Trebia River is a project carried out by WWF Italy with the contribution from the Open Rivers Programme, a Dutch foundation funded by Arcadia. I would like to express my deepest gratitude to WWF Italy for providing opportunity to carry out part of study in such a innovative project of its kind in Italy.
I would like to express my sincere gratitude to my parents, sisters, nephew, friends and relatives for their unwavering love, support, and encouragement during my academic career. Your everlasting faith in me has been my source of strength and inspiration as I've worked towards reaching this important milestone. You all have my sincere appreciation for your priceless contributions to my path.
Finally, I would like to express my gratitude to Politecnico Di Torino for providing me with the opportunity to pursue a master's degree with minimum or no tuition fees. The university has cultivated a diverse and dynamic academic environment where individuals from various backgrounds can thrive, facilitating the exchange of ideas and fostering innovation and collaboration, regardless of financial constraints.

Contents

List of Figures

List of Tables

Chapter 1

Introduction

1.1 Dam Removal Background

Rivers are of paramount importance from various perspectives, encompassing their roles in environmental, societal, economic, and ecological aspects that have close dependencies to fluvial morphology, ecology, and river ecosystem. Within the river ecosystem, sediment transportation and deposition are fundamental geomorphological processes and play a crucial role in shaping the river channel and bed forms. These processes are affected by the construction of artificial dams, barriers, and other structures that act as sediment traps, causing a significant alteration in the downstream supply of the river. [Chong et al., 2021] Along with the water, dams also store large amounts of sediment behind it. The uninterrupted flow of the river system is disturbed and impedes the natural process of sediment transport with its significant impact on the seasonal peak flows and flood peaks [Kondolf, 1997]. Dams also significantly impact the ecosystem and ecological aspects, altering the flow pattern on which aquatic species rely, causing habitat loss, and creating barriers to migration, breeding, and feeding of fishes.Some common ecological impacts of dams include a decrease in the quality of biodiversity and water quality that hinders the migration of fish and aquatic animals, oxygen, and temperature change. Dams building has been very common for centuries and millennium in Europe, as everywhere in the World. Dams offer several services to human beings, including power generation, water supply,

irrigation,navigation, flood control, and recreational activities.Although the benefits of dams are numerous, recent experiences have shown serious impacts in ecological aspects of river [Kristensen et al., 2018] and alteration of flow regime [Bonacci et al., 1992].Dams have a long-term decadal impact, causing hydrologic alterations that affect floodplain production and, eventually, the river carbon cycle [Salerno et al., 2022].As reported by [Tealdi et al., 2011] dams are considered as the most prevalent human made structures which affects the sediment transport and hydrological flows ultimately narrowing and deteriorating river bed. The study by [Im et al., 2018] shows the changes in morphology and ecological habitat due to the artificial structures such as dams in rivers systems after causing the discontinuity in physical variables such as water discharge, water depth, flow velocity and bed material within the upstream and downstream of dam.

In addition, barriers in the river affect inundation risk to the downstream areas during flooding and negatively impact biodiversity, restrict nutrients to fertilize floodplains, create wetlands, and limit a continuous supply of sediment downstream, adversely affecting many species and plants that depend on free-flowing rivers.Changes in flow and sediment caused by dams induce the loss of habitat, which weakens the river's ability to provide natural flood control and ultimately affects the communities with the flooding risk during high precipitation [open river programme, 2023].

The significant changes are attributed to river morphology and ecosystem due to dam removal. Dam removal can re-establish the natural flow of sediment transport and restore aquatic life's habitat. Within the river system, the flow of sediment is downstream and sideways and in most of the cases the removal of dams helps to restore sediment connectivity in the fluvial system.The sediment dynamics is often considered the important factor in reshaping the river in terms of morphological aspects, fluvial bed forms, and aquatic habitats.The transportation of stored upstream sediment of dam alters the river channel often creating flood plains. These changes provides the suitable place for the vegetation and it can be seen rise of extensive vegetation cover from the previous dam removal sites.This release of sediment can be associated with the large scale increase in sediment supply to the downstream shaping the fluvial landscape.The response of river in downstream of the dam site with the increased sediment is commonly associated with the

filling of riverbed pools, aggradation and channel widening [Cui et al., 2017].In addition, dam removal even provide ideas for conducting real-world experiments. For example, the influence of increment in water slope, caused by lowering the base, can be tested with the sediment transport and channel evolution [Gartner et al., 2015]. The responses due to the transported sediment and dam removal are discussed in this chapter.

1.2 Context of San Salvatore Dam on Trebbia River

Dam Removal is considered as a key component of river restoration. Dam Removal is a popular topic throughout the world, and there was a record-breaking successive year of dam removals in Europe as more than 200 dams in 2021 [Elton, 2022] and more than 325 river barriers, including dams and weirs in 2022, were removed [Green, 2023].European Water Frame Directive considered river restoration as a important tool that can be applied to most rivers in order to restore the changes in morphological and ecological state [Groll, 2017]. Open Rivers Programme was launched with the investment from Arcaida on 8th October 2021 with the aim of restoring European rivers through it's support to remove the dams and restore river and biodiversity of its ecosystem. This program is aligned with similar functioning regarding the restoration in Europe. Free Trebia river is the catchment development and river restoration through dam removals is considered as a first dam removal project in Italy with collaboration with the WWF Italy and Politecnico Di Torino. San Salvatore dam was planned to built 40m high to serve two hydroelectric project in 1920s as shown in (Figure 1.1 (a)). However, it was incomplete and left behind with 8m of height including foundation. The channel in order to divert the flow during the construction of dam was also built at that time. Construction of such dams, mining, channelization has led to channel adjustments in Trebbia river during last two centuries [Surian et al., 2004]. Although sediment mining had significant impact on the sediment fluxes in the channel in short term, the impact of dam is considerably high for the long run. [Surian et al., 2004]. The feasibility study was agreed to carry out for the removal of dam after the common understanding between the regional authorities, associations and the communities to help

restore natural habitats and enable river ecosystems of Trebbia River.

Among the various barriers within the Trebbia basin, San salvatore is one of the dam. with the preliminary analysis of Trebbia river barriers by Open rivers programme with collaboration to the Emilia-Romagnia region, San Salvatore dam was considered feasible for the removal. As, this dam is obsolete and do not have any function and left abandoned it can be seen that the large amount of sediment trapped upstream and a deep pool just downstream of dam.To access the amount of sediment trapped upstream and the amount of sediment that will be transported downstream along with its effects to the morphology and flood prone areas downstream are the aspects of this study. whether the dam removal is a feasible option for the Trebbia river restoration is a major concern and this study provide valuable insights for decision making.

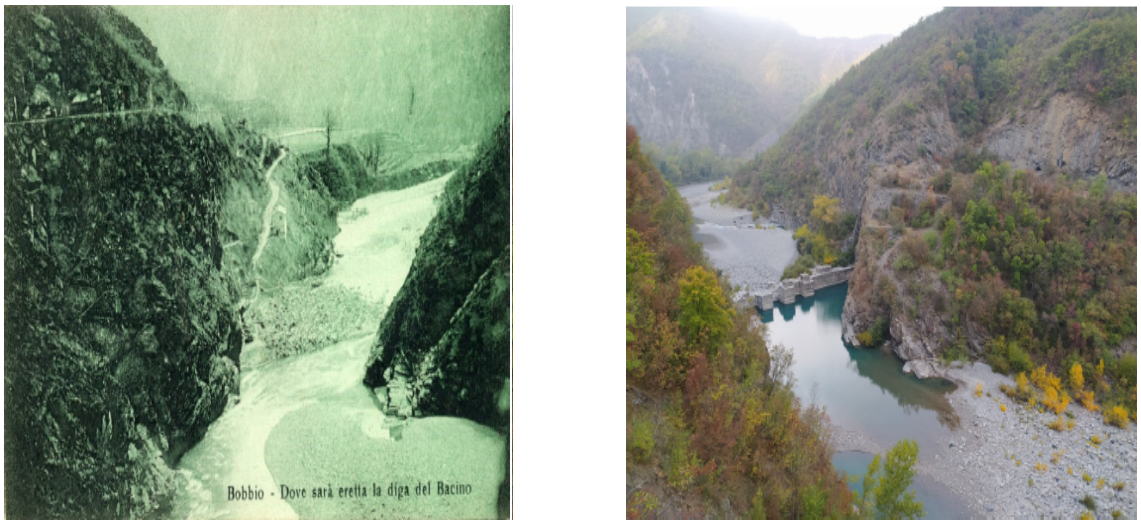

(a) (b)

Figure 1.1: a) San Salvatore dam area in 1920s. b) San Salvatore dam today Adapted from *CIRF(Centro Italiano per la Riqualificazione Fluviale)*

1.3 Dam removal responses

1.3.1 Ecological response

The ecological response is the important aspects to understand during dam removal, as in some cases can have surprising outcomes from dam removal due to the complex interaction among physical processes, ecological responses and local river conditions. In broader scale, the biological, chemical and physical components of the ecosystem, are affected by dam removal and have responses that have interconnection between them [Bushaw-Newton et al., 2002].These responses are useful to understand and decide how the dam removal should be conducted and achieve the ultimate goal of restoration.These responses varies spatially and are distinct [Foley et al., 2017b]. In addition, it depends on size and configuration of the dam and reservoir, local legacies, and the composition of the local biota, geomorphic alterations,changing bed sediment size and even the flow regimes after the dam removal [Stanley and Doyle, 2003, Schmitz et al., 2009, East et al., 2015b].
The Manatawny Creek Study by [Bushaw-Newton et al., 2002]shows the detailed integrative approach to deliver the ecological response to dam removal and how the outcomes of these responses affect spatially. He outlined responses such as movement of sediment and sediment aggradation that affects the impounded region and downstream of the dam rather than upstream; however, the responses such as the return of native species fish assemblage are found mostly upstream, impounded region, and downstream. The above mentioned statement is also underpinned by [Bellmore et al., 2019] that with the dam removal, the movement of fishes and microorganisms is found upstream and is the primary driver of ecological response. The author also developed a conceptual ecological-response model, as shown in the figure, for three regions, i.e., upstream, vicinity of the dam, and downstream of the dam that is to be removed and explored the ecological responses that re expected to arise from physical and ecological linkages in each geographical area.

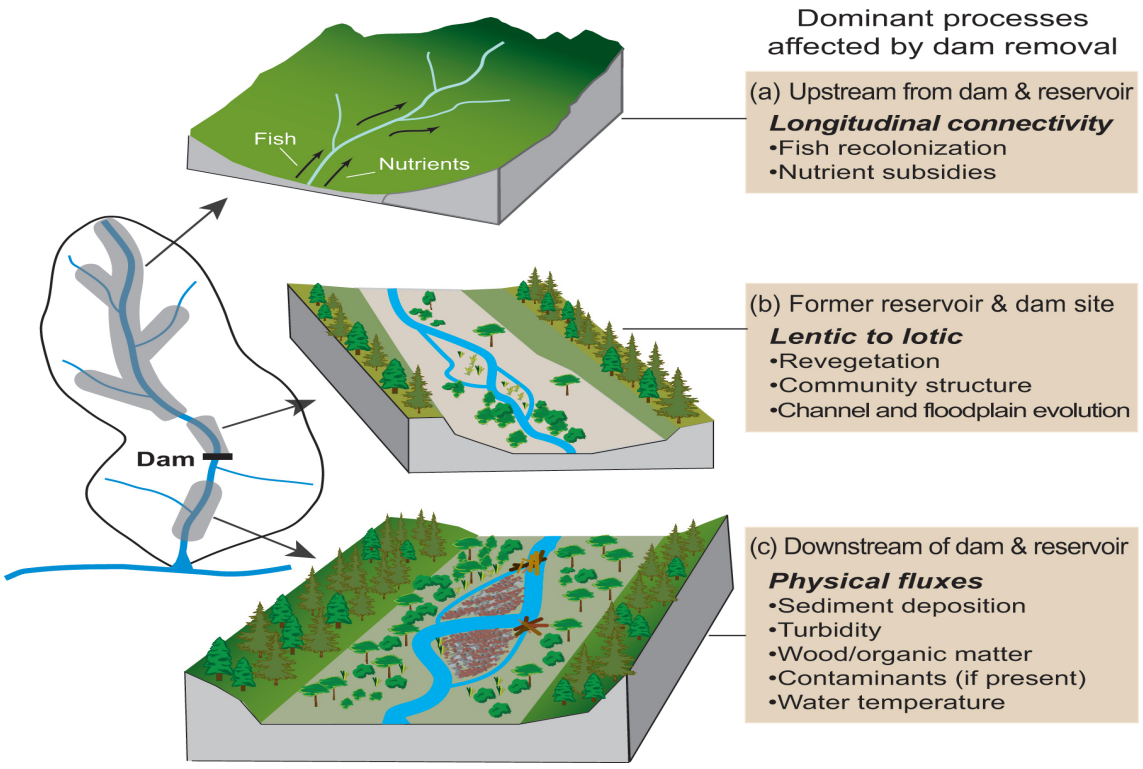

Figure 1.2: Figure shows different spatial location affected by dam removal along with the processes that affects the ecological response.(*adapted from [Bellmore et al., 2019]*)

.

The migration of sediments after dam removal can have a negative impact on downstream ecosystems, leading to a drop in fish habitats [Catalano et al., 2001]. Changes in sediment dynamics may disturb riverbeds, affecting spawning sites and interfering with the overall ecological balance required for fish survival. On the other side, vegetation have substantial influence on the evolution of river planform and shaping the river channel [Camporeale et al., 2013] and dam removal can have significant impact on vegetation, as in a study by [Orr, 2002] in a multiple dam removal sites found that vegetation quickly established following the dam removal and author stated that vegetation had important geomorphic implications. In addition, as reported by [Asaeda et al., 2011], due to the sediment transport downstream, certain plant species may sometimes predominate over others, or a new species may invade a habitat with favorable soil nutrients and features, disrupting

the ecological equilibrium. However, the study by [Stanley et al., 2002] shows that within 1 year period of dam removal there were no substantial ecological changes due to sediment transport by the flood stating that the transported sediment trapped and settled in downstream impoundment.Furthermore, [Bushaw-Newton et al., 2002] reported that sediment transport and channel adjustment after dam removal will have short term impact into the biotic responses. It is well known that, the ecological changes can occur in different range of time scale.For example, In the context of short-term changes, following the dam removal the fish start upstream movement and some faunal changes occur in within days, In contrast, some ecological attributes takes years or decades [Bellmore et al., 2019].

Due to inadequate research regarding the dam removal, it is difficult to make a conclusion to the range, magnitude of expected ecological response. The research gap in the dam removal study, which have bypass just upstream the dam and allows the water flows continuously between upstream and downstream and also the type of aquatic habitats found upstream and downstream whether varies or not is still a topic of concern in order to predict the ecological response after dam removal.

1.3.2 Geo-morphological response

Prior to dam removal,it is important to know how the river respond to dam removal following the transport of upstream trapped sediment.Different studies shows that after dam removal the sediment transport depends on the method of release, structure and nature of system [Peters et al., 2017, Sawaske and Freyberg, 2012] the grain size, cohesiveness [Robinson et al., 2000]. The spatial variability of sediment are the dominant factor for the rate and volume of sediment erosion.The types of sediment that are trapped upstream play major role for the geomorphological responses to dam removal creating a knickpoint, knickzone and promoting a headcut migration. [Kim et al., 2015, Major et al., 2017]

The earlier conceptual model of geomorphological response after dam removal by [Simon, 1989] shows the channel adjustment near the dam and later on the study by [Doyle et al.,

2002] used and modified including more data observation and described the geomorphological changes in six stages as (stage A) Pre dam removal condition, (stage B) after dam removal without sediment disturbance, (Stage C) Upstream degradation begins, (Stage D) channel widening mass wasting, (Stage E) downstream aggradation and downstream degradation as shown in Figure 1.3 .Additionally, the study by [Doyle et al., 2003] that is applicable to fine-grained, alluvial channel systems and included ecological significance due to greater incision in alluvial channel is shown in Figure 1.4

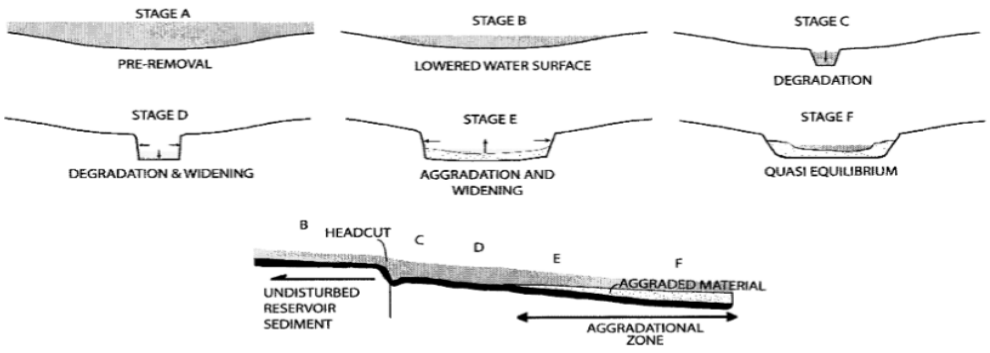

Figure 1.3: Geo-morphological evolution of channel at different stages (*adapted from [Doyle et al., 2002]*)

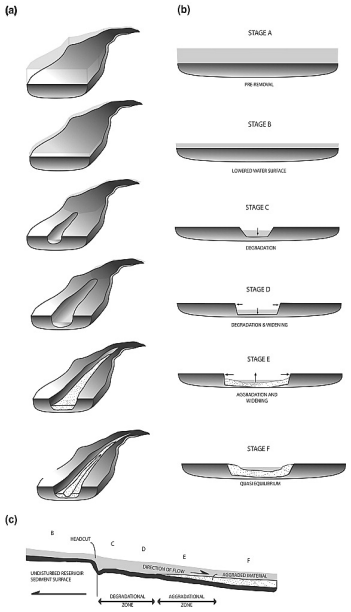

Figure 1.4: Geo-morphological evolution of channel at different stages in alluvial systems (*adapted from [Doyle et al., 2003]*)

In both the studies, the form and processes were similar and the similar pattern can be expected in other cases following the dam removal, however, channel evolution depends upon the local environmental conditions such as characteristics of sediment,consolidation of fine sediment, vertical and lateral adjustments [Doyle et al., 2003]. The research conducted in four different sites by [Csiki and Rhoads, 2014] suggest that due to the variability of pattern of channel morphology and sediment characteristics, the local site specific conditions should be taken into account for dam removal planning.

With the lack of comparable observational data ,it is difficult find out the proper documentation about the appropriate time scale for incision and recovery following dam removal. Large amount of sediment is transported and deposited after the dam removal, while the deposition in downstream occurs temporarily as depth and elevation return to near pre dam removal condition within some months [Doyle et al., 2003]. The research of river channel response after dam removal in the lower Penobscot River by [Collins et al., 2020] conducted pre and post dam removal survey and confirmed that there was not substantial change in bed elevation, channel shapes and positions.The author also stressed that physical changes in the channel are to be minimum when the little sediments are eroded from

the impoundments. Impounded sediments can be transported in two phased as shown by the [Collins et al., 2017] where half of the impounded sediments eroded rapidly in normal flows and for the second phase of erosion depended on the large floods that further eroded the sediments from newly formed channel.

The time scale for the recovery of sediments impacts downstream is difficult to predict, however in the study by [Kim et al., 2015] states the river geomorphology after low head dam removal can be in the state of quasi-equilibrium in about a decade. In contrast, the channel downstream takes months to years to achieve a degree of stability [Major et al., 2017] and geomorphic change decrease substantially after some years [East et al., 2018]. Dam removal can be done mainly in two ways, which is differentiated based on how fast the dam is removed and the rate at which draw down of reservoir is done. Firstly, During instantaneous dam removal the reservoir is emptied in a matter of hours to days.Secondly method of dam removal is staged dam removal which takes over months and years to draw down, which are generally used for the taller dam and that restores the large amount of sediment.Both the methods can be effective during different conditions, for the former method it is considered as the effective method for small dams and that also minimizes the high concentration of sediment downstream for a small amount of time, mostly for one season, minimizing the impact to the aquatic organisms.However, the latter case can be more controlled in terms of speed and rate of sediment transport and helps to minimize the effect for the high sediment sensitive organisms [Duda and Bellmore, 2022]. The geomorphic evolution after dam removal can be significantly influenced by the method of removal, gradual or instantaneous. To bolster this statement,in a experiment performed by [Cantelli et al., 2004] found that during instantaneous removal, the flow incises and rapid channel narrowing occurs at first due to which large amounts of sediment transported downstream which can have practical implications and after the rate of incision slows the narrowing is followed by slow widening that tends to propagate upstream.The author also stated that gradual removal of dam provides an option smoother and more controllable release of sediment with less impacts downstream.Similar kinds of erosion process in small dams can be observed after gradual or instantaneous dam removal. In a review study of small dam removals conducted by [Sawaske and Freyberg, 2012] shows less

percentage of sediment volume eroded at short time during staged dam removal than that of instantaneous dam removal affecting the geomorphological evolution.Sediment during the staged dam removal takes more time to erode when the sediment reservoir are partially filled but it erodes rapidly once it passes the dam area [Foley et al., 2017a].

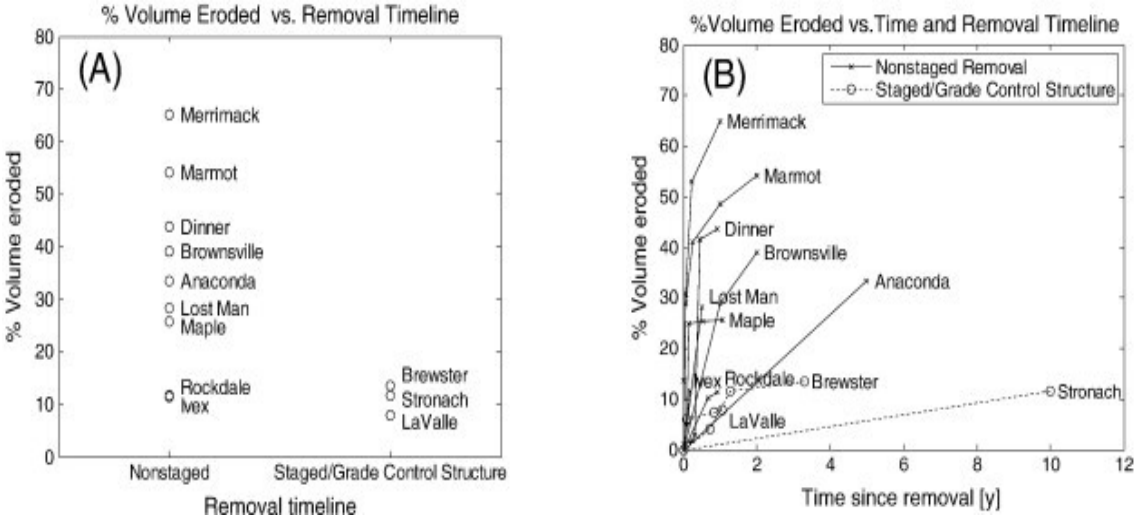

(a) (b)

Figure 1.5: a) Figure shows the percentage of sediment volume eroded during staged and unstaged showing exposure to less volume of sediment following the staged dam removal b) Figure Shows the percentage of volume eroded during a timeline showing that the significant volume eroded within the short timeline during unstaged timeline with heavy sediment load downstream in short time Adapted from *[Sawaske and Freyberg, 2012])*

After dam removal, adjustment occur to channel the channel due to the large sediment transported downstream from impoundments in initial state and sediment from upstream sources later on [Foley et al., 2017a].This transported sediment fills the downstream pool, aggradation, widening and braided configuration occurs [East et al., 2015a]. This impacts may leads the risk of inundation to the downstream of the dam.

There is a significant lack of details regarding dam removal and sediment transport after dam removal along the Trebbia River, even in Italy, and also the bypass located upstream of the dam in this study that allows constant passage of sediment downstream up to a particular flow followed by transport of sediment by dam overflow during high flows made

the evolution of geomorphological channel after dam removal even more complicated.

1.4 Dam removal for river restoration

With the emerging awareness of environmental degradation, river restoration is becoming a significant concern in different nations [González del Tánago et al., 2012]. The EU Water Framework Directive (WFD) has dramatically strengthened river restoration in Europe, supporting the improvement of water bodies' ecological state [Löfgren et al., 2009]. Restoration projects are taking place in Europe in higher numbers, with the view of attaining the high quality of rivers in Europe by 2027 [Ellwanger et al., 2012]. Different literature shows that river restoration has several definitions proposed by various authors. According to the European Center for River Restoration, river restoration encompasses a wide range of strategies, such as biological, spatial, physical, and managerial activities intended to restore the natural state and functioning of the river system. Also, The CIRF (Italian Centre for River Redevelopment) [PRATICHE et al., 2006] reported river restoration as a comprehensive approach that includes legal, financial, administrative, and structural aspects and aims to restore natural processes and ultimately its functional characteristics and bolster the connection between water course and river system, to promote the environmental value and socioeconomic objectives. Several authors have defined river restoration as a technique to improve the hydrologic, geomorphic, or ecological processes within the degraded watershed [Jähnig et al., 2011, Wohl et al., 2005, Smith et al., 2014, Palmer and Ruhi, 2019, Simon et al., 2013].

Different methods have been used to restore the rivers depending upon the aim of projects, such as creating habitats and restoring the historical river characteristics [Formann et al., 2014]. Initially, the restoration included the alteration of channel form that focused primarily on the habitat of fish [Gowan and Fausch, 1996], bio-engineering techniques using dead wood [Abbe and Brooks, 2011] or enhancing channel morphology [Rosgen, 2011]. Furthermore, other river restoration techniques that were adopted in some projects, such as in Skjern River in Denmark, the alteration of the riverbed by excavation to the historical river paths [Pedersen et al., 2007] and setting up corridors for river transitions [Dister,

1998]. Some researchers have prioritized river restoration as the process-based restoration rather than only at the river form, fostering the channel-floodplain connectivity, longitudinal connectivity, restoration of water sediment fluxes, and ecological productivity [Wohl et al., 2005, Konrad et al., 2011, Palmer et al., 2010, Shields Jr et al., 2011]

Dam removal is considered a very attractive restoration measure since it essentially restores the natural water and sediment transport, resulting in the enhancement of natural habitats and wildlife [Gough et al., 2018]. The report by the same author [Gough et al., 2018] has detailed why dam removal is considered a viable river restoration technique. For example, dam removal helps in nature enhancement and restoration, contributes to the Water Framework Directive, improves fish migration, minimizes maintenance costs, and improves socioeconomic aspects of the community. The author also stressed that dam removal is considered the most cost-effective measure desired for river restoration; however, these are achieved when we act in time. Some of the dam removal case studies that have been previously implemented in European countries are well presented by [Gough et al., 2018] which serves as an good example of the river restoration by dam removals.The author also shows the dam removal can minimize fragmentation and restore river connectivity.

Some of the studies have shown that the number of dam removal projects has been increased in the view of restoring the water, sediments, and nutrients fluxes along with the connectivity of aquatic organisms [Major et al., 2012, Wilcox et al., 2014, East et al., 2015a, Magilligan et al., 2016].

Another issues of river degradation is fragmentation and defragmenting them is a necessary condition for effective river restoration. Dam removal helps to redistribute sediments that are generated and transported in restored-healthy river-and allows for habitat creation and channel adjustment and makes rivers more resilient towards the changing climate [Garcia de Leaniz et al., 2023]. In general, the fragmentation and changes in the habitats due to the dam brings alteration in the flora, fauna resulting in different ecosystem than the one that would have occurred naturally. Dam removal is becoming a important management strategy which can be the a good potential for re-connectivity and resilience in the watershed scale.

1.5 Problem Statement

Several studies have been published evaluating the geomorphological and ecological response after dam removal as discussed in above section, however very few studies have been conducted to predict the feasibility of dam removal based on sediment volume and transport prior to the dam removal using the modeling tool, that augments the decision making for dam removal. In addition, none have conducted studies for the morphodynamic and ecological response in the particular river section having the bypass-that connects upstream and downstream of dam. In this thesis, the purpose of the study was to evaluate the feasibility analysis after dam removal and assess the geo-morphic evolution of river bed after dam removal. To that end, the section of San Salvatore Dam in Trebbia river was selected. Among other different river restoration options, dam removal was considered an optimum river restoration method for the Trebbia River. Previous studies on Trebbia River show the river has several threatened species and biodiversity threatened by inline barriers. These barriers were constructed for different functions; out of 27, most are obsolete [open river programme, 2023]. San Salvatore is one of the obsolete dams that this study is concerned about.

During low flow condition, the bypass in the upstream of the dam serves as flow passage, however during high flood, the relationship between flow that passes from the bypass and overflow the dam adds the complexity during the 1D and 2D hydro dynamical modelling. As, this dam stores of sediment upstream, the concern of sediment transport to downstream during dam removal is critical. Due to the dense settlement of people in Bobbio town in downstream of dam, effect of San salvatore dam removal and sediment transport should be well understood. There is lack of hydromorphodynamical study including the bypass channel, granulometric analysis and terrain analysis in Trebbia river especially, considering the San Salvatore dam. There is no information regarding hydro-morphological evolution of reach and its impacts to human settlement and biodiversity in the Trebbia river. Although dam removal options seems to be optimum method for river restoration, the effects and

morphological evolution of river plays a pivotal role for the decision makers.

1.6 Research Aims and objectives

This thesis aims to understand the relationship between the flow in bypass channel and overflow of dam, and 1D and 2D hydro dynamical simulations using HECRAS along with the 1D geomorphological evolution of river bed using MATLAB in order to assess the implications of dam removal for Trebbia river restoration.This thesis also considers the data collection using UAV systems to provide the terrain model and bathymetry measurement within the dam area and analyze the grain size distribution required for the numerical and hydromorphological simulations.This study utilizes the above mentioned concept, to address the following research questions.

1) What will be the relation between the flow between the river and the bypass channel and the threshold flow to overpasses the dam?

2) what would be the geomorphic response after removing the San Salvatore dam?

3) What would be the affect of sediment transport to the downstream after the dam removal? Is the San Salvatore dam removal a better option for river restoration for Trebbia River?

1.7 Organization of Thesis

This thesis consist of 7 chapters. Chapter 1 is an introduction that is followed by the Chapter 2 Study area including the topography and geography of the area. Starting from the data collection such as point cloud acquisition, granulomety analysis and the detail methodology techniques for the same are introduced in Chapter 3. Chapter 4 outline the assumptions, calibration and modelling strategy needed for the 1D, 2D hydro-dynamical modelling and 1D morphological modelling . Chapter 5 we delve into analyzing and evaluate the results obtained from numerical modeling. Finally chapter 6 includes the conclusion remarks and chapter 7 includes the appendix attached.

Chapter 2

Study Area

Trebbia is a river in the Liguria and Emilia-Romagna region in northern Italy. The Trebbia catchment is located in the north Apennines and covers an area of about 1070 km2. With a total length of around 120 km, the Trebbia is one of the principal tributaries of the Po River. The mean annual flow over the stretch of the river is estimated to be around $19.72 m^3/s$ (25 years of data from the gauging station of Bobbio from the year 1972 to 2023 (*described detail in section 3*)) with the basin area of $631 km^2$. The Trebbia catchment consists of around 85% of mountain and hilly regions with the geology mainly characterized by sedimentary, marls, sandstones,claystones. [Bollati et al., 2014]

The Trebbia river runs from Mount S. Lazzaro in the Ligurian Apennines to the Po, just west of Piacenza runs about 120km length. This river is surrounded by Mounts Penna (1,735 m above sea level) and Maggiorasca (1,799 m above sea level) run along the watershed to the south, Mount Cavalmurone (1,670 m above sea level) to the east, and Mount Crociglia (1,578 m above sea level) to the west. It has multiple tributaries, the most notable of which is the Aveto stream, which is around 30 km long and contributes a significant amount of water owing to the heavy rainfall in its basin, which has a surface area of roughly 257 km2. The Bobbio, Perino, and Dorba streams are other significant tributaries. Considering the morphological and hydraulic behavior, the Trebbia River can be divided into two regions: the mountain region up to the Rivergaro and the plain section to the confluence of Po.

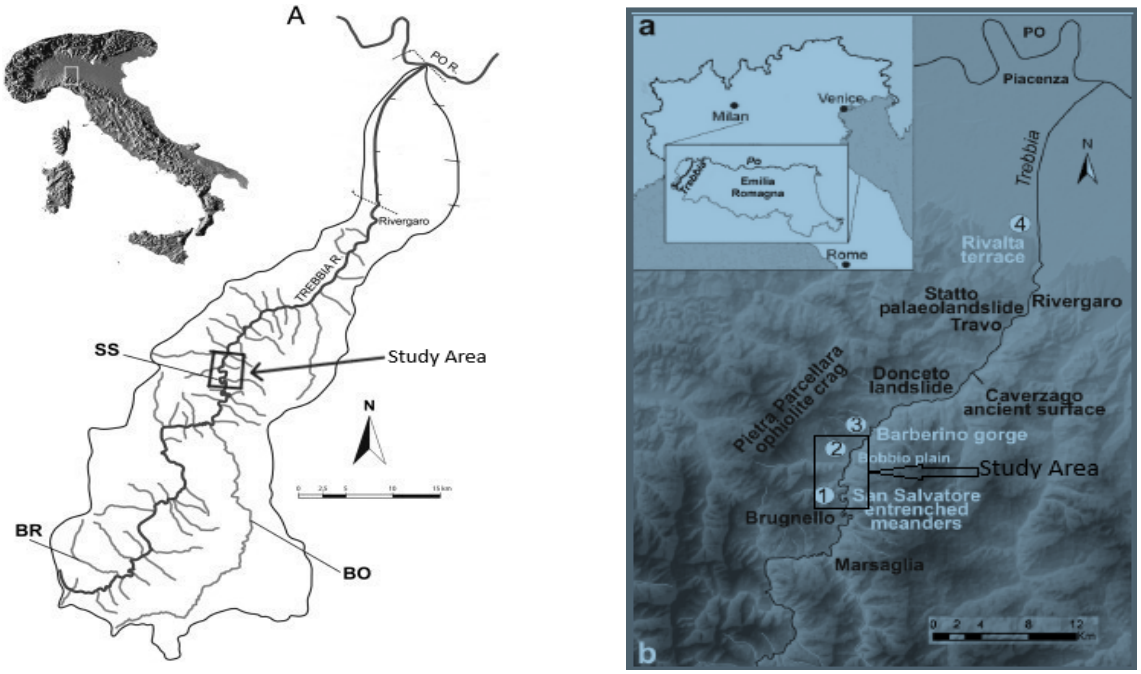

(a) (b)

Figure 2.1: Fig (a) Trebbia river catchment with the study area where, SS= San Salvatore and (b) Trebbia river Catchment: section 1 and 2 is the study area . Adapted and modified from *[Bollati et al., 2014, Bollati et al., 2011]*

The study area lies between the Marsiglia in upstream and Bobbio Town downstream as shown in Figure 2.1(b) and Figure 2.2 and the San Salvatore dam coordinates is 44°44’33.13" N and 9°23’12.10"E. The river has irregular meandering planform with high curvature and point bars in the upstream of the dam, however in the downstream the river turns into the branched and braided with large flood plain areas and alluvial deposits.The upper part of the river is considered to have rocky riverbank and steep slope.In the middle section the riverbed seems to have gravel bed and it flows in a large alluvial area before the Po river.This study is focused near the San Salvatore region reach where it has partly confined reaches crossing the hilly areas.

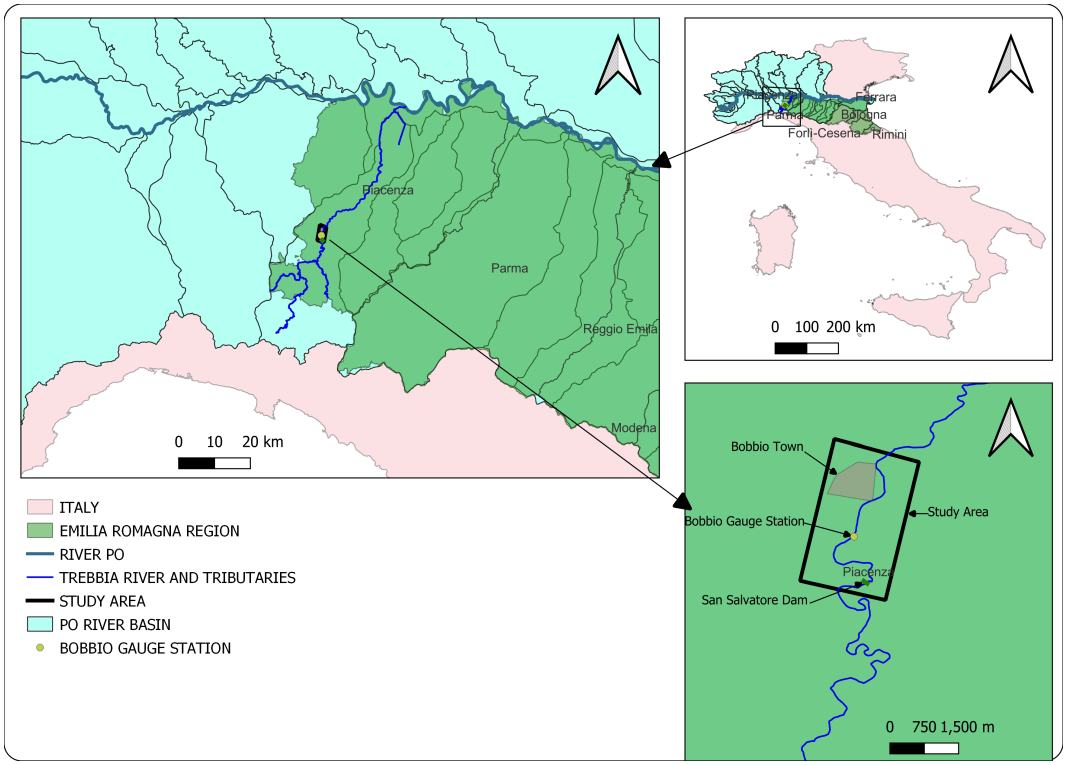

Figure 2.2: Study Area in Trebbia River indicating with the details

The San Salvatore Dam, the primary area of the research, is a dam left abandoned centuries ago and made up of concrete structures. The barrier has around 80m width, 5m height, and 4m breadth at the top, as shown in Figure 2.3. Although there is a creek as shown in Figure 2.4(a) in the barrier through which water can pass downstream, the river's trajectory is diverted towards the bypass channel, as shown in the figure below. On the dam's left side (considering the direction of flow), there is a bypass channel from where water passes to the downstream and connects the upstream and downstream channels. This bypass channel facilitates the sediment transport downstream; however, as there is no information inside the bypass channel, the morphological and biological characterization still needs to be discovered. The diameter of the bypass channel is around 4.5m, and around 240m length.During high flows, water fills the bypass channel and acts as a pressurized channel and the discharge passes also passes through the dam's overflow.

(a) (b)

Figure 2.3: a) Dam area shows the entrance and exit of flow in the bypass(present) b) Dam area shows the water overflow through dam during high flows(10/2017) Adapted from *Google Earth*

/

(a) (b)

Figure 2.4: a) Creek present in the dam(clicked from upstream of dam) b) Dam from right side (photo clicked from the right side of flow direction) *(Photo taken by researcher of Politecnico di Torino)*

The Trebbia River exhibits significant environmental and geomorphological diversity, hosting valuable biodiversity that holds critical ecological importance, due to which dam removal is considered an important aspect as it can significantly impact the river course and environment. Trebbia River runs through the protected areas that fall under the Natura 2000 sites and has the "Parco Regionale Fluviale del Trebbia" (Trebbia regional river park), which preserves the Trebbia River that has been managed by Ente di Gestione per I Parchi e la Biodiversità since 2012 and is very important for the flora and fauna that can be found there. Some of the endangered species in the Trebbia River, such as Stone Curlew, Alosa fallax, Anguilla anguilla(European eel), Barbus plebejus(Italian Barbel), Barbus meridionalis [open river programme, 2023],Rheophilous cyprinids and willow bushes, shrubs such as Juniperus communis, Clematis vitalba are found there [Wikipedia contributors, 2023]. These protected areas and regional parks stretch downstream from the San Salvatore dam, provide crucial habitat for threatened species. While the current study may not cover the full downstream region, it is critical to recognize that upstream hydrological and morphological changes due to dam removal might have negative consequences for flora and fauna both upstream and downstream of the dam. Recognizing the linked nature of the ecosystem, efforts to understand impacts on these valuable species are critical for the overall protection of the Trebbia River and its different habitats.

Trebbia river and catchment have been affected by the human disturbances such as reforestation, torrent control works, constructions of levees, dams, sediment mining during past centuries as documented by [Surian et al., 2004]. Notably, the period between the 1960s and 1980s witnessed a peak in sediment mining activities, exerting a lasting influence on the river's geomorphology. Furthermore, the trebbia catchment has seen significant land use changes over centuries [Bollati et al., 2014]. These modifications have exacerbated the ecosystem's difficulties. The study area is subjected to a variety of disturbances, such as the presence of drop structures within the riverbed, bridges, dams, and weirs. These structural alterations have caused a morphological imbalance, upsetting the river's normal flow dynamics. Such obstructions also have a negative influence on the movement patterns of fish species within the river course.

Figure 2.5: Figure showing the Bobbio Town in vicinity of Trebbia River *Adapted from Google Earth*

(a) (b)

Figure 2.6: a) Just Upstream of Bobbio Town before flooding b)The same area after flooding *(Photos adapted from ARPA Emilia Romagna Report 2015)*

Bobbio is small town in northern Italy which is 1460m (4,790 feet) above sea level, on the left bank of the river Trebbia which is around 4km downstream from the San salvatore dam as shown in Figure 2.5. From the source to the Bobbio region have irregular meanders and have erosion forms due to which the river mobilize considerable amounts of sediments and transport and deposit downstream. In one of the report by ARPA Emilia Romagna[2015] reported that the cultivated areas and residential areas were flooded as shown in Figure 2.6 just upstream the Bobbio town due to heavy rainfall and flood. The human settlement in the Bobbio town is near to the Trebbia river bank and is about some meters of height above the Trebbia river bed. Although, there is a proper river bank protection, the risk of flooding due to the sediment transport augmenting rise in river bed elevation is still there.This area is considered as the sensitive area for the flood risk due to the dam removal and sediment transport in this study.

Chapter 3

Data Acquisition and Methodology

In this study the systematic methodology has been adopted, commencing from the data collection with the drones equipped with advanced photogrammetric cameras that capture high-resolution images and integrating this with bathymetric survey of specific river section with water to generate the Digital Terrain model(DTM) .These developed DTM are then used to numerical and hydrodynamic modeling after the post processing as described below in details.

3.1 UAV Measurement and Bathymetric Survey

Data collection with Unmanned Aerial Vehicles(UAV) nowadays has been a highly used surveying technique. Common UAVs, such as drones with digital cameras and sophisticated processing software are now an excellent approach to collecting precise data to create comprehensive Digital Terrain Models (DTMs). With a proper flight planning including some parameters such as image overlap,orientation of flight lines,camera configuration and flight height the UAV carried out a flight plan automatically.Moreover, external factors such as weather conditions in the study area, battery backup, and the overall control of the UAV during flight are integral components of the planning process, The images are taken with camera attached with the UAV with its proper internal orientation parameters.The precision and speed of aligning those images also depend on the height of the UAV above

the ground level and the extent of image overlap.Having sufficient overlap ensures there are ample matching points in consecutive images for alignment. It's essential for the overlap to be adequate; otherwise, the photos won't align properly.Even the different camera configuration like Nadir, Oblique or both configuration techniques and flight pattern such as double, single or crosshatch adds the flexibility during the image acquisition.

During the UAV data acquisition, incorporating ground control points increase precise modeling accuracy. Specifically a receiver capable of real-time kinematic mode (RTK), is essential to obtain accurate coordinates for ground control points. The RTK-equipped UAV collects data with improved spatial accuracy, and the GCPs serve as control points for further refinement. In post-processing, the collected UAV data is geo-referenced by incorporating the RTK-corrected positions of both the UAV and the GCPs, resulting in a highly accurate and precisely positioned geo-spatial data set.The flow chart demonstrating the stepwise process for the UAV image acquision is shown in Figure.

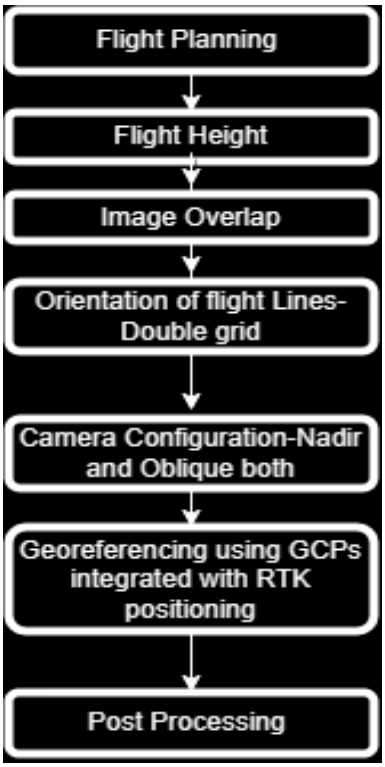

Figure 3.1: Step-wise procedure for the UAV data acquisition

These kind of technique does not provide precise information under the water. Different

factors such as weather, refraction,water turbidity can impact the quality of the images and the performance of UAV which may lead to error during terrestial data acquisition.The influence of refraction is critical in bathymetric photogrammetry since water's light refraction can misrepresent reported depths, necessitating corrective techniques. Concurrently, the quantity of turbidity determines the feasible detail levels for submerged surfaces in surface surveys using water. Turbidity, water surface roughness, and maximum light penetration depth all have the ability to suppress surface characteristics in photogrammetric photographs, reducing accuracy in underwater surveys. This highlights the need of tackling these complications in order to assure the dependability of photogrammetric data in aquatic environments. For the same, integration of bathymetric technique is normally adopted in the section with deep water as shown in Figure 3.2

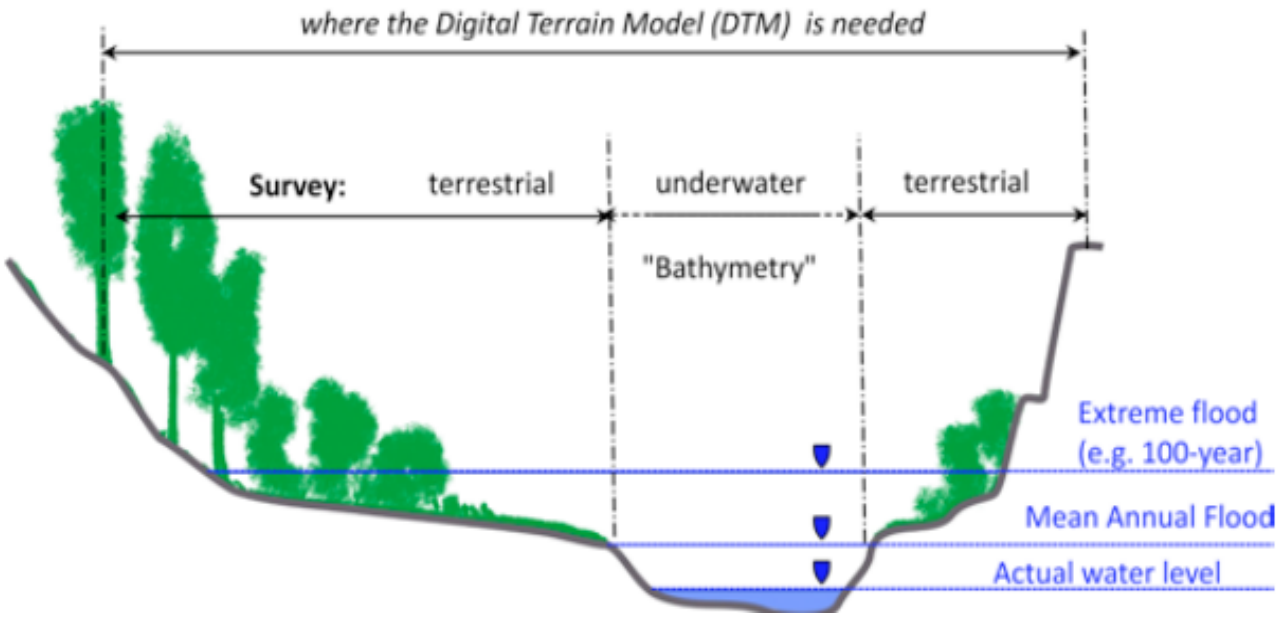

Figure 3.2: Diagram showing the terrestrial and underwater zones that require bathymetric survey *Adapted from [Zinke and Flener, 2013]*

The figure above shows the typical section requiring terrestrial and bathymetric data acquisition integration. Terrestrial data acquisition can be performed through the drone, as discussed above. Meanwhile, the bathymetric survey was conducted using the SonTek RiverSurveyor system. This system is a robust and precise Acoustic Doppler Profiler

(ADP) device developed for measuring river discharge, three-dimensional water currents, depths, and bathymetry from a moving or stationary vessel. Multiple acoustic frequencies fused with precise bandwidth control make for the most robust and continuous shallow-to-deep measurements ever for an ADP. In addition, the vertical beam system and the ability of an instrument to be integrated with RTK GPS integration with power and communication module allows the measurement of precise data and provides ease of use.9-beam ADP has been used with a velocity profiling range of 0.2 to 30 m in both shallow and deep channels from moving or stationary boats/floating devices. The M9 is housed in a 5-inch (13-cm) Delrin casing. It includes four 3.0 MHz transducers and four 1.0 MHz transducers in a Janus arrangement. Depth information is provided by a 0.5-MHz vertical acoustic beam (echo sounder) as shown in Figure 3.3

(a) (b)

Figure 3.3: a) ADP with its components b)Assembled Sontek Hydroboard integrated with the GPS *(Adapted from RiverSurveyor S5/M9 System ManualFirmware Version 2.00 September 2011)*

In this study, a high-resolution topographical survey was conducted in the 3.1Km of river section with 600m upstream and 2500m downstream of the San Salvatore dam to create the terrain in two different dates as shown in 3.1. During the first survey, smaller section images were acquired to get the orthophoto output for the Grain Size distribution near the

San Salvatore dam, and sediment sampling was carried out(discussed in a later section). During the second campaign, all the study area images were performed to get the DSM required for modeling. In addition, a bathymetric survey and flow measurement were conducted simultaneously.

S.N.	Date of Survey	Measurement performed
1	12th April 23	Image Captured by Drone (Smaller section for GSD as shown in Figure below)
		Identifying the GCP and CP
		Sediment Sampling
2	4th and 5th July 2023	Image captured by Drone(Output:DSM of full study area)
		Identifying GCP and CP
		Bathyemetric Survey
		Flow Measurement

Table 3.1: Survey Details at study area

As discussed above, the aerial captures were made using the Matrice 300 RTK drone equipped with a Zenmuse P1 camera as shown in Figure 3.4 This digital camera was equipped with full-frame ($35.9mm \times 24mm$) with a resolution of $45MP$ and a pixel size of $4.4\mu m$. Images were acquired using the 35 mm lens and flights were performed at 50-80 m above the ground, with a Ground Sampling Distance (GSD) estimate of 1 cm/pixel.

(a) (b)

Figure 3.4: a) Matrice 300 RTK drone equipped with a Zenmuse P1 camera *(Adapted from heliguy website updated in July 2022)* b)Figure during takeoff at study site

As, the Zenmuse P1 can can record tilted photos without the need for manual corrections. It automatically turns the camera to the proper angle, allowing to take straight-down (nadiral) and angled (oblique) photos in the same flight.In our study, flights were carried out with both nadiral and oblique camera orientations of 45°. Furthermore, a multi-constellation, multi-frequency GNSS instrument in RTK mode was used to determine the location of the ground control points that are used in post processing as discussed above. DJI TERRA Software was used for processing measurement data and the output was an orthophoto as shown in Figure 3.5

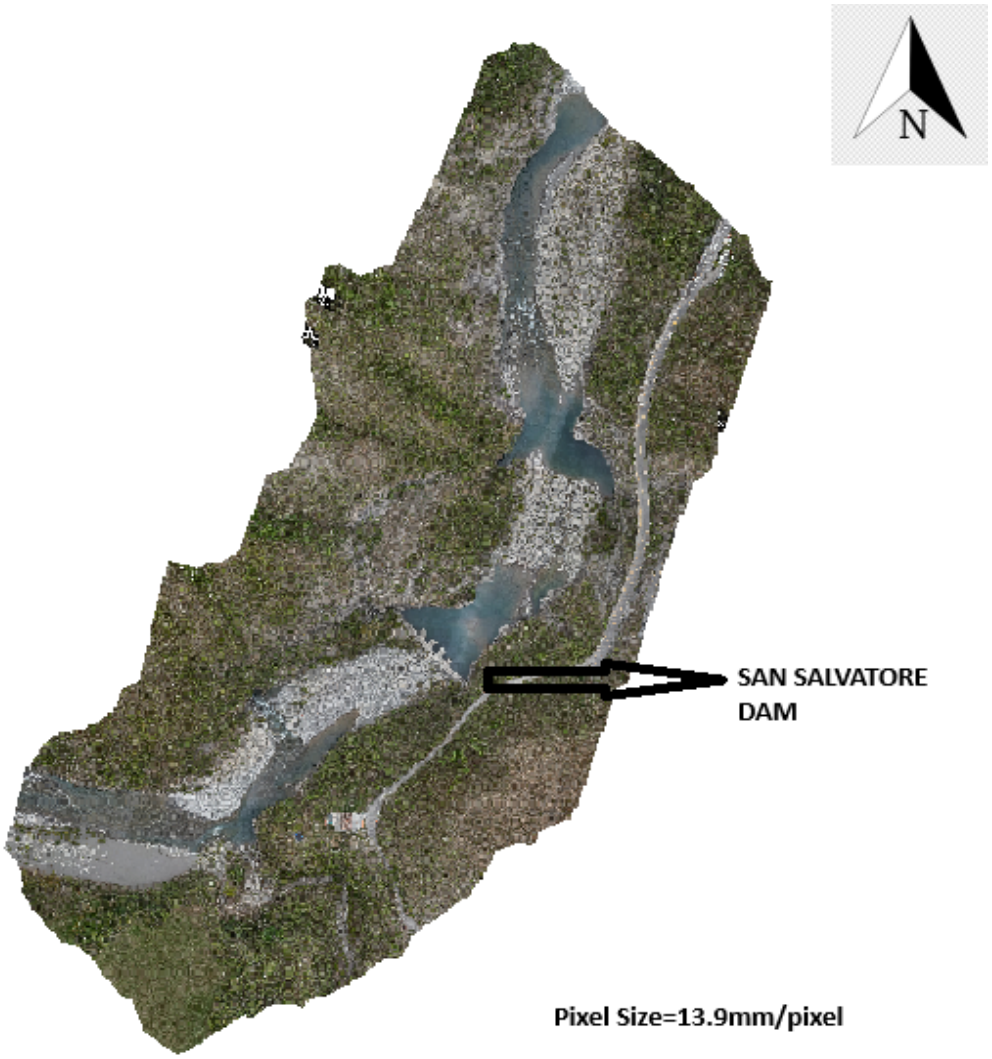

Figure 3.5: Output from the DJI TERRA Software in orthophoto format

For the bathymetric survey, the above mentioned instrument was used and five different location were selected for the survey as shown in Figure 3.6. Surveying was done with the help of the boat equipped with the bathymetric instrument and the accurate depth beneath the water surface was measured in each places.SonTek RiverSurveyor system measures a wide range of data, however this study focused to measure the depth of the selected location in order to correct the data acquired through drone in wet areas.

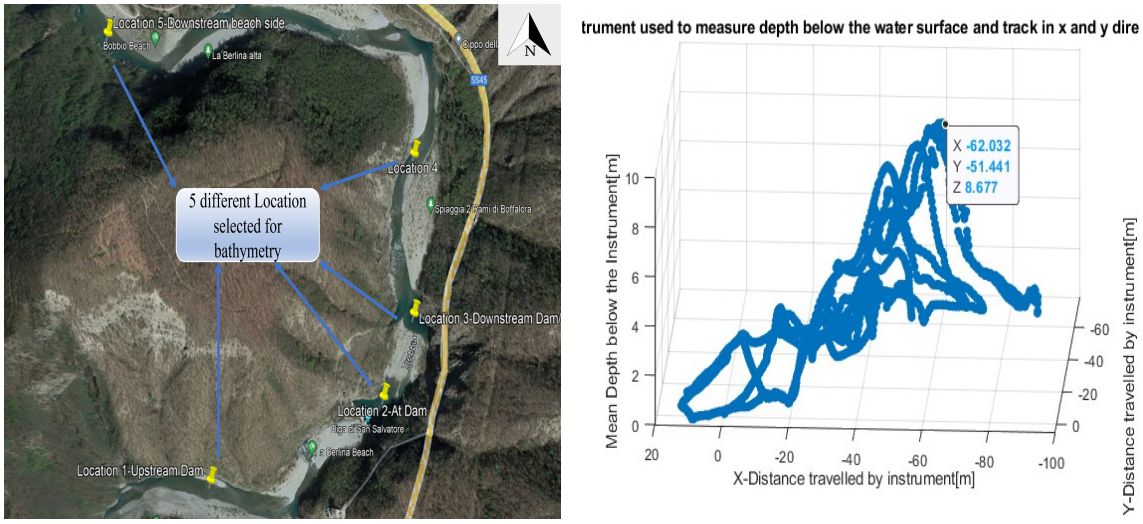

(a) (b)

Figure 3.6: a) Location of the bathymetry survey conducted (*Photo adapted from Google Earth*) b) Depth measured with the help of instrument at the Location 2 Dam area.

The maximum depth measured by the bathymetric survey at the location shown in diagram above are listed in the table below:

S.N	**Location**	**Depth [m]**
1	Location 1 Upstream Dam	0.66
2	Location2-At dam	8.67
3	Location 3-Downstream Dam	9.76
4	Location 4	4.87
5	Location 5-Downstream beach side	3.57

Table 3.2: Maximum depth measured through bathymetric survey

The maximum depth measured in the above table are further used used to correct the depth in the final digital terrain model in specific cross section. The drone data acquisition and the bathymetric survey output are used in the hydraulic and hydro-morphodynamic modeling after post-processing. Still, the DSM output generated from the post-processing contains the vegetation and shrubs that need to be removed and segmented to get the final terrain model that contains only the topography surface. To this end, segmentation and

classification of point cloud obtained from the drone and generation of final terrain model are discussed in detail in section 3.5

3.2 Hydro-meteorological Data

This research uses data from the Bobbio gauge station (Latitude 44.75, Longitude 9.38), located in the province of Piacenza at 272 meters above sea level, within the Trebbia basin. The Trebbia basin spans 1071.09km^2, with the gauge station covering the basin area of 631km^2. Annual discharge data spanning 25 years (1997-2023) were obtained from the gauge station, with gaps in the year 2013 and three months in the year 2015 due to a problem with the gauge station instrument. Hourly Data for calculating average river discharge were acquired through communication with Arpa Piemonte.

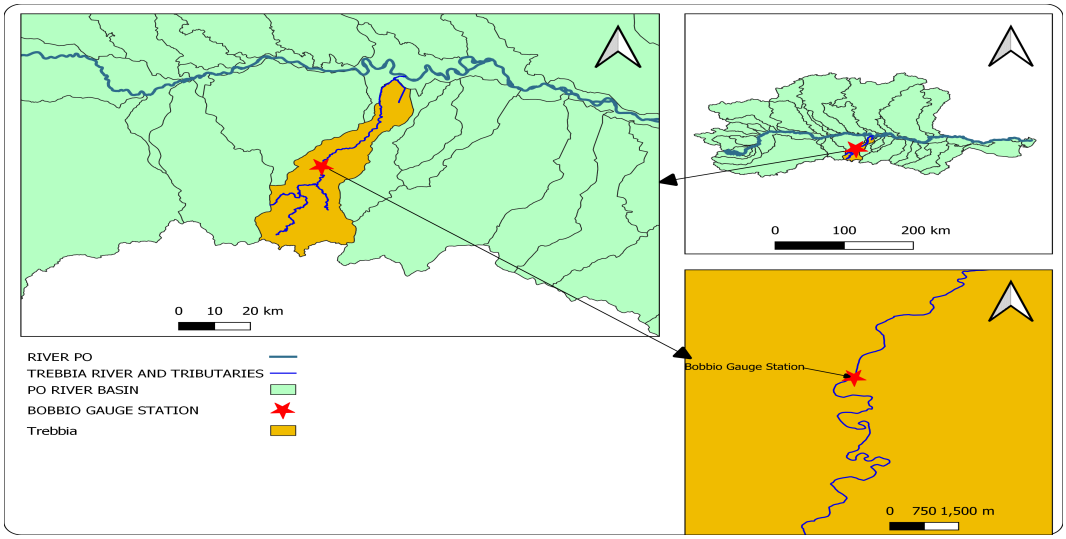

Figure 3.7: Bobbio Gauge Station and Trebbia Basin

After the pre-processing of raw data, such as identifying the non-data variables and removing them, the average discharge of Trebbia River was calculated considering the hourly data as 19.72m^3/s and the plot is shown in Figure 3.8(a).This discharge was used for further analysis in the research. Furthermore, annual maxima were calculated for the same 25 years.During those periods the extreme event reported by Arpa-Emilia Romagna in their annual reports of Sep 2015,Dec 2006, and Dec 2009 were also included for the

annual maxima calculation as shown in Figure 3.8(b)

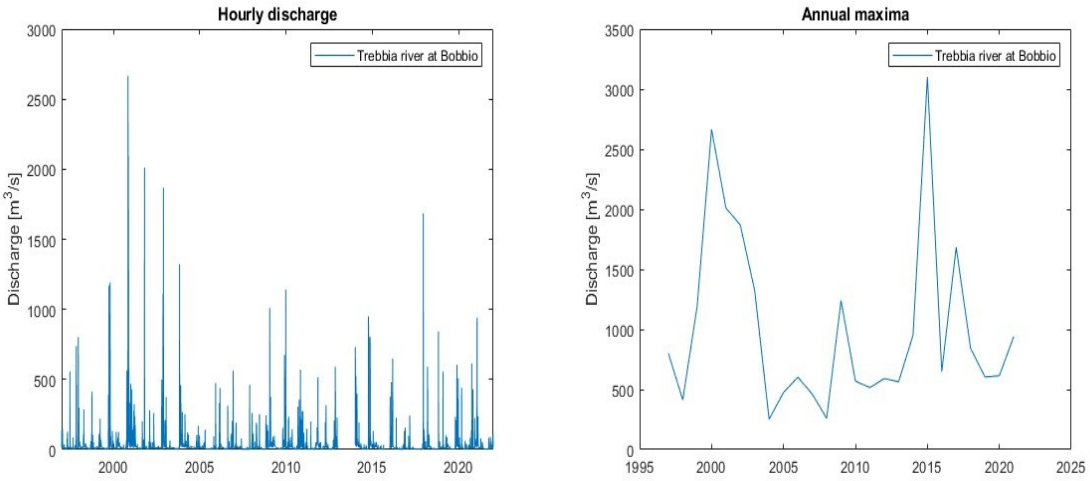

(a) (b)

Figure 3.8: a) Hourly discharge data (1997-2023) b) Annual maxima discharge(1997-2023)

Different discharges associated with different return periods were required for the hydrodynamic modeling and, eventually, the development of a flood inundation map. Flood frequency analysis(return period) is the method that gives information about how often a certain flow is reoccurring. The analysis was then performed by fitting the probability distribution model to the sample of annual extreme data recorded for an extended period. With the help of the model parameters calculated, the extreme events can be calculated for large recurrence intervals. In this study, among the many probability distributions, only the GEV, gamma, lognormal, and log-logistic probability distribution models were fitted well, as shown in Figure 3.9. The parameters estimation was done by maximum likelihood methods, and the chi-squared test, Anderson-Darling test, and Kolmogorov-Smirnov test with significance interval of 5% have passed the above distribution.

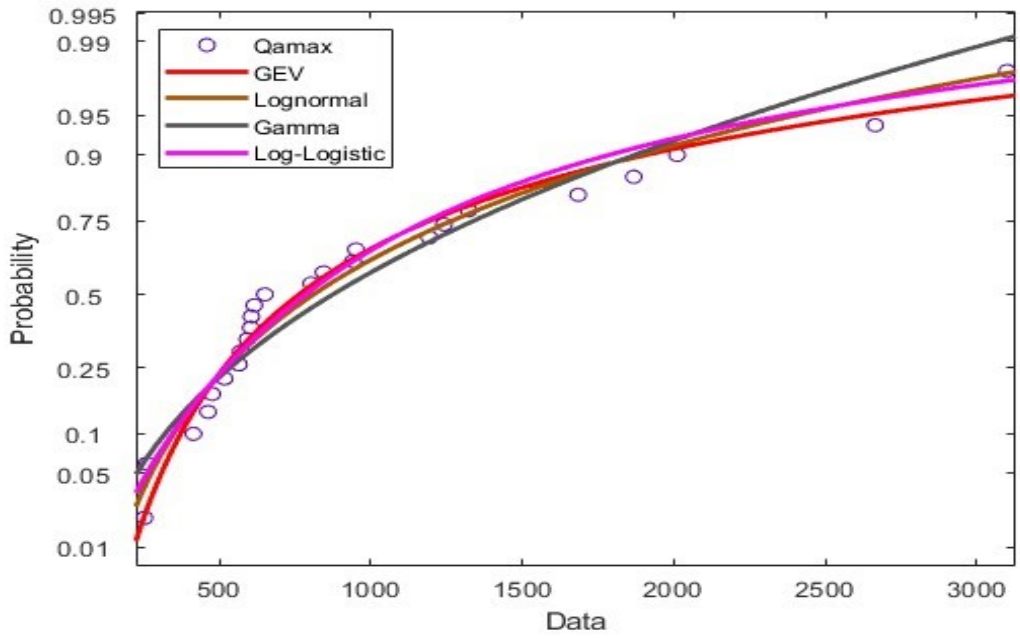

Figure 3.9: Probability distribution models plotted with annual maximum discharge

The above figure shows the good fit with the GEV, gamma, log-normal and log-logistic distribution indicating that the chosen probability distribution accurately captures the patterns and variability present in the observed data the statistical characteristics of the data set.In addition,the goodness of fit test with Anderson-Darling test, and Kolmogorov-Smirnov test determines how well a random sample fits the theoretical probability distribution and suggest that the assumptions underlying the chosen probability distribution are not violated significantly by the observed data. Then, the design discharges for different return period have been calculated for each probability distribution models as shown in the Figure 3.10.

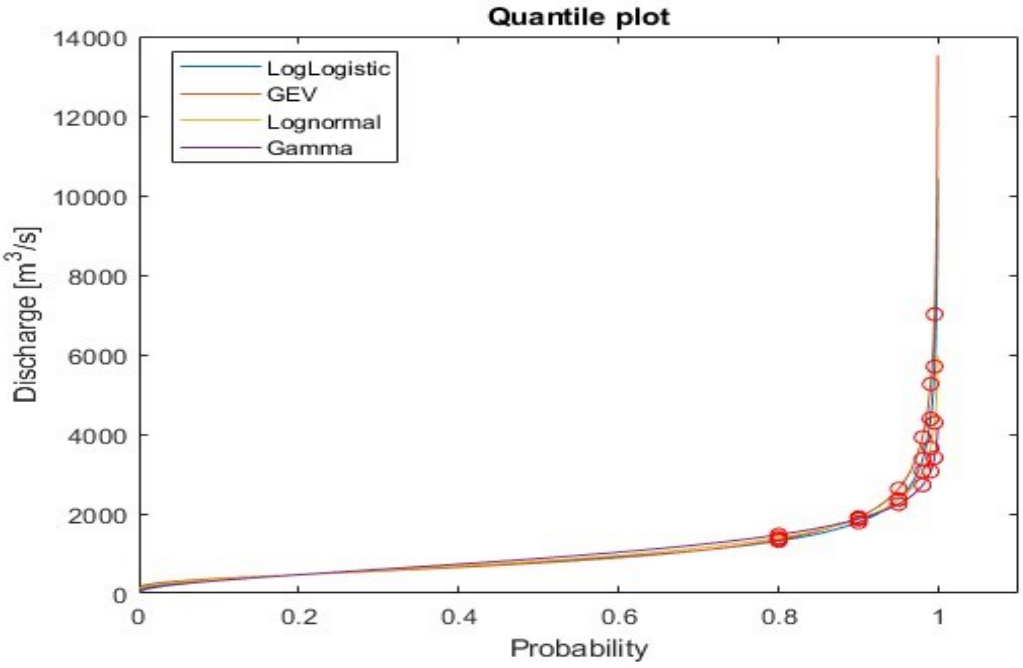

Figure 3.10: Design Discharges for each probabilistic models

As is shown in the figure above, the discharges for different return periods (5 year, 10 year, 20 year, 50 year, 100 year, 200 year) were calculated for each distribution and the average of each distribution is taken as the design discharge(as shown in table 3.3) for each return period.

S.N.	**Return Period**	**Discharge**(m^3/s)
1	5-year (Q_5)	1383.9
2	10 -year (Q_{10})	1855.5
3	20-year (Q_{20})	2396.4
4	50-year (Q_{50})	3268.3
5	100-year (Q_{100})	4091.1
6	200-year (Q_{200})	5102.9

Table 3.3: Design Discharges of Trebbia river for different return periods.

The above estimated discharges were used to perform hydro dynamical and hydro-

morphodynamic modeling in this study.In addition, these discharges are also important to generate the inundation mapping in different return period using appropriate hydraulic model, which is one of the aim of this study.

3.3 Grain-Size Distribution

Grain have wide range of size from clay-sized particle that needs microscopic instrument to boulders of large diameters that can be easily measured. Due to this wide range of sediment distribution, logarithmic or geometric scales are used to express grain sizes. The grain size scale that is mostly used is Wentworth scale which is a geometric scale. This scale, extends from $> 256mm$ to $< 1/256mm$ and divided in mainly six categories boulders, cobble, gravel ,sand, silt and clay and further subdivided.However, silt and clay categories are rarely included in the gravel bed rivers. After that, a modification was done by Krumbein and proposed logarithmic phi scale in 1934. Although applying logarithmic transformation to the particle size D would result in normal distribution, in order to make it convenient Krumbein defined particle size D as the negative logarithm to the base of 2 and referred to the resulting scale as the φ scale as shown in by a equation 3.2

$$\varphi = -\log_2 \frac{D}{D_0} \tag{3.1}$$

Where φ is Krumbein phi scale
D is the diameter of particle in mm
D_0 is reference diameter equal to 1 mm

$$D = D_0 \cdot 2^{-\varphi} \tag{3.2}$$

Scales as shown in Table 5 are essential for the graphical representation and for statistical computations. where,the Udden-Wentworth scale is more qualitative and categorical, while the Krumbein phi scale provides a quantitative and logarithmic representation of particle sizes.The Krumbein phi scale is a logarithmic scale that provides a convenient way to represent a wide range of particle sizes in a compact form and researchers and

image based analysis software often use the Krumbein phi scale for detailed grain size distribution analyses.

Scale	**Size range**	**Size range**	**Aggregate name**	**Other names**
φ	(metric)	(approx. inches)	(Wentworth class)	
<8	>256 mm	>10.1 in	Boulder	
−6 to −8	64–256 mm	2.5–10.1 in	Cobble	
−5 to −6	32–64 mm	1.26–2.5 in	Very coarse gravel	Pebble
−4 to −5	16–32 mm	0.63–1.26 in	Coarse gravel	Pebble
−3 to −4	8–16 mm	0.31–0.63 in	Medium gravel	Pebble
−2 to −3	4–8 mm	0.157–0.31 in	Fine gravel	Pebble
−1 to −2	2–4 mm	0.079–0.157 in	Very fine gravel	Granule
0 to −1	1–2 mm	0.039–0.079 in	Very coarse sand	
1 to 0	0.5–1 mm	0.020–0.039 in	Coarse sand	
2 to 1	0.25–0.5 mm	0.010–0.020 in	Medium sand	
3 to 2	125–250 μm	0.0049–0.010 in	Fine sand	
4 to 3	62.5–125 μm	0.0025–0.0049 in	Very fine sand	
8 to 4	3.9–62.5 μm	0.00015–0.0025 in	Silt	Mud
10 to 8	0.98–3.9 μm	3.8×10^{-5}–0.00015 in	Clay	Mud
20 to 10	0.95–977 nm	3.8×10^{-8}–3.8×10^{-5} in	Colloid	Mud

Table 3.4: Table showing Krumbein phi Scale and Wentworth class *Adapted from [Wikipedia, 2023]*

Average grain size is widely measured using mathematical measurements such as median, mode, and mean.The mode is determined as the steepest point on a cumulative curve and reflects the most commonly occurring particle size in a population of grains.The median size is the midway of the grain-size distribution, corresponding to the cumulative curve's 50th percentile diameter. The mean particle size is the arithmetic average of all particle sizes in a sample, and it is frequently derived by averaging chosen percentile values from the cumulative curve.The cumulative distribution curve represents the cumulative

percentage of particles finer than a given size and it provides a graphical representation of the grain size distribution. In summary, the cumulative percent on the y-axis provides a visual representation of how the cumulative distribution of particles changes with grain size. For example, D_{50} point on the cumulative curve indicates that 50% of the total weight of sediment particles in the sample is composed of particles with a size smaller than or equal to theD_{50} size. In simpler words D_{50} is size such that 50% of the sample is finer than $D_5$0.This cumulative distribution provides a comprehensive view of the entire range of particle sizes in the sediment sample, illustrating the proportion of particles finer than or equal to each size.

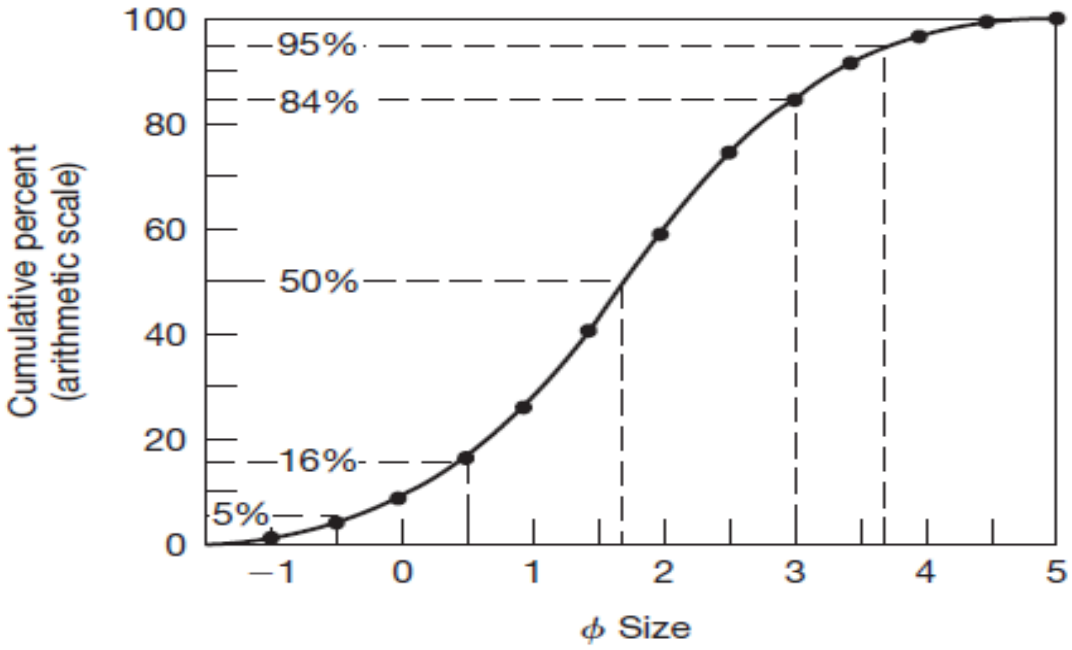

Figure 3.11: Cumulative percentage values from cumulative curve with the particle size *Adapted from [Boggs et al., 2012]*

The distribution of grain sizes in a river's bed, bars, and banks influences a variety of physical, chemical, and biological processes within river landscapes [Cattapana et al.,]. Knowing the grain sizes in a riverbed is critical for understanding and forecasting fluvial dynamics and the grading curve and characteristic grain sizes are critical charac-

teristics for modeling hydraulics and sediment transport in the case of non-cohesive bed material [Rüther et al., 2013] . Most numerical methods require information about the sediment particle sizes near the riverbed to estimate alluvial roughness accurately. Understanding the grain size distribution is also crucial for operations like identifying aquatic ecosystems and evaluating geological deposits [Chardon et al., 2022].

Grain size distribution and Grain roughness has been a important factor in the gravel bed river and is the topic of interest among the fluvial researchers [Rice and Church, 2010]. Grain roughness affects flow resistance, shear stress [Otsubo and O'Sullivan, 2018] and sediment supply [Milan and Heritage, 2012].Additionally, understanding the majority of physical and ecological processes in watercourses requires assessing the distribution of particle sizes on grain roughness. Indeed, the grain size characteristics such as hydraulic roughness, flow resistance, bed stability, habitat compatibility of stream bed surfaces are important in hydraulics, hydrology, morphology, and ecology [Cislaghi et al., 2016]. Manning's roughness coefficient is an essential parameter in hydrodynamic modeling, and this coefficient is influenced by the size, shape, and arrangement of the bed particles and grain size distribution plays important role to define these parameters.This section of the study, focuses to estimate the grain size distribution with different method and that are used to estimate the Manning's coefficient as well as use in numerical and hydrodynamic modeling.

The quantification of grain size distribution can be done by several methods.The grain size distribution method such as volumetric sampling and laboratory sieving [Kellerhals and Bray, 1971] of grain sediment, Wolman pebble-counting [Wolman, 1954], volume by number, grid by number, and area by number methods [Bunte, 2001] are most commonly used for grain size distribution.However, these methods are laborious, time and resource consuming such as equipment, staffs, laboratory facilities and also provide limited spatial coverage. Considering these methods as laborious and time consuming, significant advancement in high resolution photography have been developed to estimate the grain size distribution for large scale survey.A number of researchers have developed image-processing approaches for analyzing and classifying riverbed surface and armor layer sediments of mountain rivers in recent years. [Graham et al., 2005b, GOGOAŞE NIS-

TORAN et al., 2019, Buscombe, 2008].

Automated grain sizing methods is thus designed to be efficient, and fast and can be categorized as object-based and a statistical percentile based methods [Buscombe, 2020]. Percentile-based methods, such as simple autocorrelation algorithms, grain size prediction using image texture and semi-variance, spectral decomposition, and convolutional neural networks, estimate grain size distribution through statistical analysis of image characteristics [Carbonneau et al., 2004, Buscombe et al., 2010, Lang et al., 2021]. Object-based methods, exemplified by Sime and Ferguson (2003), and Graham et al. (2005a, b), employ grain separation algorithms to detect interstices and identify individual grains. Various techniques, including automatic edge detection, modified edge-detection algorithms, double threshold interstice-detection, and enhanced grain detecting models like BASEGRAIN, have been proposed for precise grain identification and measurement [Detert et al., 2012, Sime and Ferguson, 2003, Graham et al., 2005a, Graham et al., 2005b].Some neural networks have been also developed to estimate the GSD from the digital images [Buscombe and Carini, 2019].

Object-based approaches, also known as morphological approaches, use thresholding and segmentation processing to establish the form of each visible particle, whereas statistical approaches estimate grain size using picture texture analysis. Although object-based approaches are restricted and cannot be used beyond a single pixel, they appear to be a great tool for giving comprehensive grain size information regarding spatial variability, which can be beneficial for understanding flow processes.Furthermore, this approach employs grain separation algorithm sequences to detect grain interstices and identify each individual grain on the bed.As previously stated, many researchers used an automatic edge detection algorithm that was modified by [Sime and Ferguson, 2003] with a watershed algorithm and further improved by [Graham et al., 2005a, Graham et al., 2005b] with a double threshold intersticis detection, and finally [Detert et al., 2012] developed a software that uses a five step image-processing algorithm.In this study grain size distribution in the interested location was estimated with the help of this software and Wolman pebble count method was used at a location to verify the median grain size.

3.3.1 BASE-GRAIN

BASE-GRAIN is well known MATLAB-based object detection software tool for granulometric analysis of the surface top-view images of non cohesive gravel river bed.As already introduced,The methodlogy of the software is defined mainly by five steps.The first stage uses a double gray-scale threshold to detect interstices. The second phase employs morphological bottom-hat filtering to identify additional interstices. Step three completes the interstice identification using edge detection technique. The focus of the analysis is adjusted in step four to separate the single grain zones. A improved watershed algorithm is merged with the information collected by Canny edges in the previous stage in this step for grain segmentation. This stage produces a binary picture with completely validated single grain components that are successfully segregated by their interstices. The region attributes of each grain's top-view area and properties(for example, a-axis, b-axis orientation) are retrieved in step five. Normalized second central moments of specified object areas are used to replace these regions.The detailed explanation can be found in [Detert and Weitbrecht, 2013].

In this study, the orthophoto was obtained that was used for the analysis as discussed in section 3.1.The area near the San Salvatore dam at upstream and downstream was selected.The orthophoto has been divided into sections as shown in the Figure 3.12. Only the areas with clear without deep water, obstacle- and vegetation-free surface, displaying gravel accumulation were considered.The one area of each sections such as point bars were normally selected where the gravels were exposed and was easier and effective for the analysis.

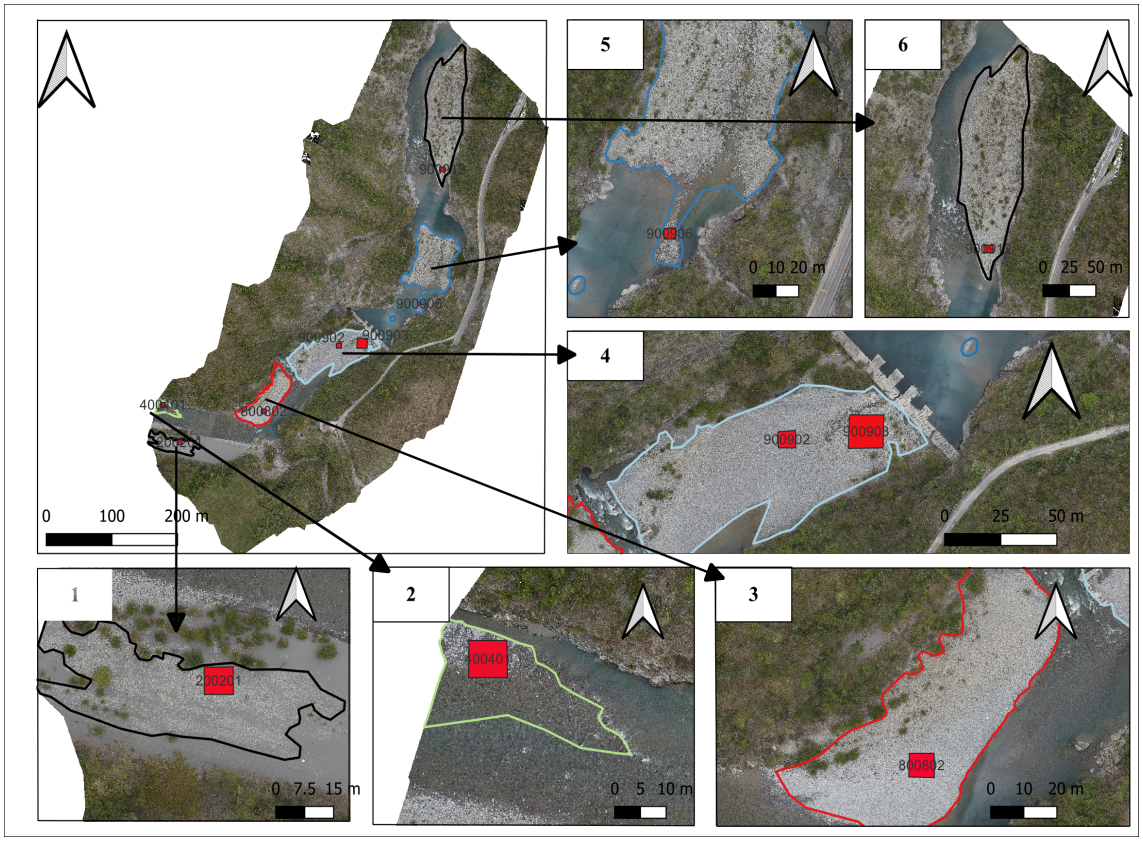

Figure 3.12: Orthophoto showing the location of the selected area for GSD analysis

	Location and Image number					
	1	2	3	4	5	6
S.N.	**Sub-divided region(Image ID)**					
1	200201	400401	800802	900902	900906	900912
2				900903		

Table 3.5: Location and Image ID as shown in Figure 3.12.

The image from each area was extracted from QGIS and used for the BASEGRAIN software. The top-view photograph of a granular bed according to the object detection involving steps 1–5 was performed, applying the line-sampling method according to Fehr's (1987) method. At first, the image was imported to the BASEGRAIN software,

and pre-processing, such as scale and crop section(if required), was performed. Now, the five-step processing was applied to the image of each location. During this process, at the first step [medfiltsiz10, facgrayhr1, facgrayhr2, blocSizG, mfG]=[3 px, 0.8, 0.1, 8 px, 1] and in the second step [medfiltsiz20, criteriCutL2] = [1 px, 0.1] was chosen and regarding the 4th step [areaCutLfA, areaCutWW] = [100, 40]. Post-processing, such as the departing objects function, was used to remove unwanted objects, such as wood in the image. Also, the merge objects were used if the single gravel was divided into smaller ones during processing.The image of section 3 (Image ID-800802) is shown in Figure 3.13 and additional images are attached to the appendix.

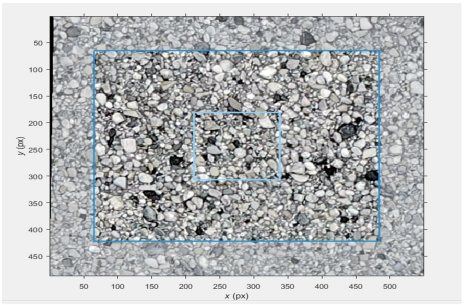

Fig. A

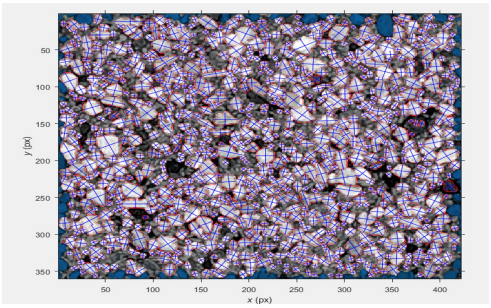

Fig. B

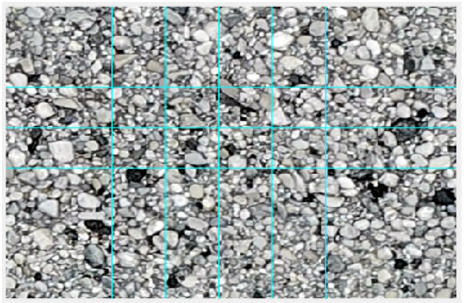

Fig. C

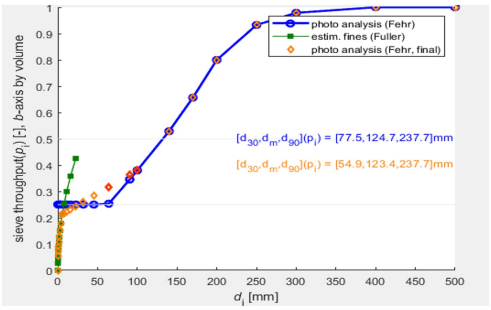

Fig. D

Figure 3.13: Figure shows the process GSD analysis in BASEGRAIN software. Fig A: Pre-processing of the raw image. Fig-B: Output of object detection after five steps processing. Fig-C: Analysis based on Fehr(1987), Fig-D: GSD curve by volume with calculated grain size diameter

.

For each location and Image ID the same process was performed. Output of the BASEGRAIN as the excel sheet was extracted and and the grain size distribution curve were generated as shown in Figure 3.14.

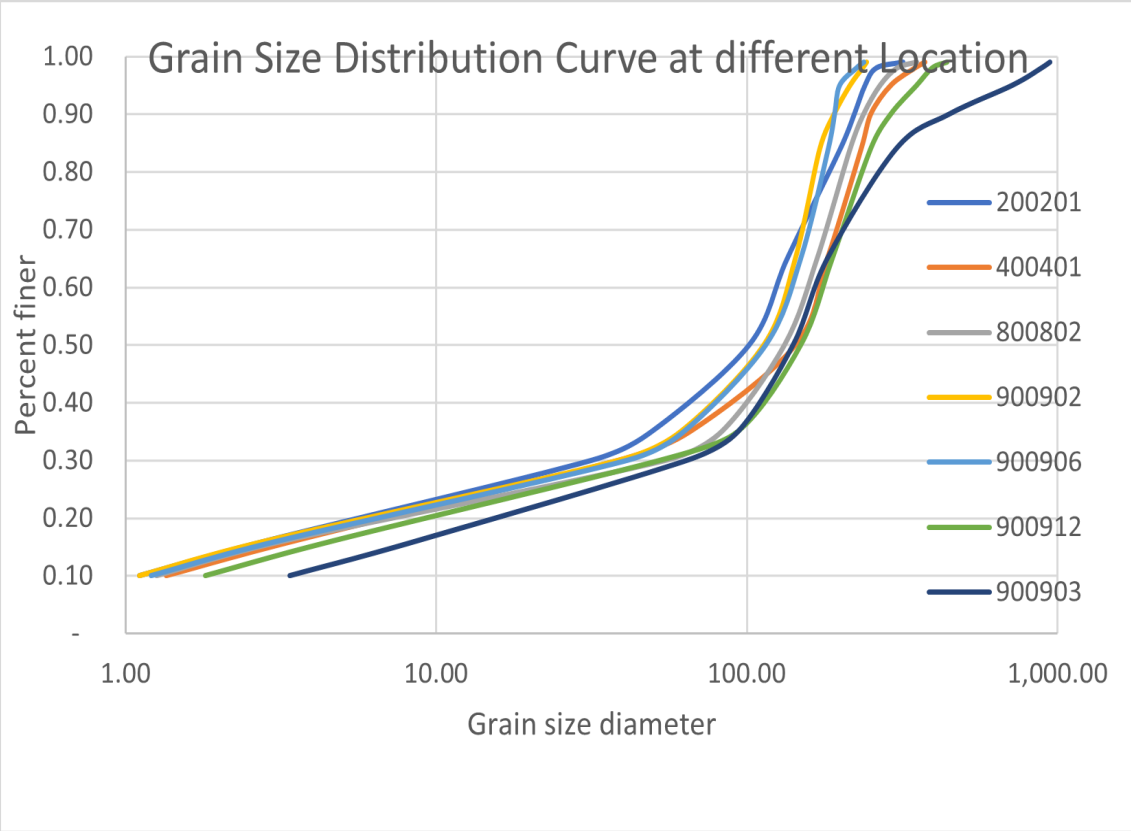

Figure 3.14: Grain size distribution curve obtained from the BASEGRAIN Software

.

As shown in the figure above, seven different curves at each location listed in Table **??** were calculated by plotting the percent finer on the Y-axis and the grain size diameter on the X-axis. The cumulative distribution curve obtained shows a minor variation within the different locations except for one location of ID 900903, which might be the case that the deposition of large gravel material upstream of the dam is present.As inferred from the figure, smaller variations can be observed in finer grains and higher variations between the coarser grains. All these locations lie in the deposition part of the river reach and point bars just upstream and downstream of the dam placed; in this study, these areas are

taken as the representative sample of the interested river reaches. Even some parts of the river reach contain sand deposition, which was neglected for the grain size distribution analysis.

All the grain sizes obtained from the Excel sheet of the BASEGRAIN analysis based on Fehr, Final, each (D10, D16, D30, D35, D50, D65, D84, and D90) values in all selected location were plotted as shown in Figure 3.15.This Fehr, Final curve was selected for the analysis as it also includes the values of D10 and D16 through interpolation of the Fehr photo analysis curve.

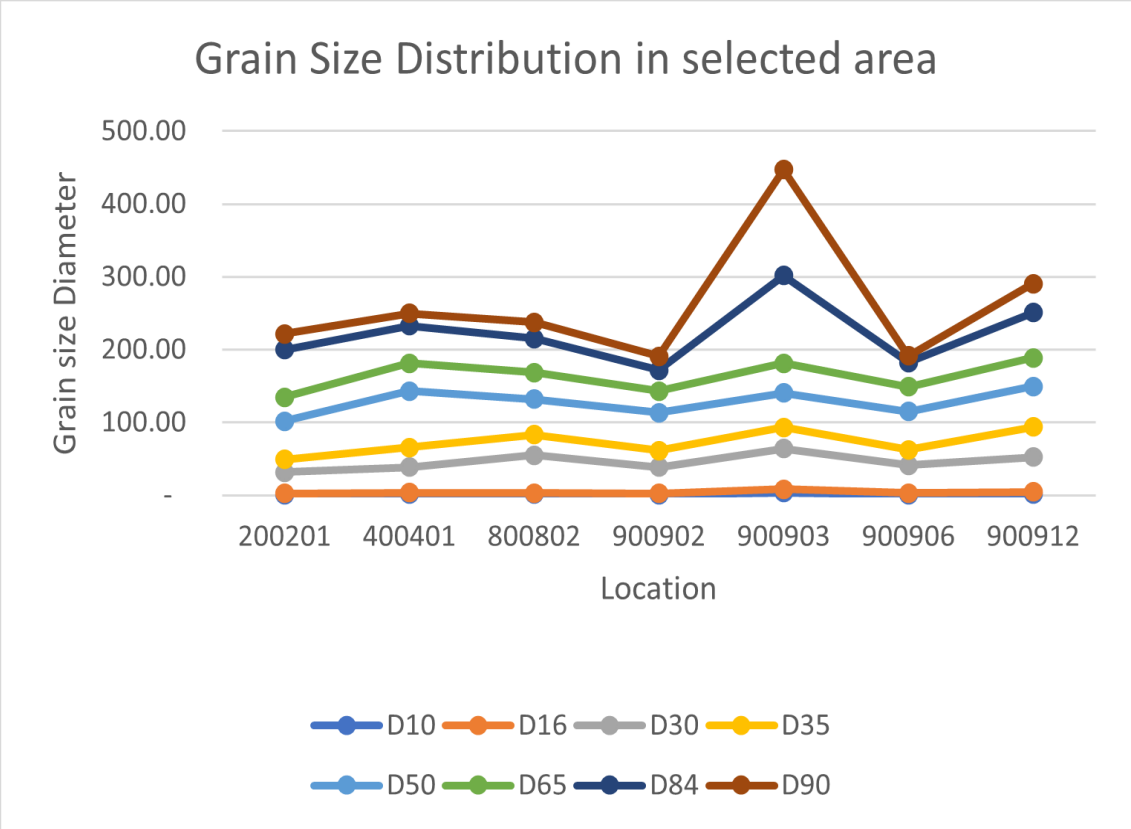

Figure 3.15: Comparison of different grain sizes at different location

.

The eight percentile values (D10, D16, D30, D35, D50, D65, D84, and D90) indicate the sediment grain size (in mm) for a particular "percent finer" value, which is used to compare individual values. Among the values obtained, in location 900902 the values

variability is significant due to which the values of that location was excluded during calculation ofaverage values of D10, D16, D30, D35, D50, D65, D84, and D90 at each location. Values of different percentile of grain size varies in different locations. For example, the values for D10 varies from 0.011m to 0.018m and D30 varies from 0.316m to 0.548m shows some variation in each location and were also shown in figure above. The mean value of each grain size of all location have been calculated and summarized in the Table 3.6.

Grain Size	**D10**	**D16**	**D30**	**D35**	**D50**	**D65**	**D84**	**D90**
[mm]	1.31	3.34	42.95	69.30	125.79	160.87	208.75	230.35

Table 3.6: Mean grain size for different percentile in all the location selected

D50 values is one of the most essential characteristics determining the effective particle size of a group of particles or the grain size distribution curve, and it can also be used to show grain size variations in different locations.The D50 values was also a important parameter that was used in the numerical as well as hydrodynamic modelling in this study.In addition with this, R^2 values were evaluated for D10, D16, D30, D35, D50, D65, D84, and D90 values and 3rd order polynomial was a good fit.

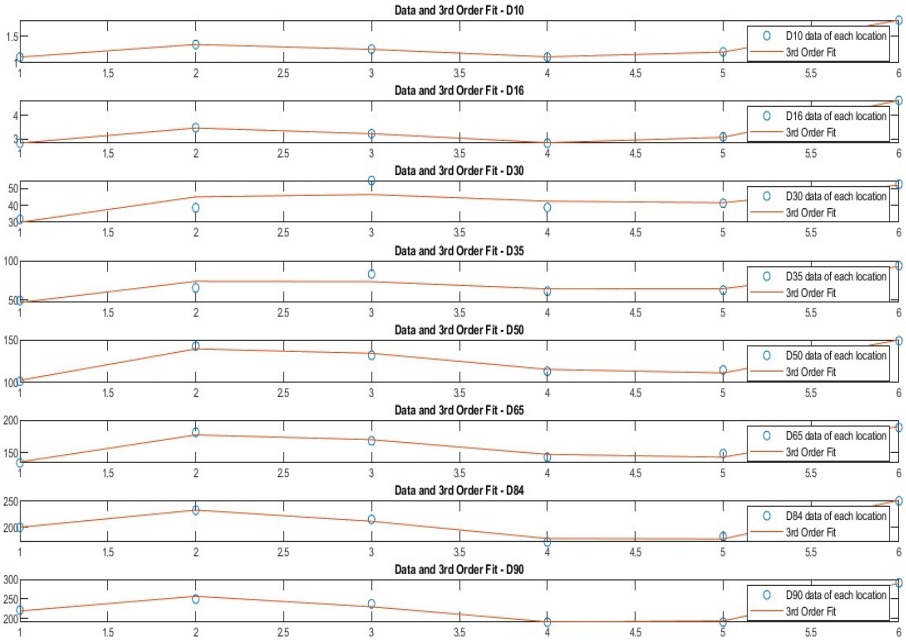

Figure 3.16: 3rd order polynomial curve fitting for the grain size values of different location

.

Grain Size	**D10**	**D16**	**D30**	**D35**	**D50**	**D65**	**D84**	**D90**
R^2	0.9998	0.9995	0.6778	0.8626	0.9794	0.9696	0.9812	0.9833

Table 3.7: R^2 values of the values at different locations

The R^2 values quantify how well a 3rd order polynomial equation fits grain size values across different locations. Higher R^2 values indicate a better fit, reflecting the proportion of variability in the data explained by the model.

Furthermore, at one of the Location 800802, the pebble count method was conducted in order to calculate the D50 and check the grain size value obtained from the BASEGRAIN Software.

3.3.2 Wolman pebble count method

Pebble-count techniques are utilized to characterize the surface layer's particle size and are in-situ methods developed to gain grading curves mainly on the surface made up of coarser materials like gravel. In this method, one should physically measure or describe the axis of the individual grains. To obtain % finer frequency-by-number GSDs, grains were counted by size [Wolman, 1954]. Pebble-count methods need minimum field equipment and are thus ideal for gathering particle size data in remote regions. This is especially true when the spacing between grains is determined by a person's foot. In this method, the zigzag routes in the riffles, pools, and point bars were taken, and the approach consisted of the random selection and measurement of gravel particles that were taken from the riverbed layer found at the toe of the sampler at each of three steps without looking [Bunte, 2001] as shown in the Figure 3.17. As suggested by the [Bunte, 2001], 100 or more gravel particles should be taken in a specified area for a better result. In this study, 71 samples were taken into account due to constraints in the time and particular location width. A cumulative size distribution curve of particle diameters was determined using the measured particle and the Wentworth grain size scale as shown in the Figure 3.18.

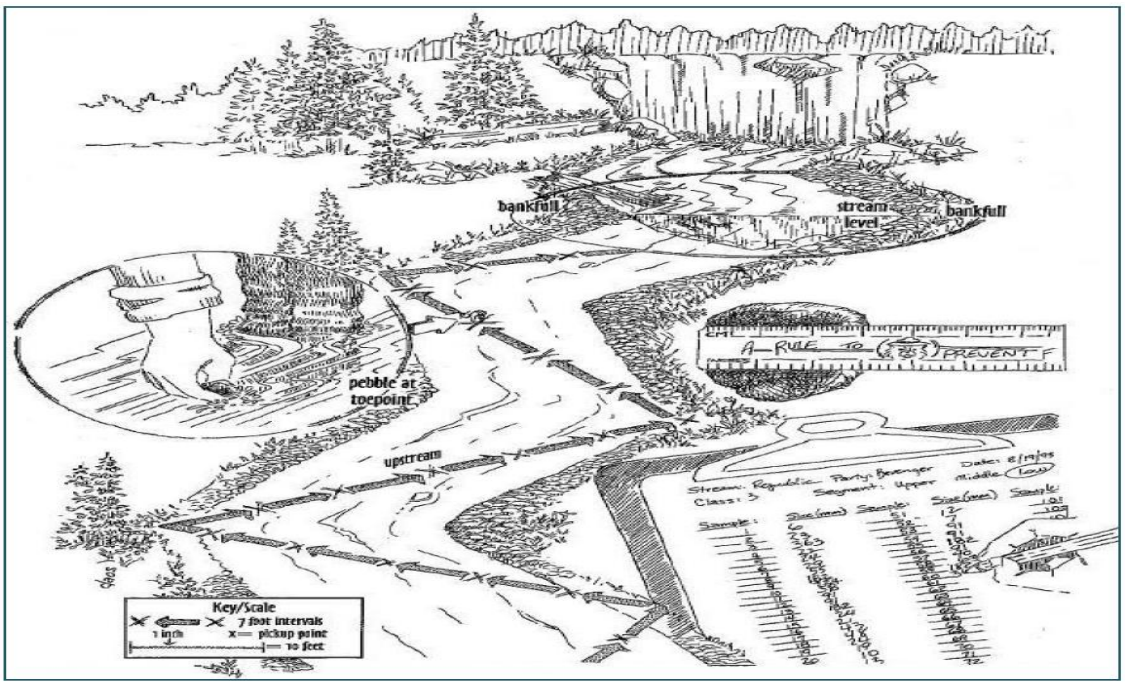

Figure 3.17: Wolman method(1954) *Adapted from website of west virginia department of environmental protection*

.

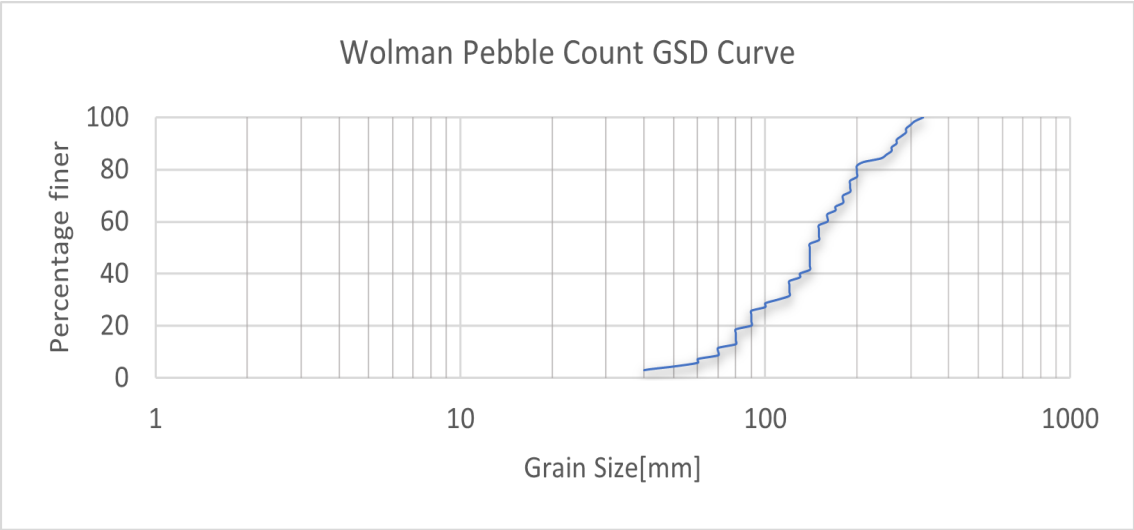

Figure 3.18: Wolman method for Grain size distribution analysis

.

From the cumulative grain size distribution curve of the in-situ sample collected and applying the Wolman method, D50 has been calculated as 140 mm, which is slightly greater than the D50 as 132.3 mm that was calculated from the BASEGRAIN software at the location 800802. The results obtained with the Wolman method validate the results of the BASEGRAIN software. As the BASEGRAIN analysis was comprehensive and detailed, the grain size required for further numerical modeling and the hydrodynamic modeling grain size that was calculated from the BASEGRAIN software and listed in Table 3.6 were taken.

3.4 DEM Generation

Digital Elevation Models (DEMs) are the digital representation of the Earth's surface that shows the variation in elevation. These 3D models are used in numerous applications such as hydrogeomorphology, hydraulics, hydrology, natural resources management, and many more. As discussed above in section 3.1, structure-from-motion (SfM) photogrammetry, which uses images taken by UAVs, is increasingly being utilized to generate high-resolution DEMs.These DEMs are divided into the Digital Surface model(DSM) and the Digital Terrain model(DTMS). DSMs are the digital representation of the elevation that describes the physical surface, including all-natural and artificial things, including ground and non-ground points. DTMs are similar to DSMs but do not include the non-ground natural and artificial things representing the bare Earth. DTms are typically used for various applications such as environmental planning and management, flood risk evaluation and hydraulic modeling.

The river section also contains various terrain elements such as woods, debris, vegetation, and hydraulic structures such as bridges and culverts. These elements should be removed during the terrain modeling to get the DTMs that are further used for numerical and hydraulic modeling. In this section, the generation of DTMs after processing the point cloud (generated through the UAV measurement) in the software CloudCompare has been thoroughly discussed and the output as DTMs without the noise were obtained.The methodology to obtain the final DTM from the initial phase of data acquisition is shown

in the Figure 3.19.

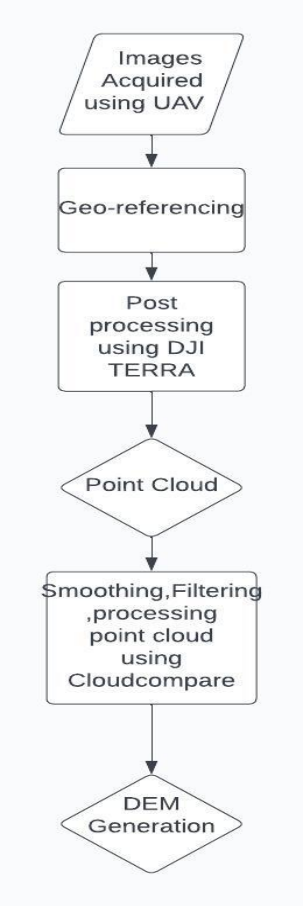

Figure 3.19: Workflow of DEM Generation

.

3.4.1 Point Cloud

Point clouds are a group of three-dimensional data points that often depict the exterior surface of an object. These points are specified by their spatial coordinates (x, y, z) and may be acquired using a variety of techniques, including LiDAR (Light Detection and Ranging), photogrammetry, and 3D scanning technologies.This study focus on the LAS point clouds generated from UAV measurement and the point clouds can be segmented, classified and filtered as per the requirement in CloudCompare software. Cloudcompare (CC) also has an option to merge the LAS files into a single LAS file or segment options to split in smaller LAS files.The complete point clouds that was the output of UAV

measurement as discussed in section 3.1 is shown in figure below:

Figure 3.20: Complete LAS Point Cloud in the study area

.

This study area consists of dense vegetation, woods, debris, houses, and bridges that need to be removed to obtain the ground point clouds. The dense vegetation can be found on the upstream side of the study area, whereas the structures and buildings can be found on the downstream side of the area, as shown in Figure 3.20. Also, the noises and artifacts are common in photogrammetric-generated 3D point clouds due to the mismatches. This can be seen under the terrain surface, as shown in the Figure 3.20. It is difficult to use a filtering algorithm as these mismatches were closely found near the terrain surface.
In the later sub-section, the methodology to remove such noises and other unwanted structures and items has been discussed.

3.4.2 Segmentation

Manual segmentation and classification is the technique of finding and categorizing individual points within a point cloud based on their attributes. Manual segmentation and classification can take long, especially with big point cloud data sets. They are useful techniques, however, when clarity and knowledge of certain aspects are crucial to the study. The complete LAS point cloud file was complex and had a high number of point clouds. As this study area contains a steep slope, flat areas, and irregular slopes, high precautions should be taken to segment and classify point clouds.The basic steps that was implemented during the manual segmentation were:

- The large clouds points were splitted into a small clouds points
- Segmentation of the unwanted things such as vegetation, houses, woods was done and classified to their respective groups.
- The smaller clean point cloud containing only the ground point clouds were merged.

Furthermore, the manual segmentation methodology is shown in the figure below. First, the larger point cloud section was split into smaller sections, and then orienting the smaller point cloud section parallel to the ground points, other point clouds, such as vegetation and other unwanted things, were removed from that section. After repeating the same task, only the ground points without noise were obtained.All the smaller sections were finally merged to create the complete section. The holes created after removing the unwanted clouds from ground points were further filled with different interpolation techniques. Manual segmentation method is essential even after applying various filtering techniques. Some of them were also applied in this study and discussed in the following sub-section.

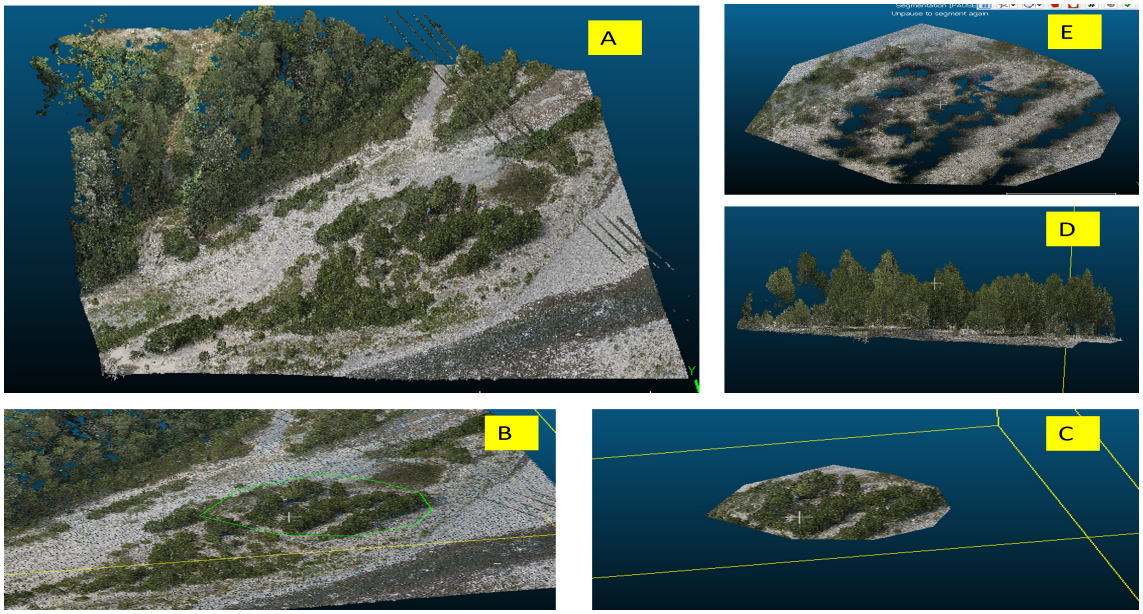

Figure 3.21: Fig A: (shows the a part of the whole LAS file). Fig B: (Smaller section of Fig. A was selected for segmentation). Fig C: (Output of smaller section). Fig D: (Orientation of the section to remove unwanted parts such as vegetation). Fig E: (Output after removing vegetation).

.

3.4.3 Filtering

Colorimetric segmentation using RGB filtering and CSF filtering plugins of CloudCompare were used in this period. Former is a common technique in image processing and computer vision. It involves isolating specific colors or color ranges within an image to identify and segment objects of interest.During this method the color range in the RGB space was determined in the section where we want to segment. Basically, this method was used in order to separate dense vegetation point cloud from other point clouds. This was due to the fact that the study section has dense green vegetation which was easy to visualize and efficient to segment with the help of RGB filtering. A example of the RGB segmentation is also depicted in the Figure 3.22, where, minimum and maximum values for the R, G, and B channels to filter out points that fall outside the desired color range

were defined. Normally, the R,G,and B values were selected automatically after choosing the desired color in the clouds.Based on the color intensity in different sections, RGB values were selected with certain deviation limits(5%).

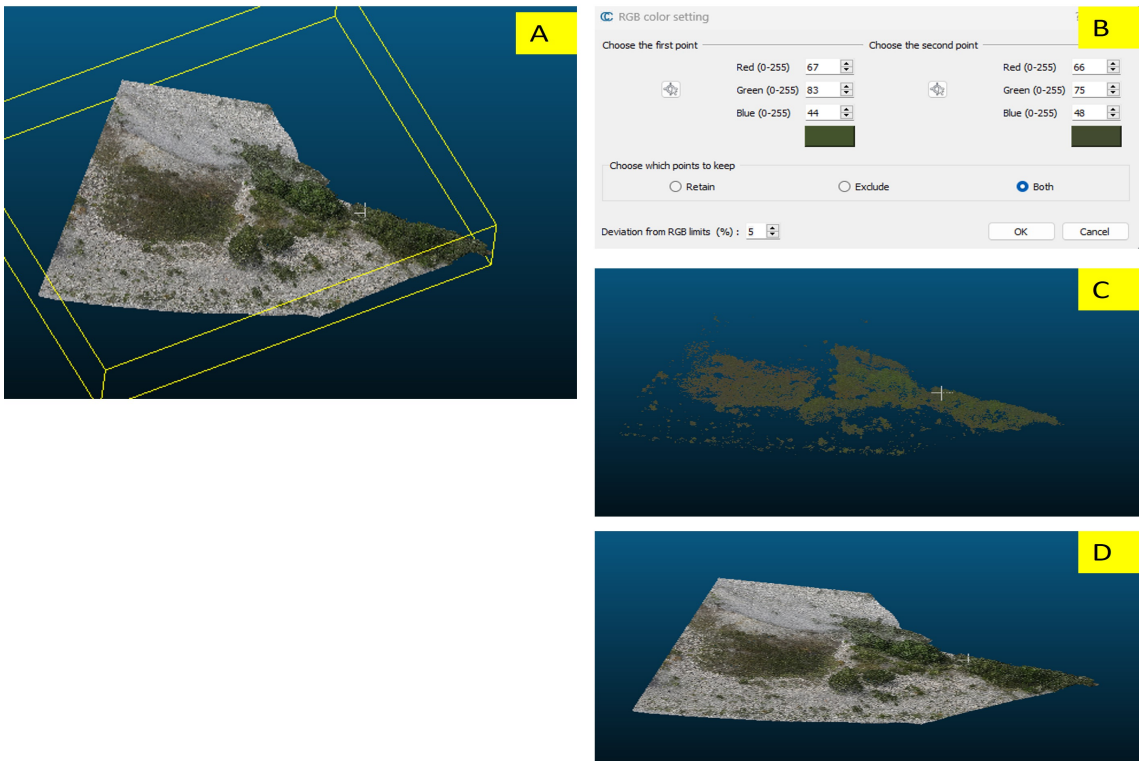

Figure 3.22: Fig A: (original section). Fig B: (RGB values with deviation limits). Fig C: (Vegetation that was filtered out). Fig D: (Remaining points clouds after filtering).

.

The final result can be produced after repeating the process numerous times with different RGB values. However, the generated point clouds also contain some point clouds with elevation greater than the ground points, necessitating manual segmentation. This strategy was beneficial on slopes with dense vegetation. Throughout the point cloud segmentation procedure, RGB filtering was used in conjunction with manual segmentation in numerous parts.

Other filtering technique, cloth simulation filtering (CSF) was also implemented in this study. This is one of the plugin of the CloudCompare software and works on the principle

that the cloth drops on the terrain due to gravity.Considering the cloth as soft and sticks to the terrain, that will produce DSM however, overturning the terrain would produce the DTM.This cloth simulation technique was proposed by [Weil, 1986] and was also used in this study.The principle of this filtering technique is also shown in Figure 3.23.

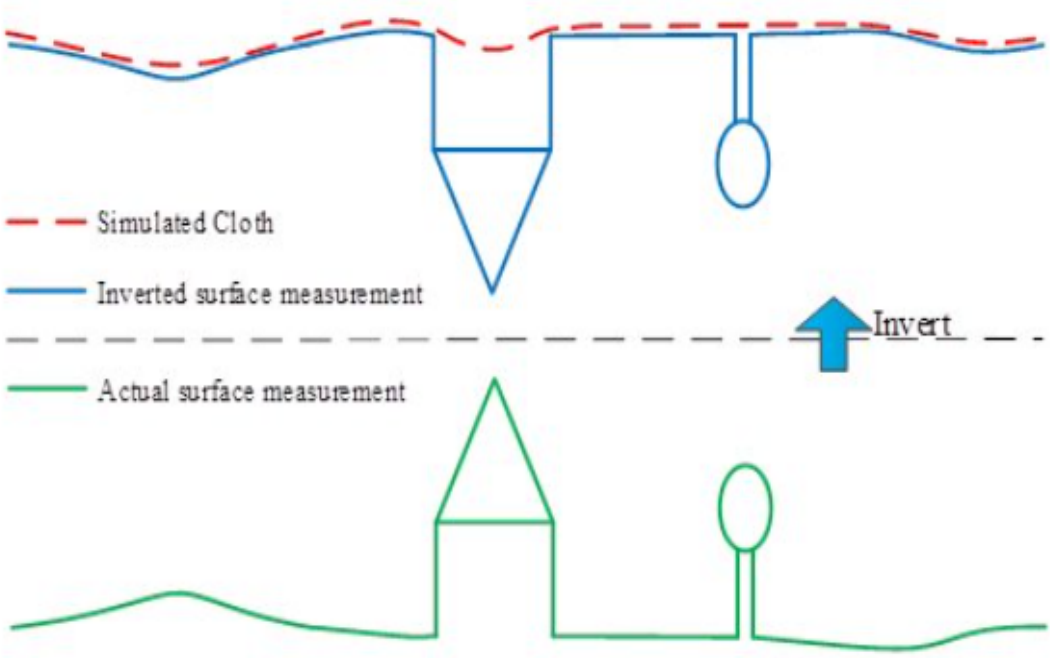

Figure 3.23: Overview of Cloth Simulation Filter(CSF) *Adapted from Wikipedia "CSF Filter"*.

.

This technique was applied in the section where there was a flat section during the survey and followed by the manual segmentation as well. In the general parameters setting, relief was selected, and the cloth resolution of 0.5 was taken, other value were taken as default as shown in Figure 3.24. This technique separates the selected point clouds into ground and off-ground points, providing them with two files, and the off-ground points were further segmented according to the types of point clouds.

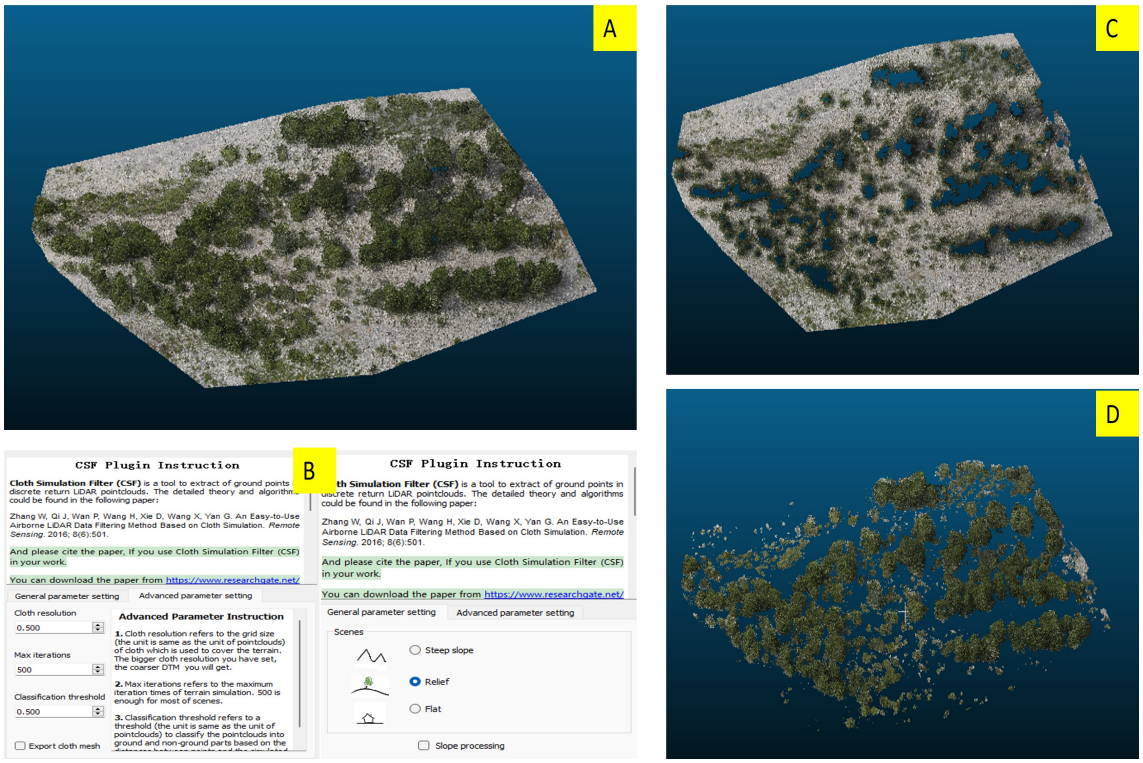

Figure 3.24: Fig A: (Selected section for the CSF filtering). Fig B: (CSF plugin parameter setting). Fig C: (Ground points after filtering). Fig D: (Off-ground points after filtering)

After applying the filtering and manual segmentation the whole point clouds needs to be classified into different classification in order to handle large las files effectively and only select the ground points that are used for modeling, and are discussed detail in the following sub-section.

3.4.4 Classification

Classification of point clouds is a daunting task due to the complex nature of point clouds. It is defined as the task of assigning a specific label to the point clouds based on their characteristics which is also known as semantic segmentation due to the fact that once the point cloud has been segmented each segment group has been named with a class to give a meaning. In this study, the points clouds of the study area were defined in six classes as:

1. Wet Area

2. Dry Bed

3. Vegetation

4. Banks

5. Logs-Trunks

6. Dam and bridges

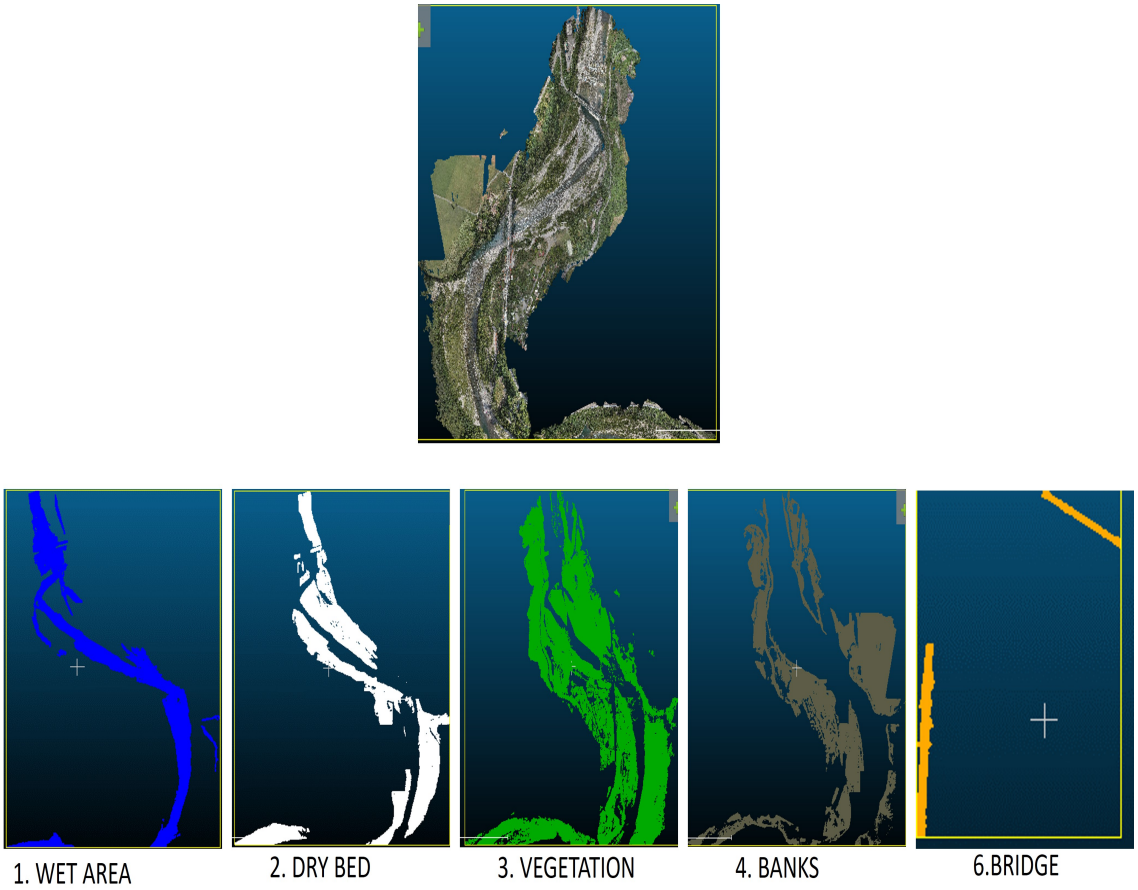

Figure 3.25: Upper figure shows the part of whole study area point clouds. Lower images are the points clouds that are segmented and classified in different classes).

After the classification into different groups, the handling of point clouds was easier and even allows for the removal or reduction of noise and irrelevant data points such as

vegetation, woods, and logs.Additionally, it helped selectively process or analyze specific groups of points such as the wet area, dry bed and banks that are only affected by flood. Consequently all these selective features were merged and the final point clouds was generated as shown in Figure 3.26.

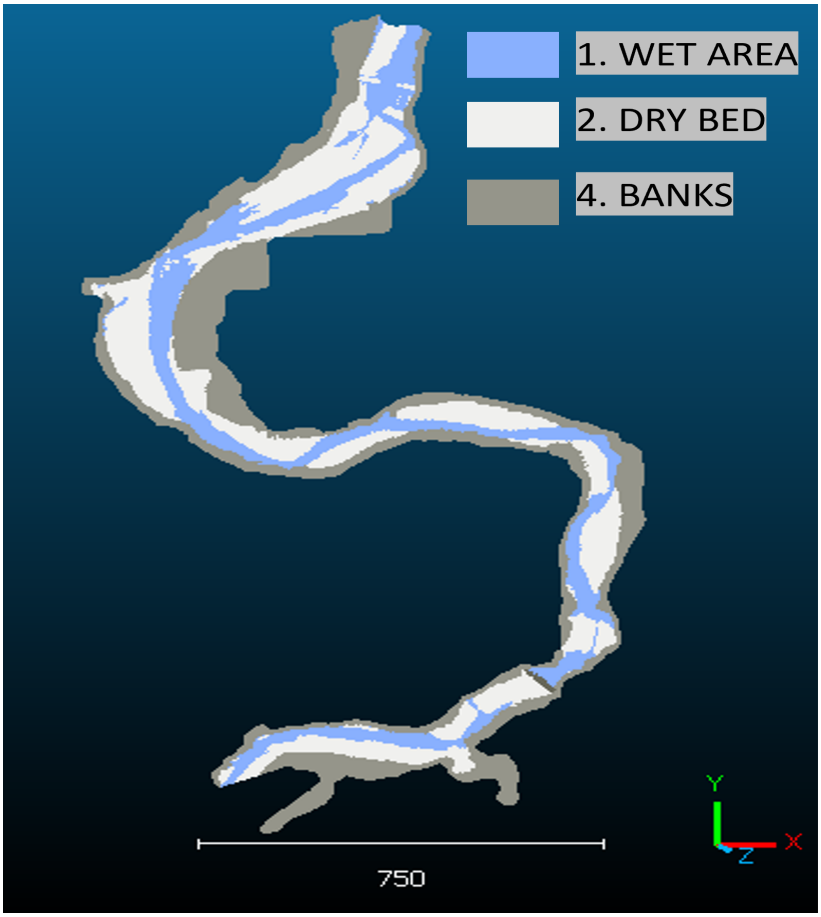

Figure 3.26: Final point cloud with wet area, dry bed and banks after removing vegetation and irrelevant point clouds

3.4.5 DTM Generation

First of all, smaller section of the point cloud without vegetation and noise were taken that contains holes which were then linearly interpolated and extracted as cloud and all the smaller section were merged after filling the holes. Also, the holes in the final point clouds chosen were small, due to which CloudCompare can be used for linear interpolation to construct the raster as output. During the procedure, the grid step size was set to 0.2, and

the height of each grid cell was calculated as the average of all points within that cell. The average height of the entire grid was used for empty cells, followed by linear interpolation with the nearest non-empty surrounding cells. Because the clouds had varying scalar fields, the interpolation was done by taking the average SF value of all the locations in this cell. Finally, a GeoTIFF raster file was exported, as shown in Figure 3.27, which relies on the GDAL for this procedure.

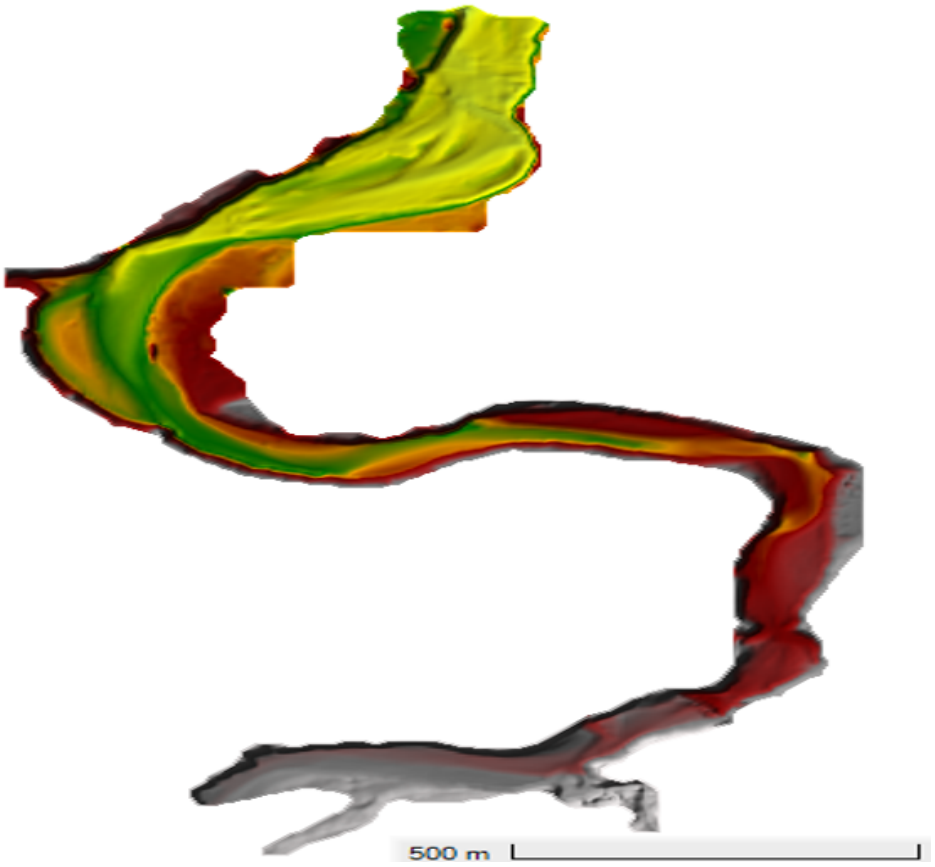

Figure 3.27: Final DTM generated

A Digital Terrain Model (DTM) was methodically derived after a complex data-collecting procedure and the execution of several tasks. This extraction needed the removal of both vegetation and noise, yielding a refined dataset suited for sophisticated numerical modeling.

Chapter 4

Numerical Modelling

The third chapter focuses on obtaining critical input parameters for further numerical and hydrodynamic modeling assessments. The data provided includes discharge data for various return periods, grain size distribution, and the Digital Terrain Model (DTM). The major parameters gained in this chapter provide the foundation for the subsequent modeling effort.

The amount of sediment transported downstream along with the morphodynamical evolution of river bed after dam removal can be calculated solving non-linear parabolic equation of sediment transport formulae by Engelund and Hansen (1967) and for the further analysis of 1D and 2D hydrodynamical modeling provides the flood mapping before and after the dam removal taking into account the sediment calculated through numerical simulation. In addition, the relation between the flow in the main river channel and the bypass during different return period flood can be evaluated through 1D hydrodynamical modeling using HECRAS.

This approach provides the affects that can be encountered after the dam removal in the fluvial bedforms and helps to provide information regarding the flooding during extreme events that augments the dam removal decision making.

4.1 Hydrodynamic Model with bypass:HEC-RAS

Different hydraulics models such as 1D, 2D and combined 1D/2D models have been common these days. Generally, HEC-RAS software uses these models for flood mapping and calculate depth under different extreme scenarios.The hydraulic modeling system is open-source software created by the United States Army Corps of Engineers (USAC, 2010) that is built to model steady and unsteady hydraulic modeling the river system. The hydrodynamic modeling in this study was carried out using HECRAS 6.4. The modeling approach would be to incorporate the channel bypass functioning and dam structure and the flow distribution within them, which provide important information for numerical morphodynamical simulations. The general methodology adopted for this purpose:

4.1.1 Key assumptions

In 1D model, all flow are considered in longitudnal flow and One-dimensional models represent the terrain as a sequence of cross-sections and simulate the flow to provide the outputs such as depths and velocity. Considering the discharge at different return period unsteady simulation with constant discharge in each return period was implemented.HEC-RAS employs the one-dimensional Saint-Venant equations to model open channel flow. The Saint-Venant equations describe the conservation of mass and momentum in open channels with gradually varying flow. The shallow water equations are a simplified version of the Saint-Venant equations for shallow flows.

Continuity equation:

$$\frac{\partial A}{\partial t} + \frac{\partial (Q)}{\partial x} = 0 \tag{4.1}$$

where:

A : Cross-sectional flow area

Q : Discharge

t : Time

x : Longitudinal direction

Momentum equation:

$$\frac{\partial Q}{\partial t} + \frac{\partial (QU)}{\partial x} + gA\frac{\partial h}{\partial x} - S_f Q = 0 \tag{4.2}$$

where:

U : Flow velocity

h : Water surface elevation

g : Gravitational acceleration

S_f : Friction slope

To simulate the flow of rivers and open channels, these equations are generally solved numerically. HEC-RAS solves the Saint-Venant equations using finite difference techniques and predicts water surface profiles, flow velocities, and other hydraulic parameters under various scenarios. To produce realistic simulations of river hydraulics, the program also takes into account aspects such as channel geometry, roughness coefficients, and boundary conditions.

4.1.2 Parameters and Input

The parameters and Input for the simulation of the flow in HEC-RAS Manning's coefficient, lateral structures, inline structure, flow data and boundary conditions.

Geometry and cross section

The DEM calculated in section 3 was used and uploaded in the RAS mapper of HEC-RAS, which has approximately 3km streamline. The cross-sections were drawn within reach and interpolated between each pair of cross-sections to obtain an approximate interpolated cross-section—every 15m of longitudinal distance.Also, the bed of the cross section was modified manually in a specific areas where bathymetry was conducted.The geometric data and cross-section are as shown in Figure 4.2.

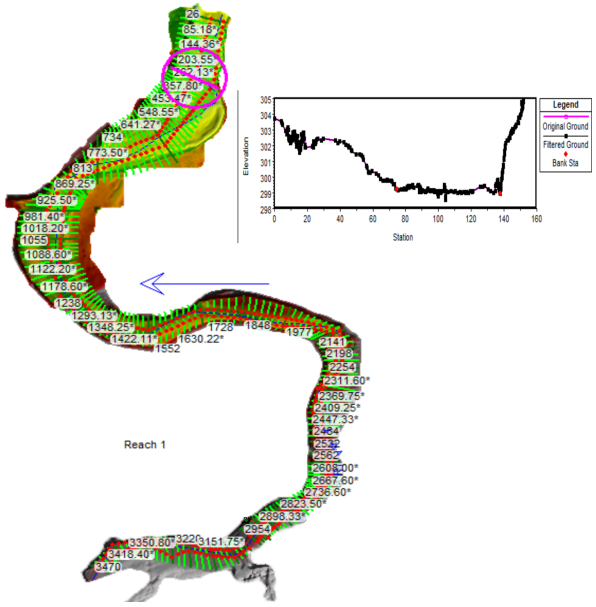

Figure 4.1: Geometry and cross section

Bypass and dam structure

As already stated the bypass channel was modelled as the lateral structure in this study and the dam structure was considered as the inline structure. Due to the inaccessibility of the bypass, the condition inside the bypass channel was unknown. For the lateral structure, first, the weir was modeled, and the height of that weir was set such that even extreme events could not pass over and then the circular culvert was planned, with the tailwater connection considered out-of-system. The diameter of the circular culvert's intake was measured as 4.5m. It functions as the water will pass from culvert to the out of the system. The same flow will be resupplied as in the form of inflow in the same area where the

bypass mix with the river again in downstream. This kind of arrangement was one of the effective way to model the bypass channel in Trebbia river and shown in the figure below:

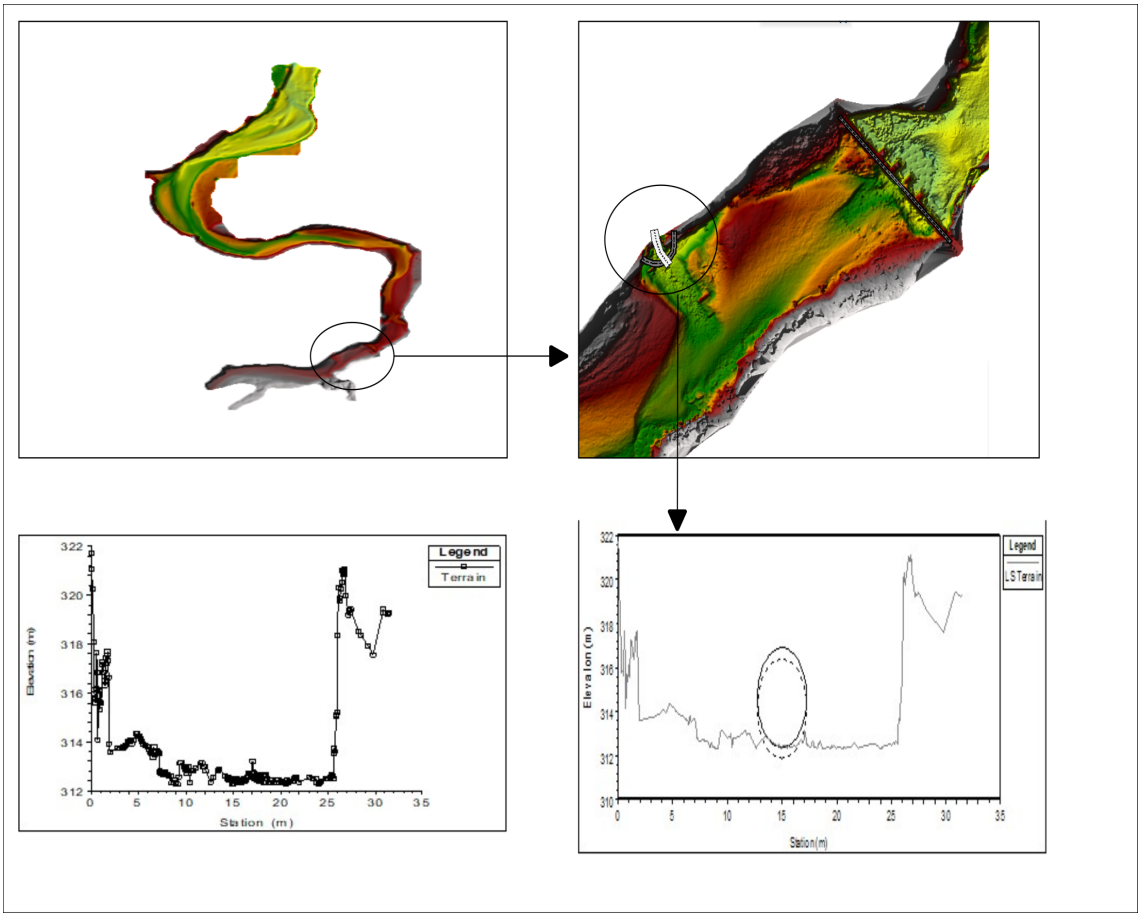

Figure 4.2: Bypass as lateral structure.Top left figure shows the full DTM and the right top figure shows the area of bypass inlet.The bottom left figure shows the terrain profile at that location whereas bottom right figure shows the culvert in the terrain.

During the modeling, the real terrain cross section dam profile was taken from the DEM as a inline structure. The dam was considered as the broad crested weir and was without the gated spillway and culvert.The stations and elevations of the top of the embankment and weir were taken from profile and the distance between the upstream side of the weir and the cross section immediately upstream of the structure was 2.7m.

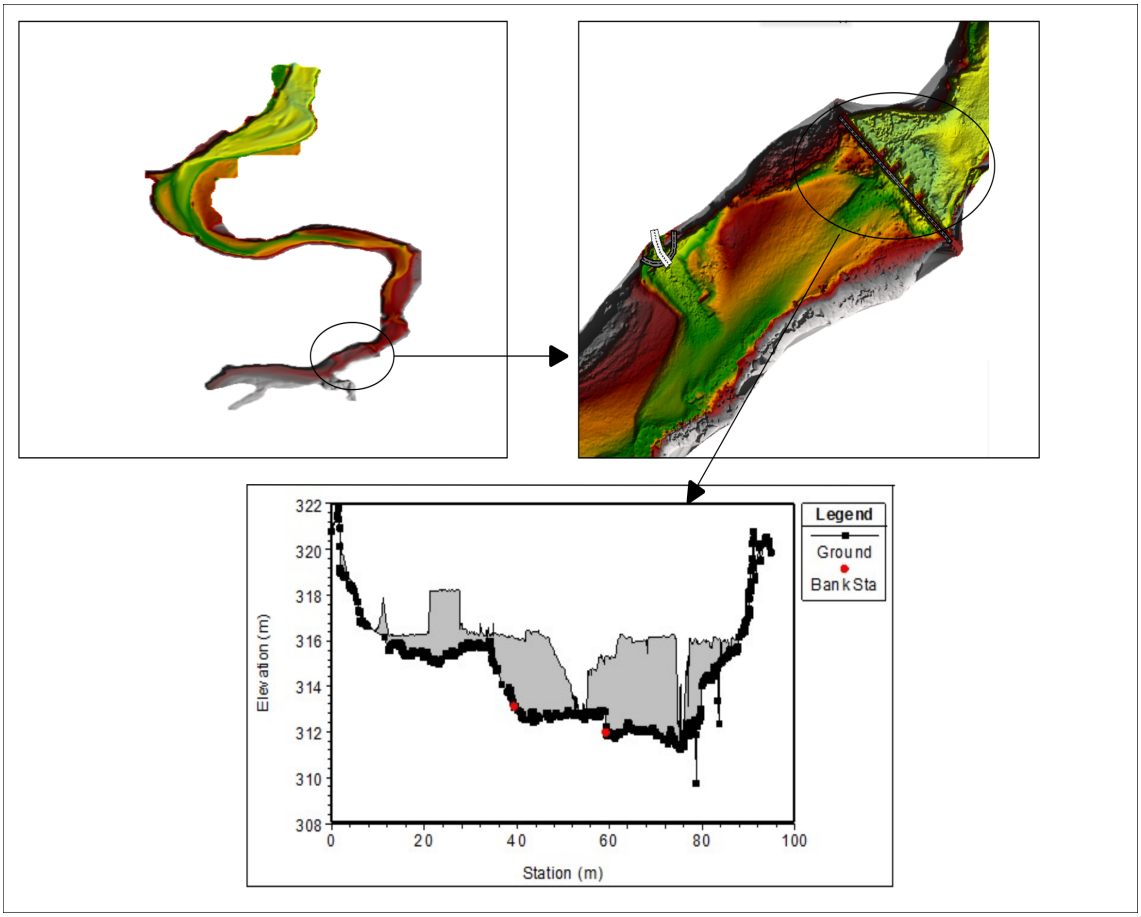

Figure 4.3: Dam as Inline structure.Top right figure shows the dam location in DTM. Bottom figure shows the actual profile of the existing dam.

Manning's roughness

Manning's n values are used by HECRAS to compute surface water profiles.This indicates Manning's roughness coefficient are important parameter for hydraulic analysis. Manning's Coefficients for the channel and flood plain were used constant throughout the reach for the modeling.The channel values were selected based on (Modified from Aldridge and Garrett, 1973) that ranges from 0.30-0.50 and also calculated through the emperical equation $n = 0.0431 D_{90}^{1/6}$ [McKay and Fischenich, 2011] with a $D_{90} = 230.35$ grain size distribution calculated in section 3. The selected mannings roughness for the channel was 0.035 and for the floodplain roughness was 0.055 considering the vegetation

and minor degree of irregularity as listed USGS guide for selecting Manning's roughness coefficients for natural and channels and flood plains.

Boundary Conditions

Flow hydrograph was taken as the upper boundary condition.The steady hydrograph was taken into account with the different return periods discharge values as calculated in hdyrological analysis.The downstream boundary condition was the normal depth with friction slope that was calculated from the terrain as 0.003. Also in this case, another lateral hydrograph(same as the outflow from the lateral structure discussed above) was introduced where the bypass connects the river in downstream.

4.2 1D Morphodynamical Simulation

For the morphodynamical simulation the Engelund and Hansen(1967) equation can be solved which was based Bagnold's stream power theorum and similarity principle that is expressed as :

$$q_b = \Gamma(\tau_* - \tau_c)^a \sqrt{\Delta g D^3} \tag{4.3}$$

Where:

q_b Bedload sediment transport rate (m^3/s)

Γ Dimensionless coefficient

τ_* Dimensionless shear stress

τ_c Critical shear stress for sediment motion (N/m^2)

a Dimensionless exponent

Δ Relative density of sediment particles (dimensionless)

g Acceleration due to gravity (m/s^2)

D Median sediment particle diameter (m)

Further, modifying the equation:

$$\tau_* = AS^{7/10} \tag{4.4}$$

$$A = \left(\frac{q}{K_s}\right)^{3/5} \frac{1}{D\Delta} \tag{4.5}$$

Where:

τ_* Dimensionless shear stress

A Constant coefficient

S Channel slope

K_s Gauckler-sticler coefficient

Putting value of τ_* in equation 4.1:

$$q_b = \Gamma\sqrt{\Delta g D^3}\left(AS^{7/10} - \tau_c\right)^a \tag{4.6}$$

Again, Differentiating w.r.t to x the equation becomes,

$$\frac{\partial q_b}{\partial x} = \Gamma\sqrt{\Delta g D^3}\frac{7A}{10}S^{-\frac{10}{7}}\left(AS^{\frac{7}{10}} - \tau_c\right)^{a-1}\frac{\partial S}{\partial x} \tag{4.7}$$

$$S = -\frac{\partial \eta}{\partial x} \tag{4.8}$$

Where:

S Bed slope (channel gradient)

$\frac{\partial \eta}{\partial x}$ Partial derivative of bed surface elevation with respect to x

The negative sign indicates that S represents the slope in the direction of increasing x, commonly associated with downstream flow. In the Exner equation, the bed slope is a key parameter influencing sediment transport and bed morphology.

Substituiting value of S we get:

$$\frac{\partial q_b}{\partial x} = \Gamma\sqrt{\Delta g D^3}\left(\frac{7A}{10}\left(-\frac{\partial \eta}{\partial x}\right)^{-\frac{10}{7}}\left(A\left(-\frac{\partial \eta}{\partial x}\right)^{\frac{7}{10}} - \tau_c\right)\right)^{a-1}\frac{\partial^2 \eta}{\partial x^2} \tag{4.9}$$

Then, the equation can be compared with the non-linear parabolic equation integrated with the exner equation:

$$\frac{\partial \eta}{\partial t} = F\left(\frac{\partial \eta}{\partial x}\right)\frac{\partial^2 \eta}{\partial x^2} \tag{4.10}$$

Where:

$$F = -\Gamma\frac{a}{1-p}\sqrt{\Delta g D^3}\left(\frac{7A}{10}\right)\left(-\frac{\partial \eta}{\partial x}\right)^{-\frac{3}{10}}\left[A\left(-\frac{\partial \eta}{\partial x}\right)^{\frac{7}{10}} - \tau_{*c}\right]^{a-1} \tag{4.11}$$

$$(1-p)\frac{\partial \eta}{\partial t} = -\frac{\partial q_b}{\partial x} \tag{4.12}$$

The Exner equation is a one-dimensional morphodynamic equation that is widely utilized in investigations of fluvial geomorphology and sediment transport. It represents the temporal history of a river's or channel's bed surface elevation (η) as a result of sediment transport and deposition processes.where (p) represents the porosity of the riverbed and $-\frac{\partial q_b}{\partial x}$ is the negative partial derivative of the bedload sediment transport rate with respect to the horizontal coordinate. It accounts for the transport of sediment within the river, influencing the bed surface elevation. The Exner equation was used and integrated with the sediment transport formulae in numerical models to simulate and analyze the evolution of riverbed profiles over time under the influence of sediment transport processes.
Adopting the Engelund and Hansen formulae where:

$$a = \frac{5}{2}$$

$$\Gamma = 0.05C^2$$

$$\tau_{*\mathrm{c}} = 0$$

where the conductance (c) :

$$c = 6.74\left(\frac{h}{D_{50}}\right)^{1/6} \tag{4.13}$$

and the flow depth (h):

$$h = \left(\frac{D_{50}^{1/6} q}{6.74} \right)^{3/5} (9.81S)^{-3/10} \tag{4.14}$$

Providing the parameters such as grain size distribution was taken calculated before with basegrain software 125.5mm, the width was calculated taking the mean value of the channel in 116 sections that were already state and the width calculated was 76.05m, unitary discharge was calculated as $(Q - threshold)/width$, conductance and flow depth and slope in all the above equation and solving the non linear parabolic equation with the pdepe function in MATLAB provides the geomorphic evolution of the river bed.

Firstly, the terrain profile can be extracted from the DTM that was calculated in section 3. Along with this, the DTM provided by Emilia-Romagna surveyed in 2015 helped to generate the longer section. where, the river profile was divided into 162 sections, the average of each traverse section provide the points for the profile as shown in figure below:

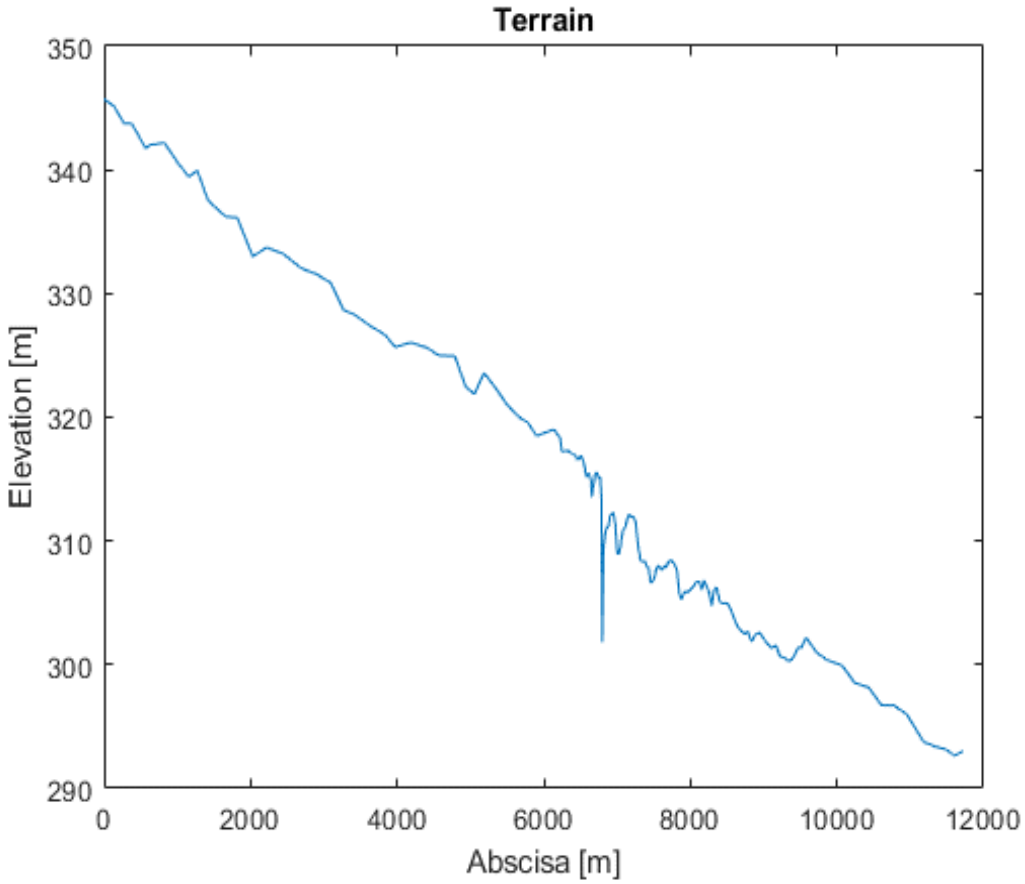

Figure 4.4: Terrain profile

The PDEPE function in MATLAB as in the format; pdepe(m, @pdefun, @icfun, @bcfun, xmesh, tspan) where the initial condition, boundary condition and the PDE itself are to be determined.

- **Initial Condition(icfun):** The initial condition for the pdepe function was the profile of the terrain that was extracted from the DTM as well as the smoothing with different interpolation such as linear interpolation, moving mean smoothing and spline interpolation function can be performed.
- **PDE function:** The parabolic equation mentioned earlier with the function that depends on $\frac{\partial \eta}{\partial x}$ that needs to be solved was used.
- **Boundary Conditions:** Upstream and Downstream boundary condition that should

be introduced in pdepe function was to be taken from the terrain profile of end upstream point and end downstream point.

Furthermore, due to the complexity having the bypass near the dam for morphological simulations, the flow that just overpasses the dam (threshold discharge) and the flow that fills the bypass channel was important which can be obtained through the 1D hydrodynamic simulations.

4.3 2D Hydrodynamical Model

The 1D HEC-RAS model has already been built as in earlier section, therefore the work was expanded to the 1D/2D environment. The HEC-RAS 6.4 is completely solved using the 2D Saint-Venant equation.It simulates flood by solving shallow water equations, which show the motion of water as depth-averaged 2D velocity and depth in line with the forces of gravity and friction. Continuity equation:

$$\frac{\partial \zeta}{\partial t} + \frac{\partial p}{\partial x} + \frac{\partial q}{\partial y} = 0 \tag{4.15}$$

Momentum equations:

$$\frac{\partial p}{\partial t} + \frac{\partial}{\partial x}\left(\frac{p^2}{h}\right) + \frac{\partial}{\partial y}\left(\frac{pq}{h}\right) = -\frac{n^2 p g\sqrt{p^2+q^2}}{h^2} - gh\frac{\partial \xi}{\partial x} + pf + \frac{\partial}{\partial x}\left(h\tau_{xx}\right) + \frac{\partial}{\partial y}\left(h\tau_{xy}\right) \tag{4.16}$$

$$\frac{\partial q}{\partial t} + \frac{\partial}{\partial x}\left(\frac{pq}{h}\right) + \frac{\partial}{\partial y}\left(\frac{q^2}{h}\right) = -\frac{n^2 q g\sqrt{p^2+q^2}}{h^2} - gh\frac{\partial \xi}{\partial y} + qf + \frac{\partial}{\partial x}\left(h\tau_{xy}\right) + \frac{\partial}{\partial y}\left(h\tau_{yy}\right) \tag{4.17}$$

Here, ζ represents the water surface elevation, p and q are the velocity components in the x and y directions, respectively, h is the water depth, n is the Manning's roughness coefficient, g is the acceleration due to gravity, ξ represents the bed elevation, f is the Coriolis parameter, and τ_{xx}, τ_{xy}, and τ_{yy} are components of the shear stress tensor.
Two-dimensional models was used to observe and predict spatially distributed, flood maps.

In this case, a 2D hydrodynamic model integrated with the storage and connected to flow area with the help of culvert was modelled in order to simulate the bypass present. ft

Inputs and Parameters

Beginning with the previously generated DTM, a precise 4m x 4m computational mesh was created, including break lines and a refinement area. The flow area was connected using Storage region/2D Flow Area connections (SA/2D Area Conn). The storage area's size was assumed to hold the volume of water passed from the flow area during the simulation. Inflow in the storage area was the important parameter that was used as the lateral hydrograph in the outlet of bypass, which helps to simulate the bypass in this research. This SA/2D Area connection used the advanced culvert connection type, which was made more efficient by utilizing the 1D model's existing culvert editor. To draw the culvert, first, the center line of the barrel was drawn with the convention from the upstream side to the downstream side.

After the mesh generation and SA/2D Area Connection, the boundary condition, at the upstream and downstream and the lateral boundary condition near the outlet of bypass was imposed.The upstream boundary condition was taken the hydrograph with the constant discharge of different return years, the lateral hydrograph was the inflow in the storage area whereas for the downstream boundary condition the terrain slope was taken into account.

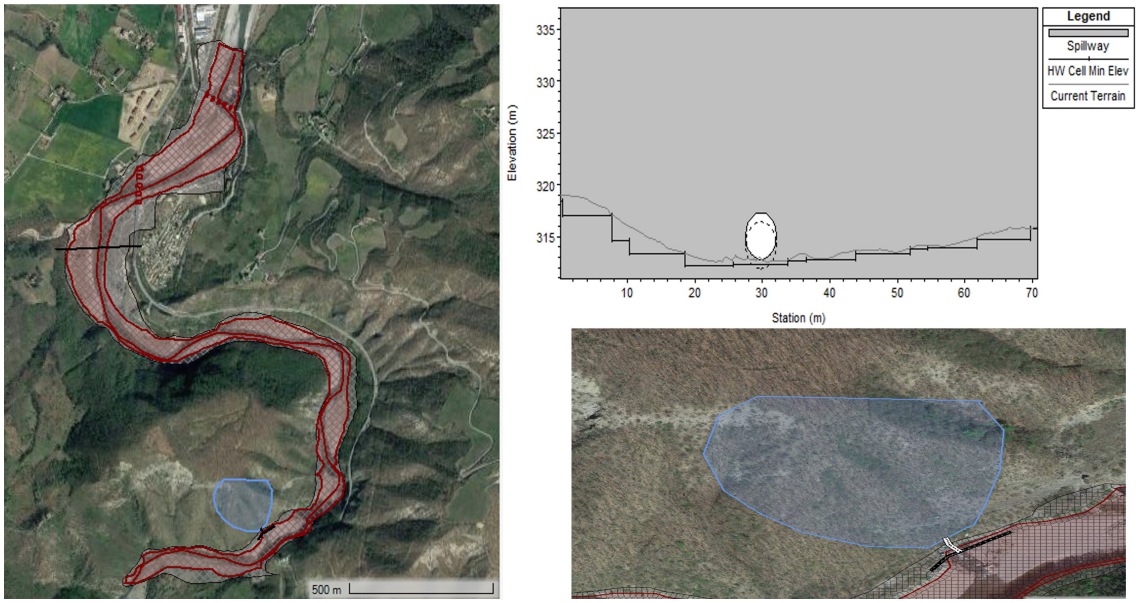

Figure 4.5: Left figure shows the geometrical properties of the model. Right top figure shows the culvert imposed and the right bottom shows the connection between the flow area and the storage area

The Manning roughness was used as per the classification of the Corine land cover, which was classified as open water(0.030), Aquatic bed(0.030), shrubs (0.040), and trees(0.045) as per Chow(1959) in the interested region. Variable time step courant number has been taken whereas the maximum courant number was 0.7, minimum courant number as 0.3, and a number of steps below Minimum before doubling as two that ensured the stability of the model.Finally, the time step of 1hr was taken into account and simulated for 35 hours during different return period discharges.

The simulation was done for two different scenarios. First, the whole DTM acquired through the drone was selected, and flood mapping was assessed, which shows the area that could be affected during different flow conditions. Second, only the DTM downstream of the dam was selected in order to see the changes in the downstream side due to the sediment transport after dam removal.

The study is more focused on the second case, as the sediment volume calculated from

the 1D morphodynamical analysis was used to see the changes in the flood plain in the downstream area. This sediment transported downstream was uniformly distributed to the flooded area and the DTM was modified considering the changes in terrain due to the increase in depth after sediment deposition. This helps to access the risk of inundation in the human settlement areas in the downstream.

The DTM collected with the help of the drone was for the limited region, the additional DTM was used that was provided by the Emilia -Romagna. As this DTM covers large area in this region, which would be very effective to observe the flood inundation impacts in the downstream of dam. The similar methodology that was performed in the previous DTM was implemented in this case.

Chapter 5

Results and Discussion

As stated in chapter 4, one dimensional simulations in HEC-RAS was done taking into account the different year return period discharges. In order to observe the relation between the flow between the bypass called lateral structure and the dam as inline structure, multiple simulation have been performed. Although the primary focus was to find out the threshold flow value that overpass the dam so that it can be used for the morphodynamical simulations, the spatial depth and velocity changes was also observed to the downstream in different extreme events.This also helps to know the flood mapping downstream in presence of the dam at different return periods.

The constant hydrograph with 5,10,20,50,100 and 200 return periods discharges.In this model the inline structure flow stability factor has been raised to 3 that helped to dampen the higher oscillations of energy slope occurred during the simulation.In addition under the htab parameter function the points were increased to 500 and Starting Elevation was set as the minimum channel elevation by pressing copy invert.The discharge through the bypass was again used as an lateral hydrograph in this case.The flow in the river and bypass channel after the several simulations has been observed as below:

Discharge in River(Q_{riv}) [m^3/s]	Discharge from culvert(Q_{cul}) [m^3/s]
10	10
20	15.28
50	21.17
100	27.41
120	29.39
200	34.59
500	43.5
1000	51.88
1383.9	56.51
1855.5	61.11
2396.4	65.45
3268.3	72.05
4091.1	78.16
5102.9	85.02

Table 5.1: Discharge in river and culvert

During the simulation process, the hydrograph with small discharge was used and at a small discharge most of the river discharge flow through the bypass channel. After increasing the river flow, the increment in the flow of bypass channel was also observed as shown in the Table 5.1. During the simulations, the overflow that exceeded the dam height, reaching a notable $120 m^3/s$ was observed and larger than this flow it was estimated that the river flow is divided into bypass channel flow and the flow that overpass the dam.However, at this discharge level, the bypass channel did not reach full capacity.

The bypass channel functions similarly to a pressure pipe when the flow rate surpasses $150 m^3/s$. The major goal of this simulation series is to calculate the distribution of discharge values between the bypass channel and the riverbed (dam overtopping). This knowledge is critical to understanding sediment movement in morphodynamic simulations. Given the sediment-filled upstream portion of the dam, it is clear that only discharges

that surpass the dam overtopping threshold may successfully carry silt downstream. This discovery expands our understanding of sediment dynamics, as even after the dam removal the upstream of dam filled with sediment would be transported only the discharge larger than the threshold discharge. The Figure 5.1 shows examples of simulations,

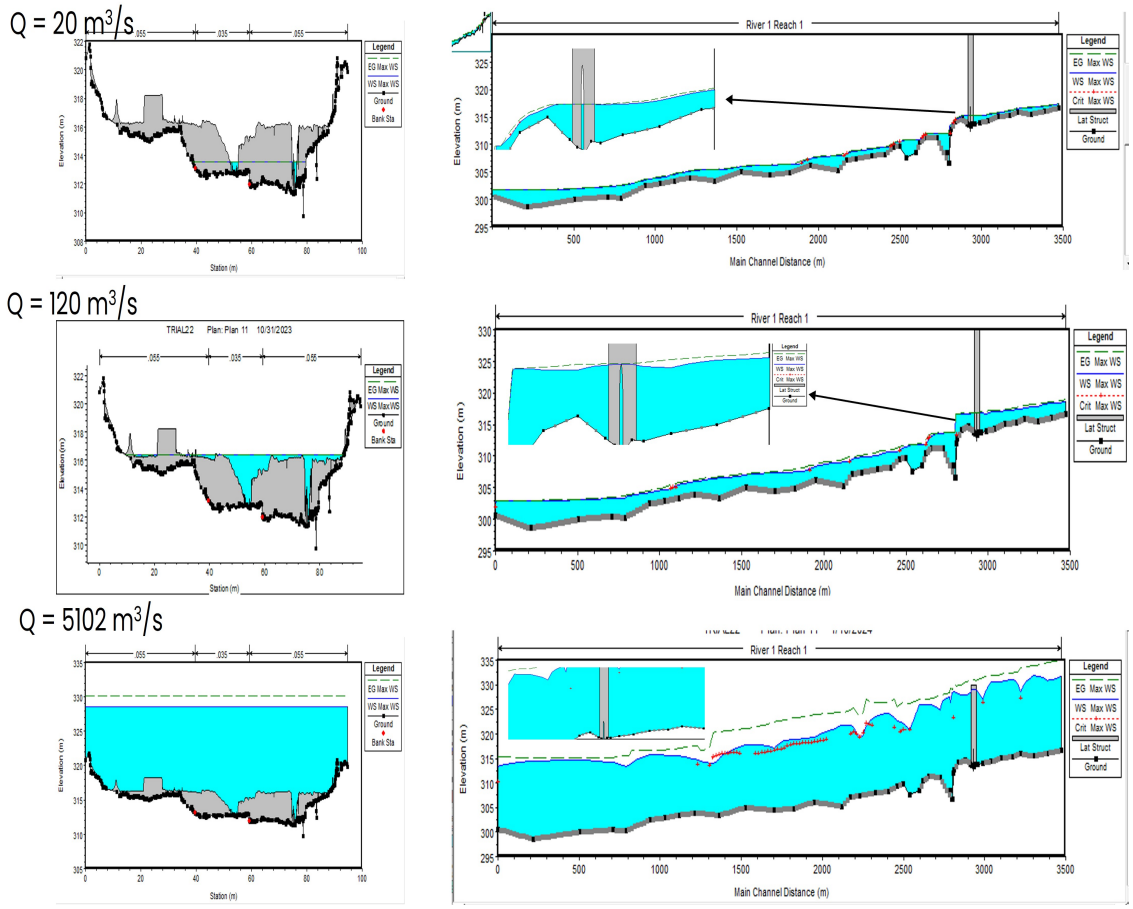

Figure 5.1: Discharges at Dam and lateral bypass channel during different discharges

A important relation have been derived between the discharges of the dam and bypass channel after performing the different simulations. The power-law relationship is a mathematical form that describes a functional dependence between two variables, typically expressed as $y = a \cdot x^b + c$. Additionally, parameters of the power-law model can be estimated from empirical data, and the resulting model can be used for predictive purposes. For example, predicting the flow rate of water through a culvert based on the

river discharge. In this case, the scaling factor a was calculated as $a = 10.81$ with a 95% confidence interval of $(5.132, 16.5)$ and $b = 0.248$ with a 95% confidence interval of $(0.1972, 0.2989)$ that represents the rate at which the culvert discharge changes concerning changes in river discharge and $c = -7.414$ with a 95% confidence interval of $(-17.08, 2.248)$ which is a constant term as a baseline. These coefficients and the model as a whole can be used to predict or simulate culvert discharge based on different levels of river discharge that can help in future detailed research as well.

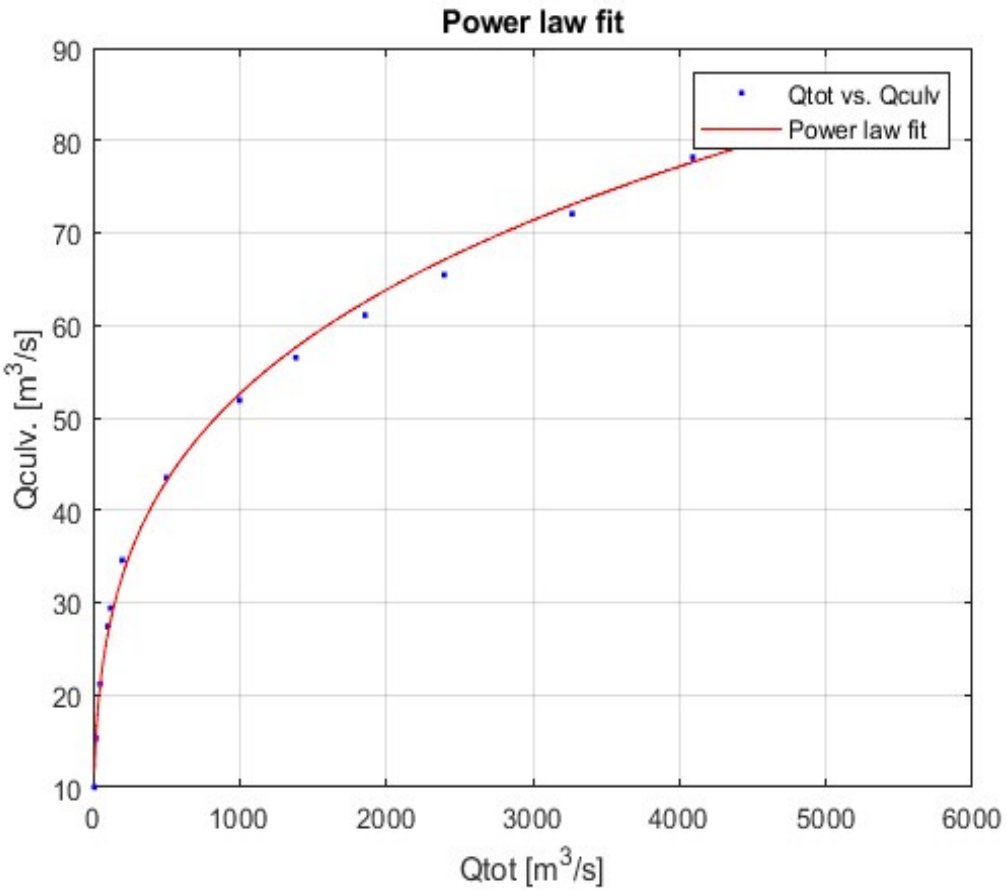

Figure 5.2: Relation between the discharge in river and the discharge in bypass channel

The threshold discharge of $120 m^3/s$ is the important parameter for the geomorphological simulation. 1-D morphodynamical simulation was performed considering the threshold value and for the 10 years of time frame to observe the evolution of river bed and sediment

transport. The two scenarios has been assessed. First, the geomorphic evolution of river bed and volume of sediment transport has been calculated without considering the bypass and secondly, the realistic scenario considering the bypass was evaluated. In both the cases the maximum sediment deposited were observed in the 500m upstream of the dam and same length of the profile was taken into account for the analysis of transport of sediment. For the first scenario, the instant dam removal was considered and the bypass was not taken into account. The mean daily discharge data as already calculated in section 3.2 was used and moving window of 10 years starting from the year 2005 with 9 simulation windows were taken as shown in Figure 5.3

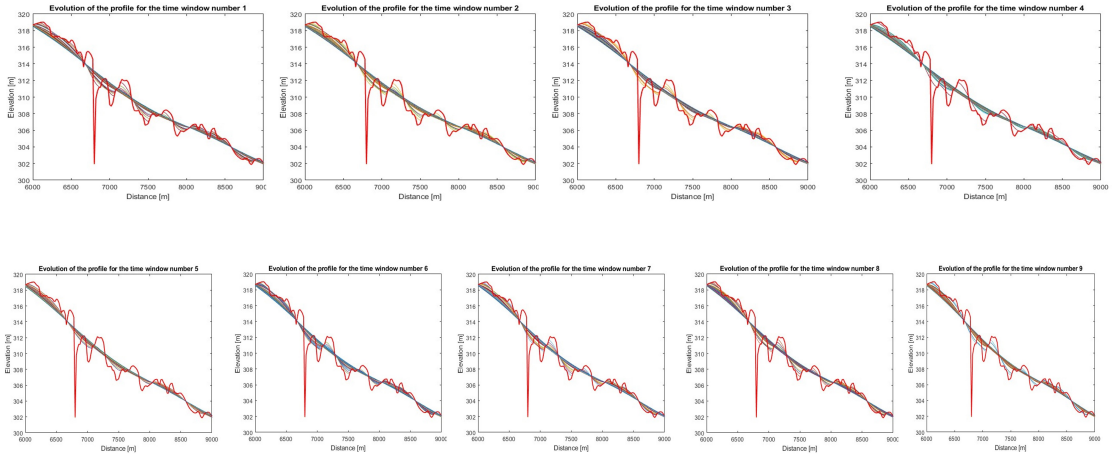

Figure 5.3: Figure above shows the 9 windows of simulation taking 10 years of data at each window for evolution of river bed without considering bypass

The change in geomorphic elevation in each window was seen higher during the initial stage however was reduced significantly afterwards.The average profile from the 9 simulation window was considered to calculate the final profile which is shown in Fig. 5.4(a). Furthermore, it has been seen that change in elevation near the dam was considerable and area shows the aggradation and degradation in that area as shown in figure below. Additionally, the amount of sediment transport considering the bypass was higher for first year and decreases significantly afterwards as shown in figure 5.4(b). Finally the cumulative volume has been calculated was 44753 m^3/s as shown in figure 5.4(c).

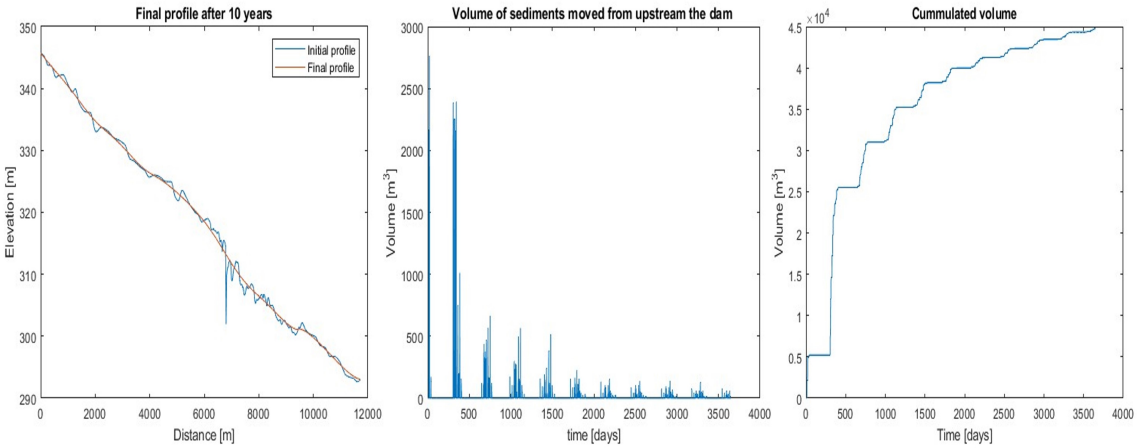

Figure 5.4: Figure in left 5.4(a) shows initial and final profile of the riverbed, figure in middle 5.4(b) shows the sediment transport in time and figure in right 5.4(c) shows the cumulative sediment transport for 10 years without considering bypass.

Similarly, for the second scenario considering the bypass during the simulation the different 9 window was taken containing 10 years in each window as shown in figure below.

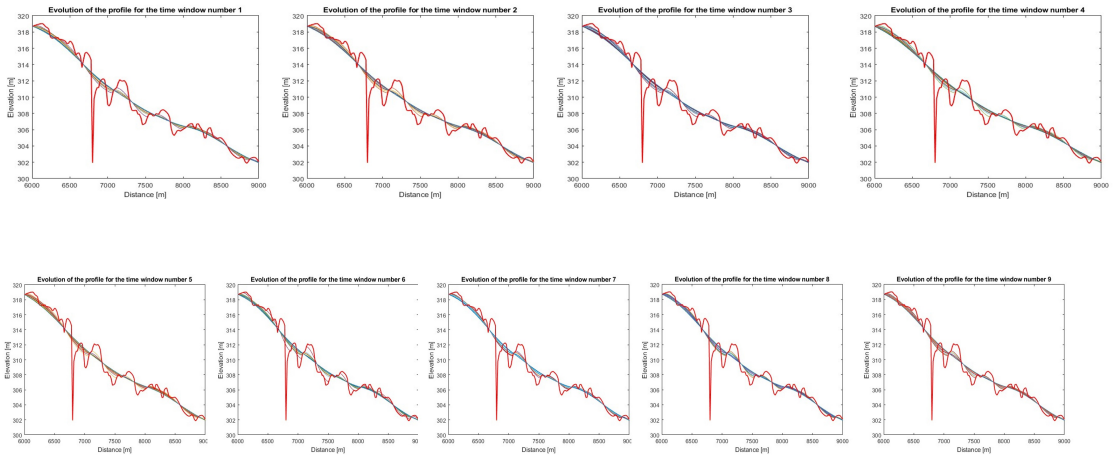

Figure 5.5: Figure above shows the 9 windows of simulation taking 10 years of data at each window for evolution of riverbed considering bypass

The profile of riverbed considering the bypass before and after dam removal has been shown in Figure 5.6(a) and the sediment transport in time has been shown in Figure 5.6(b) where it has been seen that the sediment transport has been higher for few years and then decreases afterwards. Also the cumulative volume as shown in figure has been calculated

in Figure 5.6(c).

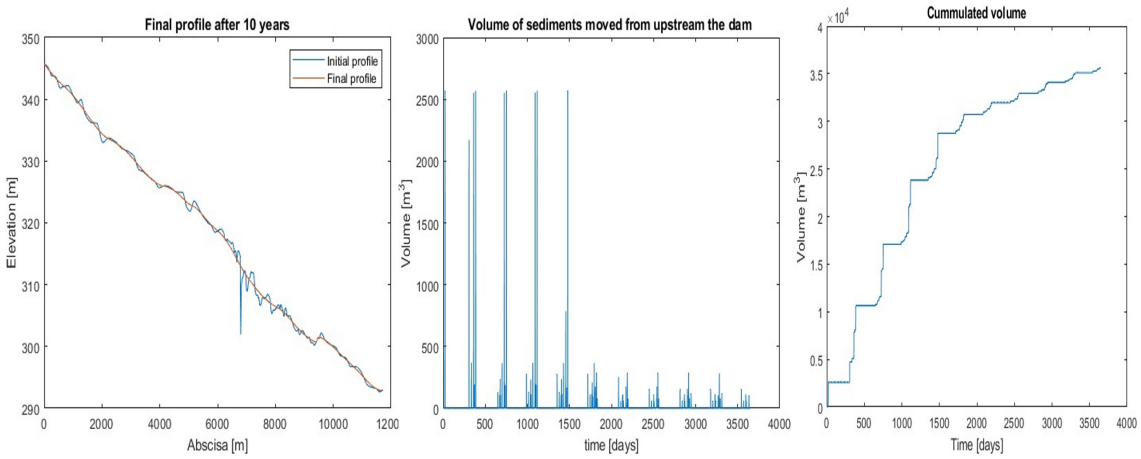

Figure 5.6: Figure in left 5.6(a) shows initial and final profile of the riverbed, figure in middle 5.6(b) shows the sediment transport in time and figure in right 5.6(c) shows the cumulative sediment transport for 10 years considering bypass

In both the scenario it has been depicted considerable variations in bed elevation over certain years, and then decreases in following years. The sediment pulse propagation in both the cases was observed as similar to two phase model where during the initial phase the large sediment is transported following to transport limited condition. However, the differences in the initial propagation phase in the first scenario without considering bypass and the second scenario with considering bypass shows that the presence of bypass in the river channel has its impacts on sediment transport and temporal variation in sediment pulse propagation in Trebbia river. To represent the realistic case in Trebbia river containing bypass the results from second scenario has been taken for further analysis. Notably, downstream aggradation and upstream degradation occurred near the dam, resulting in a quasi-equilibrium state caused by sediment transfer from upstream to downstream. The simulation of riverbed alterations concentrates on the bypass portion between the outflow and inlet, which activates when the discharge exceeds $120m^3$, suggesting a crucial threshold for investigation in the dam section.

Furthermore, the volume of sediment moved downstream peaked in the first four years,

followed by a significant reduction, highlighting the importance of sediment transport in the early stages. The cumulative volume of $35645m^3$ shown in the above figure illustrates this tendency. Additionally, the amount of the downstream pool near the dam, which is critical for sediment trapping during transport, was calculated as $12143.15m^3$. As discussed earlier in section 2 there is human settlement in the Bobbio town downstream which could be affected by the increase in flood due to the transport of sediment. For this reason, the 2D hydrodynamic simulation was performed to show how the depth of flow changes after the transportation of sediment.

The 2D hydrodynamic simulation was carried out under present circumstances to determine the downstream flood implications. Unfortunately, the Digital Terrain Model (DTM) developed does not cover the full Bobbio region, nonetheless, the impact of floods at different return times has been closely monitored. The analysis shows that, even in the current scenario, without considering dam removal and sediment transport the right bank at Bobbio Beach Ponte floods during the Q200 return period. Furthermore, the depth of flow has increased significantly throughout the Q200 return period, increasing up to 10 meters from the initial level near the bridge and shown in Figure 5.7. During different return periods such as Q5, Q20, Q100 the maximum depth observed was 4.8m,6.6m and 9.2m at the location near the bridge shows the substantial increase in depth of flow during higher return periods. With that increase in depth, houses in the right bank seems to be inundated. This analysis was done to access the condition during the extreme flood condition even without considering dam removal. So it could be anticipated that, there might occur some adverse effects due to the sediment transport after dam removal at this stage. Not only this, the analysis showed the applicability of 2D/Storage area connection effectively to generate the inundation map, flood velocity, depth in this kind of complex geometry simulating the bypass.

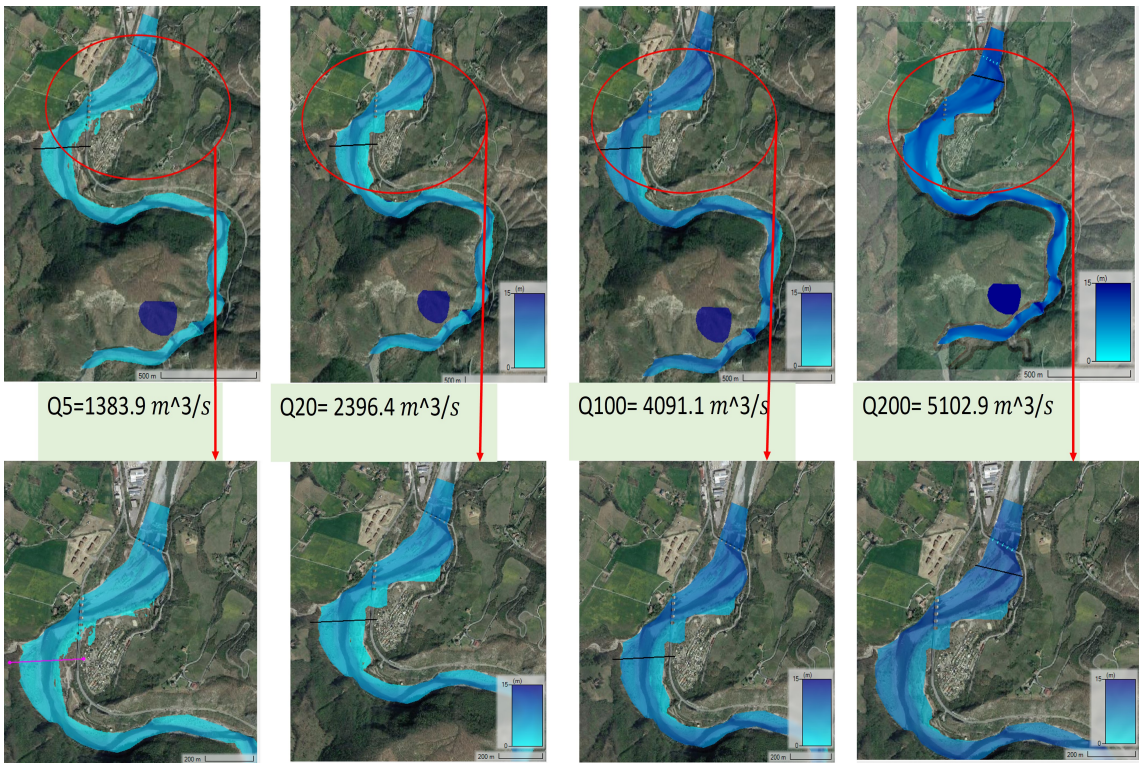

Figure 5.7: Flood mapping during different return periods

As discussed earlier, the volume of sediment transport was already calculated and the river bed profile after the dam removal has been obtained through 1D morphodynamical numerical simulations. However, this simulations lack the capacity to offer a detailed spatial overview of the study area. To address this constraint, a supplemental 2D hydrodynamic analysis was conducted, focused on the flood-prone area downstream of the dam. The flooded area was determined using 2D hydrodynamic modeling with a return period of 200 years, as shown in Figure 5.9. First the flood map, was exported from the HECRAS in QGIS and masked with the full DTM.The sediment computed above was divided by the total area i.e.305842m^2 to determine the change in bed elevation of the Digital Terrain Model (DTM), amounting to 12cm and elevation of the selected flood section was increased with 12cm as shown in Figure 5.8. After that the increased elevation masked raster is then merged with the full raster to obtained a new DTM that was used for HECRAS to obtain the flood map results after increasing the elevation due to sediment deposition after dam removal.

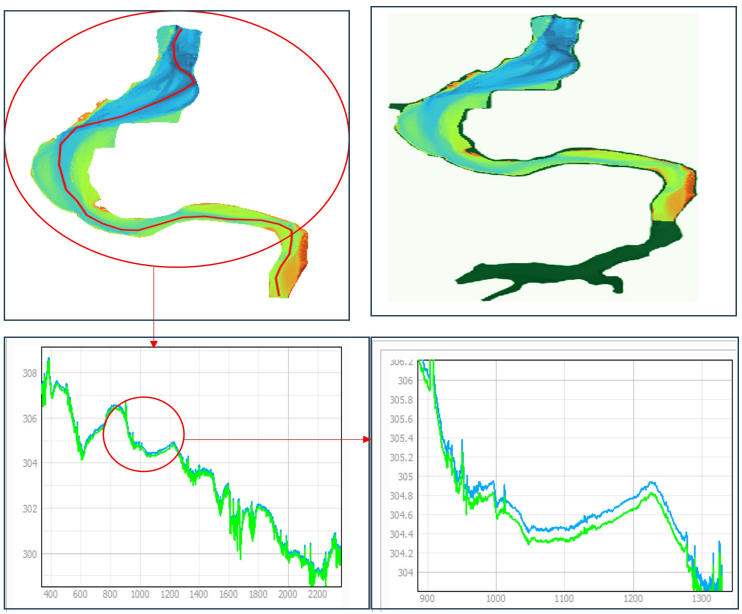

Figure 5.8: Figure on top left shows the flood map extracted from the HECRAS results in 200 year return period,Figure on top right shows the merged layer after changing the elevation of the flooded map section and figure below shows the profile after increasing elevation

The following Figure 5.9 shows the flooded area after the modified DTM after post dam removal condition. It is crucial to note that these simulations are based on the assumption of a single-stage dam removal, and the volume of the pool immediately downstream of the dam which has a volumetric capacity of 12143.15m^3 has not been taken into account. These assumptions were made to simulate the most critical case for a thorough study.Also, in this case the smaller DTM section was taken and only 12 cm change has been observed and it is very small change in such a small section. As shown in Figure 5.9., the change in the flow depth of the flooded areas in downstream with Q200 return period before and after the dam removal was less than 10 cm in most of the areas.

Even assuming the worst-case scenario, in which no sediment deposition occurs in the aforementioned pool, and with such a small DTM section the data show that the rise in water levels downstream is not particularly substantial.

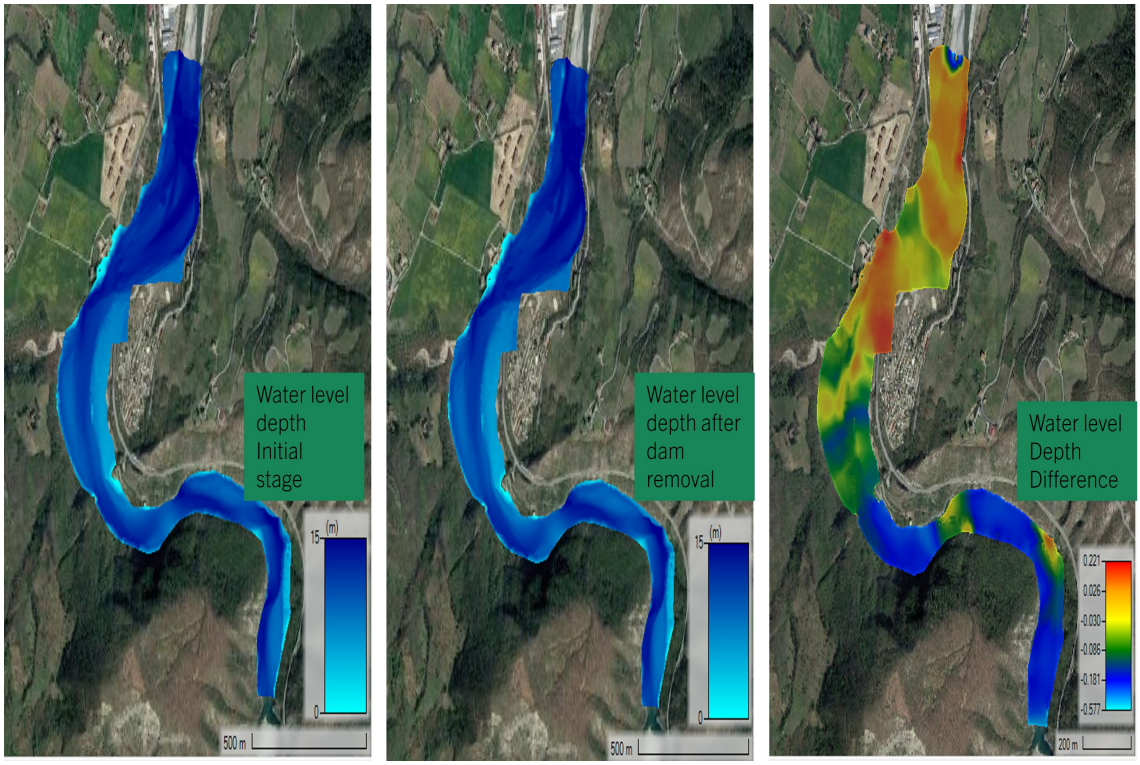

Figure 5.9: First figure shows the flood mapping in downstream of dam before considering dam removal and second figure shows after dam removal and the third figure shows the difference between the two cases

Similarly, the terrain that include the large section was also evaluated in this study. The DTM was provided by the Emilia-Romagna region. Additionally, the DTM was then smoothed with the SAGA Gaussian filter. As, this DTM includes the large area and covers the Bobbio town where the human settlement is high, potential flooding has been depicted in that area during higher return period after the hydrodynamic modeling as shown in figure. In this case, the similar methodology was conducted as before and the flooded area during Q200 return period was calculated as $1062481.69m^2$. And again dividing the sediment transported in the flooded area results in the 3.3 cm change in elevation.Figure shows the difference in the water depth in the two scenarios before and after the dam removal. The change in the depth of water level was seen with maximum 4 cm after the sediment deposition. Furthermore, this change was seen in very few areas whereas most of the areas contains even smaller change.

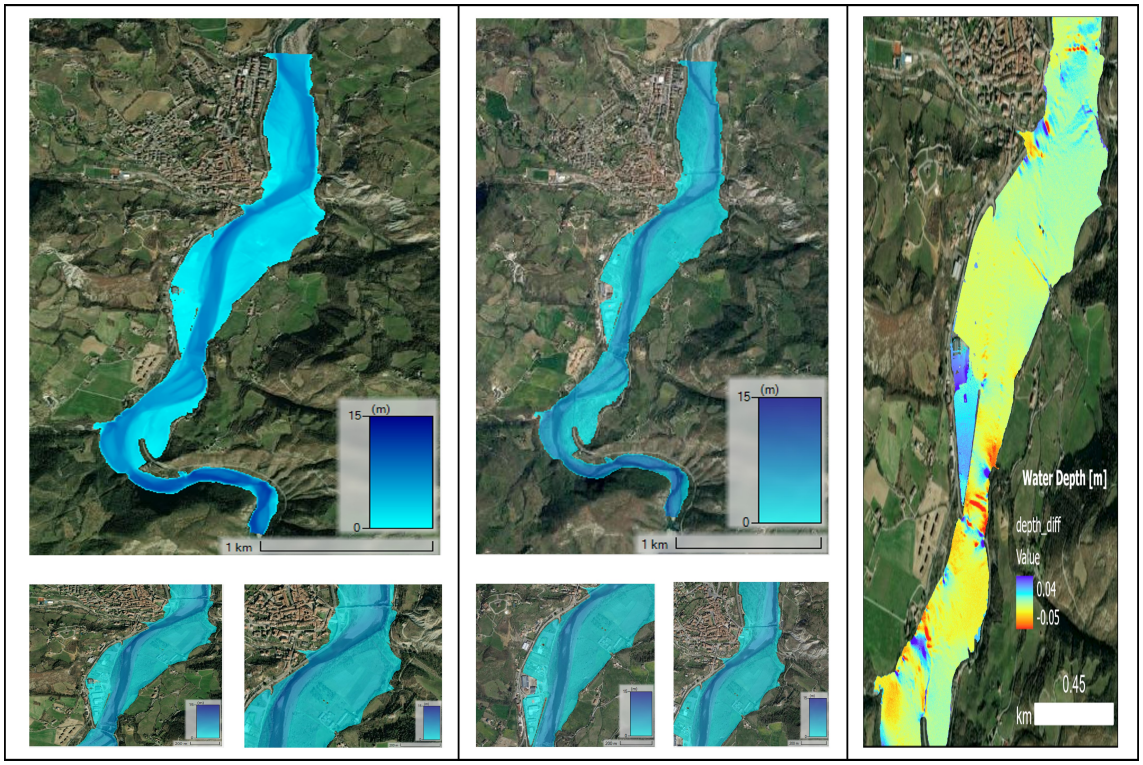

Figure 5.10: Figures in first and second column shows the flooded areas before and after considering dam removal and figure in third column shows the difference between two cases

The results obtained after the simulations considering two different DTM also shows the minimal change in the flow depth after the dam removal. As was expected, this results bolster the fact that there is insignificant effects in the downstream settlement after the sediment transport. The amount of sediment transported is quite low even without considering the pools and depression along the downstream of the channel. Although the through knowledge of the volume of sediment that can be stored in these pools needs very detailed analysis, the profile of the terrain shows the number of depressions and pools that can store sediments. The results obtained from the morphological analysis are of great importance as that shows the time frame of around four years is critical as the sediment transport is large comparing to the following years that could have some impacts to the ecological habitats in the downstream, however the ecological aspects can be expected to recover after these few years effects as it depends on the types of ecological habitats

downstream that needs further detailed analysis.

Starting from the complexity attributed due to the presence of bypass just upstream the dam and the relation between the dam and bypass with the discharge threshold value of $120m^3$ also caused the sediment transport last longer for four years and affected the geomorphic evolution of river bed. Although the cumulative volume of sediment transport was taken into account, if the sediment transport each year was taken the effects to the downstream would have much less.

This results shows that the San Salvatore dam removal in the Trebbia has less effects in the downstream and the sediment transported have short-term effects in the geomorphology of the river and the flood risk to the settlement downstream. This feasibility analysis of the pre and post-removal geomorphic assessments revealed that the majority of the geomorphic alterations occur within a short period of time, driven mainly by the initial base level modification - an observation common to dam removals elsewhere, indicating that post-removal long-term sediment production may not occur or may impair downstream geomorphic and ecological stability.

Although, there could be some impacts in the ecosystems due to the migration of sediments after dam removal can leading to a drop in fish habitats and changes in sediment dynamics may disturb riverbeds, affecting spawning sites and interfering with the overall ecological balance required for fish survival however the case is different in this study as very small volume sediment transport has been depicted and this volume of sediment could have minimal impacts for those species. In addition, some positive impacts could occur in resident fish and at-risk species and would have better access to formerly inaccessible habitat, and the restoration of sediment flow would most certainly aid the formation of critical fluvial habitats downstream.

These findings in this feasibility study are significant given the rising number of dam removals over the previous decade in different part of the world. To fully comprehend the influence of dam removal on river geomorphology and its impacts downstream, it's crucial to collect post-removal data and validate the findings of this study in this particular river.

Chapter 6

Conclusion

Over the last several years, academics have focused more on the potential usefulness of dam removal in river restoration. The expanding number of scientific research gives a significant opportunity for learning how to better manage watersheds and increase our grasp of the science of river restoration. To this end, feasibility study was carried out starting from the initial phase of data acquisition and the hydrodynamic and morphodyanamical simulations has been performed to produce some important results that bolster the decision making in the dam removal and river restoration in Trebbia river in this dissertation.

Initially, the parameters needed for hydrodynamic and morphodyanmic analysis were calculated such as grain size and distribution using the Matlab-based object detection software called BASEGRAIN, different return period discharge were calculated through statistical method of return period analysis, drone data acquisition was done to generate high resolution digital terrain model using CLOUD-COMPARE software.

The study included a comprehensive analysis taking into account the bypass that connects the dam's upstream and downstream zones. The discharge threshold was determined using one-dimensional hydrodynamic modeling in HEC-RAS. This also addresses the first research questions of finding the threshold value that overpasses the dam. Notably, it was determined that exceeding a certain threshold value is required to transport sediment present immediately upstream of the dam under such conditions. Furthermore, the study used 1D morphodynamic modeling using threshold discharge and the results showed that

the cumulative volume of sediment transfer in 10 years following dam removal was negligible. The results also showed that in the presence of bypass, the sediment transport resembled those observed in the staged dam removal condition-with the certain amount of sediment transported each year during when the discharge overpass the threshold discharge. During the first four years, the geomorphic evolution of river bed was high comparing with the following years, however after that period the change in river bed was unnoticeable suggesting that the San Salvatore dam removal have effects for few years in the geomorphic evolution of river bed. This results also allowed to answer the second research question.

To further investigate, 2D hydrodynamic modelling in HECRAS was performed in two steps. First, the flooded area was calculated in 200 year return period discharge and the elevation that needs to be added to the flooded area was calculated with the ratio of sediment transport volume by flooded area.The total volume of sediment calculated was uniformly distributed along downstream area to resemble the worst case scenario assuming that all the cumulative sediment transported downstream at once. And secondly, again the 2D hydrodynamic simulation was conducted with elevation changed DTM to see change in the flood area and the flow depth to the downstream. The results indicated a modest increase of only 12cm and 4cm in flow depth for both smaller and larger Digital Terrain Models (DTMs) selected, following sediment transport subsequent to dam removal. Importantly, the study found no significant spatial alterations in the flooded area.

In this feasibility study, it has been found that the geomorphic evolution of riverbed occurs only over few years transporting low amount of sediment and the effect of sediment transport to downstream Bobbio town regarding the flood risk was minimum after the dam removal. Due to sediment transport downstream after the removal of San Salvatore dam, it is believed that the aquatic habitat will be reconnected and the dam removal would also result in the restoring sediment budget downstream that would help native fish species by creating the gravel bars and substrates.Although more research is also required to understand linked biotic-abiotic responses to the removal of dams and to inform efficient and successful dam removal and restoration strategies in an array of physio-graphic contexts. However, detail analysis is required in terms of a cost benefit analysis in removing the dam

as well as long-term monitoring is important to fully understand ecological effects.Also,the study area is important from the recreational point of view, that needs to be well understood in consultation with appropriate regional agencies and in a public dialogue with residents in the area. In addition, different channel evolution model should be studied and validated regarding the geomorphological changes, forms and processes during pre and post dam removal condition.

Based on the fact that, the transport of impounded sediments following dam removal is not expected to result in significant downstream deposition and even most of the sediment would be trapped in pool just downstream of the dam. Finally, comparisons of "before" and "after" scenarios for dismantling the dam demonstrate that there is negligible change in terms of depth or lateral extent of flooding in the downstream suggest that the Free Trebbia River Project conducted by the Open rivers programme to remove the San Salvatore dam appears to be a commendable option for river restoration.

Chapter 7

Appendix

7.1 BASEGRAIN Analysis

Location and details are provided in details in Section 3.3.1

LOCATION: 200201

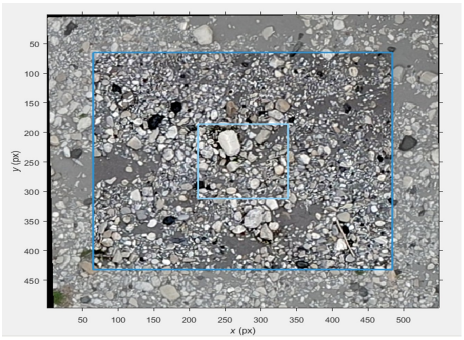

Fig. A200201

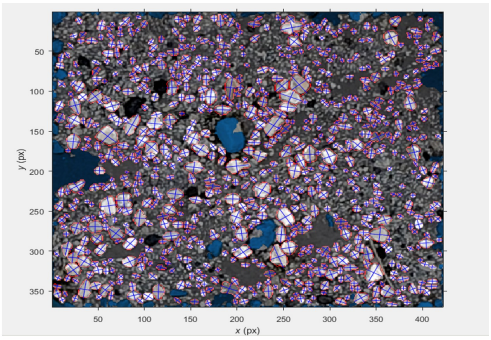

Fig. B

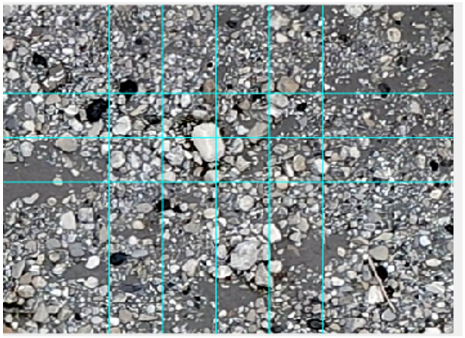

Fig. C

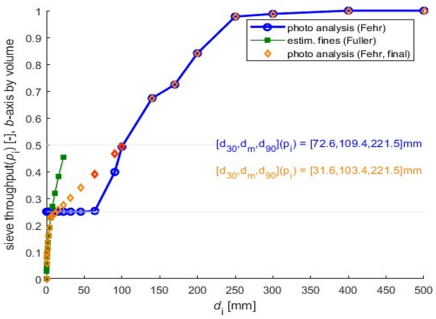

Fig. D

Figure 7.1: Figure shows the process GSD analysis in BASEGRAIN software. Fig A: Pre-processing of the raw image. Fig-B: Output of object detection after five steps processing. Fig-C: Analysis based on Fehr(1987), Fig-D: GSD curve by volume with calculated grain size diameter

.

LOCATION: 400401

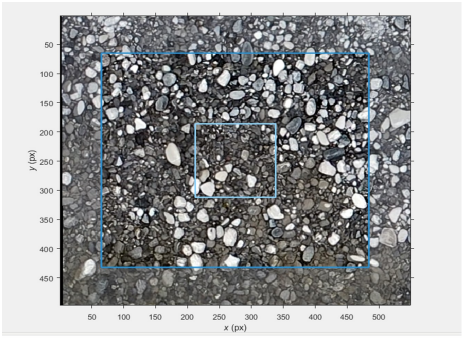

Fig. A

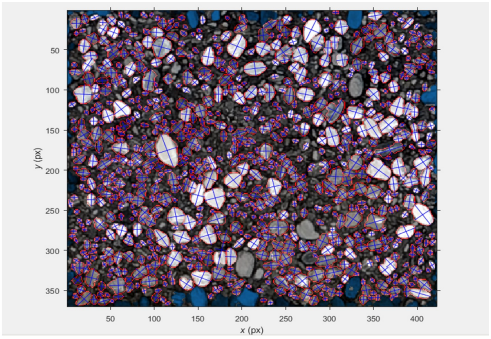

Fig. B

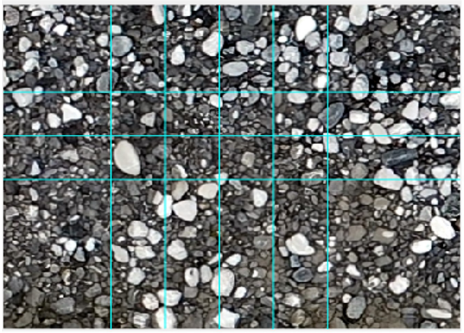

Fig. C

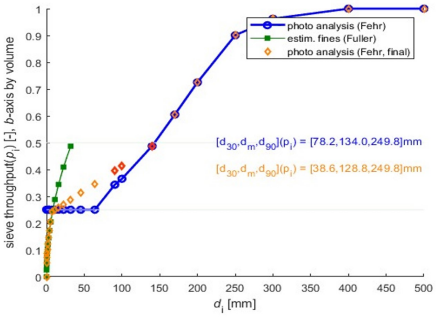

Fig. D

Figure 7.2: Figure shows the process GSD analysis in BASEGRAIN software. Fig A: Pre-processing of the raw image. Fig-B: Output of object detection after five steps processing. Fig-C: Analysis based on Fehr(1987), Fig-D: GSD curve by volume with calculated grain size diameter

.

LOCATION: 900902

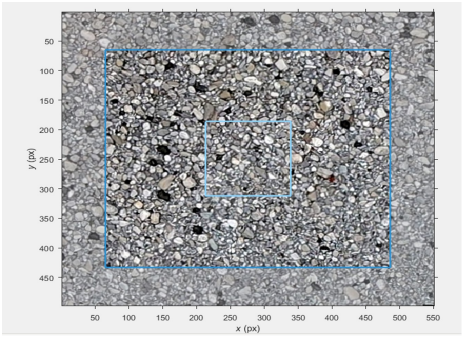

Fig. A

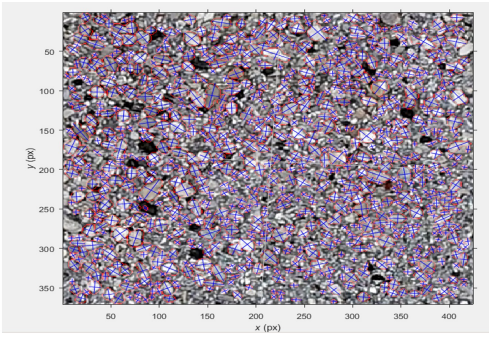

Fig. B

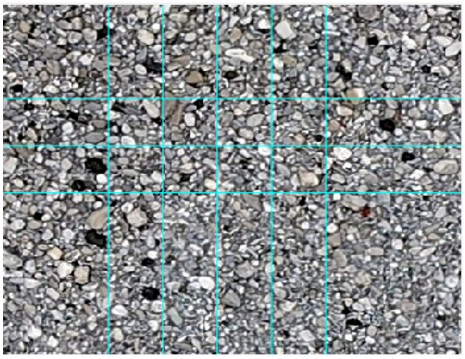

Fig. C

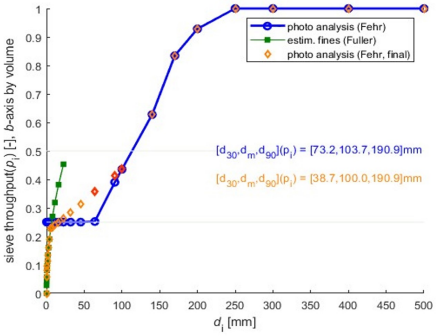

Fig. D

Figure 7.3: Figure shows the process GSD analysis in BASEGRAIN software. Fig A: Pre-processing of the raw image. Fig-B: Output of object detection after five steps processing. Fig-C: Analysis based on Fehr(1987), Fig-D: GSD curve by volume with calculated grain size diameter

.

LOCATION: 900903

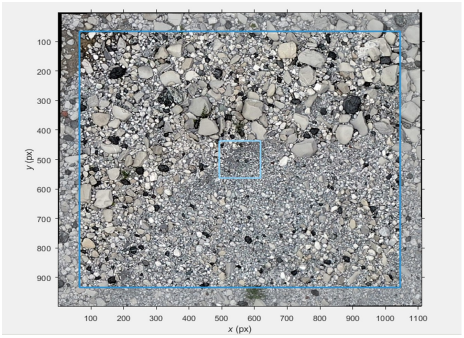

Fig. A

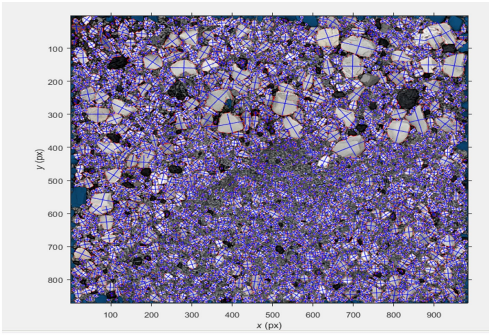

Fig. B

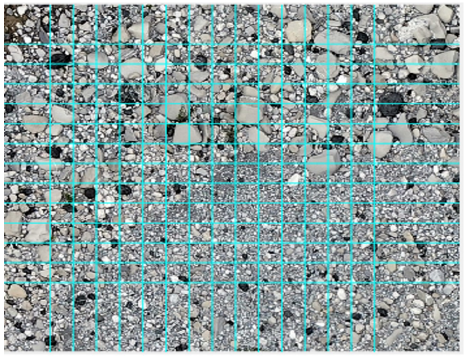

Fig. C

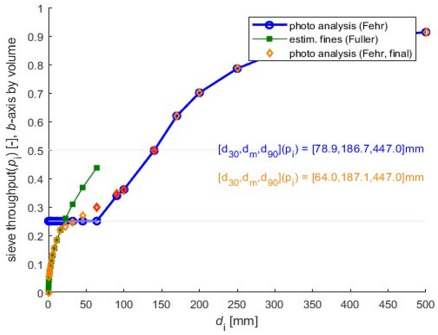

Fig. D

Figure 7.4: Figure shows the process GSD analysis in BASEGRAIN software. Fig A: Pre-processing of the raw image. Fig-B: Output of object detection after five steps processing. Fig-C: Analysis based on Fehr(1987), Fig-D: GSD curve by volume with calculated grain size diameter

.

LOCATION: 900906

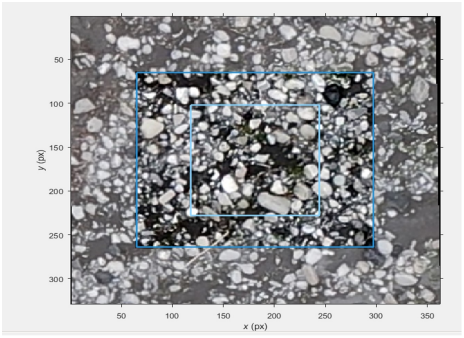

Fig. A900906

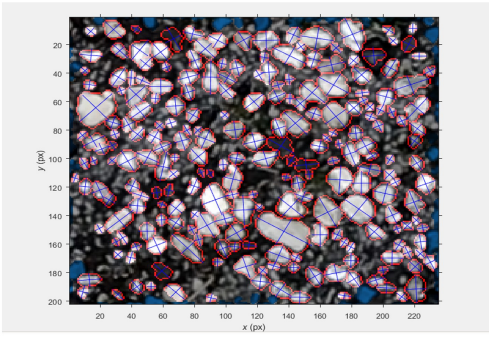

Fig. B

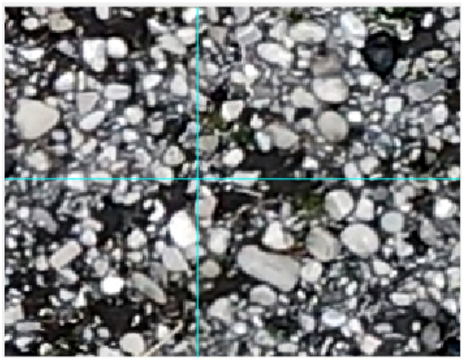

Fig. C

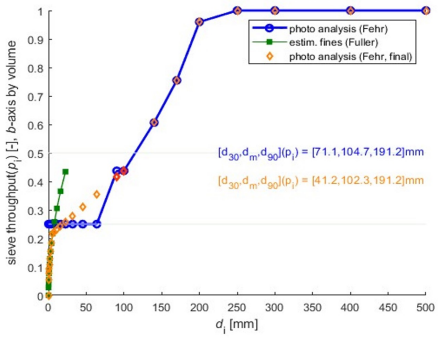

Fig. D

Figure 7.5: Figure shows the process GSD analysis in BASEGRAIN software. Fig A: Pre-processing of the raw image. Fig-B: Output of object detection after five steps processing. Fig-C: Analysis based on Fehr(1987), Fig-D: GSD curve by volume with calculated grain size diameter

.

LOCATION: 900912

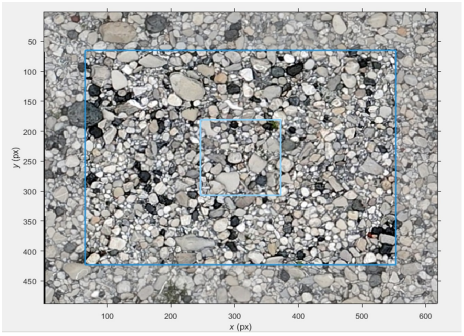

Fig. A

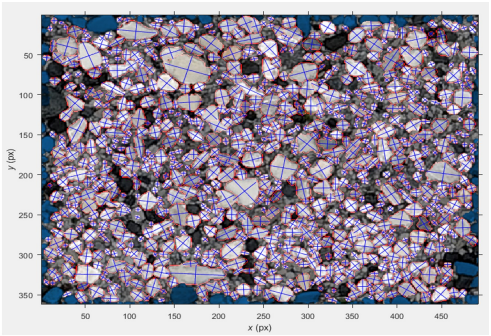

Fig. B

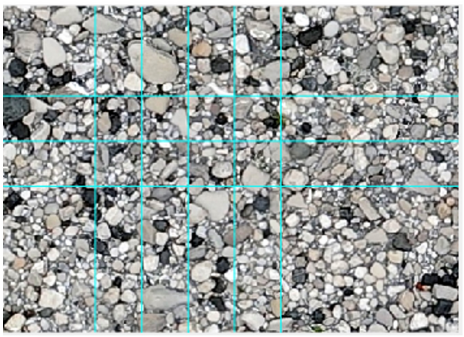

Fig. C

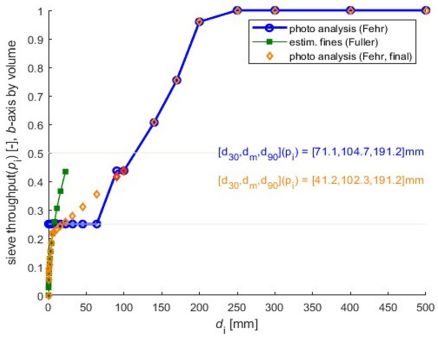

Fig. D

Figure 7.6: Figure shows the process GSD analysis in BASEGRAIN software. Fig A: Pre-processing of the raw image. Fig-B: Output of object detection after five steps processing. Fig-C: Analysis based on Fehr(1987), Fig-D: GSD curve by volume with calculated grain size diameter

.

Bibliography

[Abbe and Brooks, 2011] Abbe, T. and Brooks, A. (2011). Geomorphic, engineering, and ecological considerations when using wood in river restoration. *Stream restoration in dynamic fluvial systems: Scientific approaches, analyses, and tools*, 194:419–451.

[Asaeda et al., 2011] Asaeda, T., Rashid, M. H., Kotagiri, S., and Uchida, T. (2011). The role of soil characteristics in the succession of two herbaceous lianas in a modified river floodplain. *River Research and Applications*, 27(5):591–601.

[Bellmore et al., 2019] Bellmore, J. R., Pess, G. R., Duda, J. J., O'Connor, J. E., East, A. E., Foley, M. M., Wilcox, A. C., Major, J. J., Shafroth, P. B., Morley, S. A., Magirl, C. S., Anderson, C. W., Evans, J. E., Torgersen, C. E., and Craig, l. S. (2019). Conceptualizing Ecological Responses to Dam Removal: If You Remove It, What's to Come? *BioScience*, 69(1):26–39.

[Boggs et al., 2012] Boggs, S. et al. (2012). Principles of sedimentology and stratigraphy.

[Bollati et al., 2011] Bollati, I., Pelfini, M., Pellegrini, L., Bazzi, A., Duci, G., et al. (2011). Active geomorphosite and educational application: an itinerary along trebbia river (northern apennines, italy). In *Les géosciences au service de la société*, pages 219–233. Géovisions, 37. Institut de géographie, Université de Lausanne.

[Bollati et al., 2014] Bollati, I., Pellegrini, L., Rinaldi, M., Duci, G., and Pelfini, M. (2014). Reach-scale morphological adjustments and stages of channel evolution: The case of the trebbia river (northern italy). *Geomorphology*, 221:176–186.

[Bonacci et al., 1992] Bonacci, O., Tadic, Z., and Trninic, D. (1992). Effects of dams and reservoirs on the hydrological characteristics of the lower drava river. *Regulated Rivers: Research & Management*, 7(4):349–357.

[Bunte, 2001] Bunte, K. (2001). *Sampling surface and subsurface particle-size distributions in wadable gravel-and cobble-bed streams for analyses in sediment transport, hydraulics, and streambed monitoring*. US Department of Agriculture, Forest Service, Rocky Mountain Research Station.

[Buscombe, 2008] Buscombe, D. (2008). Estimation of grain-size distributions and associated parameters from digital images of sediment. *Sedimentary Geology*, 210(1-2):1–10.

[Buscombe, 2020] Buscombe, D. (2020). Sedinet: A configurable deep learning model for mixed qualitative and quantitative optical granulometry. *Earth Surface Processes and Landforms*, 45(3):638–651.

[Buscombe and Carini, 2019] Buscombe, D. and Carini, R. J. (2019). A data-driven approach to classifying wave breaking in infrared imagery. *Remote Sensing*, 11(7):859.

[Buscombe et al., 2010] Buscombe, D., Rubin, D., and Warrick, J. (2010). A universal approximation of grain size from images of noncohesive sediment. *Journal of Geophysical Research: Earth Surface*, 115(F2).

[Bushaw-Newton et al., 2002] Bushaw-Newton, K. L., Hart, D. D., Pizzuto, J. E., Thomson, J. R., Egan, J., Ashley, J. T., Johnson, T. E., Horwitz, R. J., Keeley, M., Lawrence, J., et al. (2002). An integrative approach towards understanding ecological responses to dam removal: The manatawny creek study 1. *JAWRA Journal of the American Water Resources Association*, 38(6):1581–1599.

[Camporeale et al., 2013] Camporeale, C., Perucca, E., Ridolfi, L., and Gurnell, A. (2013). Modeling the interactions between river morphodynamics and riparian vegetation. *Reviews of Geophysics*, 51(3):379–414.

[Cantelli et al., 2004] Cantelli, A., Paola, C., and Parker, G. (2004). Experiments on upstream-migrating erosional narrowing and widening of an incisional channel caused by dam removal. *Water Resources Research*, 40(3).

[Carbonneau et al., 2004] Carbonneau, P. E., Lane, S. N., and Bergeron, N. E. (2004). Catchment-scale mapping of surface grain size in gravel bed rivers using airborne digital imagery. *Water resources research*, 40(7).

[Catalano et al., 2001] Catalano, M., Bozek, M., and Pellett, T. (2001). Fish-habitat relations and initial response of the baraboo river fish community to dam removal. *Bulletin of the North American Benthological Society*, 18:177.

[Cattapana et al.,] Cattapana, A., Parona, P., and Francaa, M. J. Deriving grain size distributions from uavs images. *NCR DAYS 2018*, page 90.

[Chardon et al., 2022] Chardon, V., Piasny, G., and Schmitt, L. (2022). Comparison of software accuracy to estimate the bed grain size distribution from digital images: A test performed along the rhine river. *River Research and Applications*, 38(2):358–367.

[Chong et al., 2021] Chong, X. Y., Vericat, D., Batalla, R. J., Teo, F. Y., Lee, K. S. P., and Gibbins, C. N. (2021). A review of the impacts of dams on the hydromorphology of tropical rivers. *Science of The Total Environment*, 794:148686.

[Cislaghi et al., 2016] Cislaghi, A., Chiaradia, E. A., and Bischetti, G. B. (2016). A comparison between different methods for determining grain distribution in coarse channel beds. *International Journal of Sediment Research*, 31(2):97–109.

[Collins et al., 2020] Collins, M. J., Kelley, A. R., and Lombard, P. J. (2020). River channel response to dam removals on the lower penobscot river, maine, united states. *River Research and Applications*, 36(9):1778–1789.

[Collins et al., 2017] Collins, M. J., Snyder, N. P., Boardman, G., Banks, W. S., Andrews, M., Baker, M. E., Conlon, M., Gellis, A., McClain, S., Miller, A., et al. (2017). Channel response to sediment release: Insights from a paired analysis of dam removal. *Earth Surface Processes and Landforms*, 42(11):1636–1651.

[Csiki and Rhoads, 2014] Csiki, S. J. and Rhoads, B. L. (2014). Influence of four run-of-river dams on channel morphology and sediment characteristics in illinois, usa. *Geomorphology*, 206:215–229.

[Cui et al., 2017] Cui, Y., Booth, D. B., Monschke, J., Gentzler, S., Roadifer, J., Greimann, B., and Cluer, B. (2017). Analyses of the erosion of fine sediment deposit for a large dam-removal project: An empirical approach. *International Journal of River Basin Management*, 15(1):103–114.

[Detert and Weitbrecht, 2013] Detert, M. and Weitbrecht, V. (2013). User guide to gravelometric image analysis by basegrain. *Advances in Science and Research; Fukuoka, S., Nakagawa, H., Sumi, T., Zhang, H., Eds*, pages 1789–1795.

[Detert et al., 2012] Detert, M., Weitbrecht, V., et al. (2012). Automatic object detection to analyze the geometry of gravel grains–a free stand-alone tool. In *River flow*, volume 2012, pages 595–600. Taylor & Francis Group London, UK.

[Dister, 1998] Dister, E. (1998). Die bedeutung natürlicher flußdynamik am beispiel von loire und allier. *Schriftenreihe für Landschaftspflege und Naturschutz*, 56:67–78.

[Doyle et al., 2002] Doyle, M. W., Stanley, E. H., and Harbor, J. M. (2002). Geomorphic analogies for assessing probable channel response to dam removal 1. *JAWRA Journal of the American Water Resources Association*, 38(6):1567–1579.

[Doyle et al., 2003] Doyle, M. W., Stanley, E. H., and Harbor, J. M. (2003). Channel adjustments following two dam removals in wisconsin. *Water Resources Research*, 39(1).

[Duda and Bellmore, 2022] Duda, J. J. and Bellmore, J. R. (2022). Dam removal and river restoration. *Encyclopedia of Inland Waters, eds K. Tockner and T. Mehner (Oxford, UK: Elsevier Ltd). doi*, 10.

[East et al., 2018] East, A. E., Logan, J. B., Mastin, M. C., Ritchie, A. C., Bountry, J. A., Magirl, C. S., and Sankey, J. B. (2018). Geomorphic evolution of a gravel-bed river

under sediment-starved versus sediment-rich conditions: River response to the world's largest dam removal. *Journal of Geophysical Research: Earth Surface*, 123(12):3338–3369.

[East et al., 2015a] East, A. E., Pess, G. R., Bountry, J. A., Magirl, C. S., Ritchie, A. C., Logan, J. B., Randle, T. J., Mastin, M. C., Minear, J. T., Duda, J. J., et al. (2015a). Large-scale dam removal on the elwha river, washington, usa: River channel and floodplain geomorphic change. *Geomorphology*, 228:765–786.

[East et al., 2015b] East, A. E., Pess, G. R., Bountry, J. A., Magirl, C. S., Ritchie, A. C., Logan, J. B., Randle, T. J., Mastin, M. C., Minear, J. T., Duda, J. J., Liermann, M. C., McHenry, M. L., Beechie, T. J., and Shafroth, P. B. (2015b). Large-scale dam removal on the elwha river, washington, usa: River channel and floodplain geomorphic change. *Geomorphology*, 228:765–786.

[Ellwanger et al., 2012] Ellwanger, G., Finck, P., Riecken, U., and Schröder, E. (2012). Gefährdungssituation von lebensräumen und arten der gewässer und auen in deutschland. *Natur und Landschaft*, 87(4):150–155.

[Elton, 2022] Elton, C. (2022). Why is a record-breaking year of dam removals good news for europe's wildlife? `https://www.euronews.com/green/2022/05/16/why-is-a-record-breaking-year-of-dam-removals-good-news-for-europe-s-wildlife`. Accessed: 2023-10-17.

[Foley et al., 2017a] Foley, M. M., Bellmore, J., O'Connor, J. E., Duda, J. J., East, A. E., Grant, G., Anderson, C. W., Bountry, J. A., Collins, M. J., Connolly, P. J., et al. (2017a). Dam removal: Listening in. *Water Resources Research*, 53(7):5229–5246.

[Foley et al., 2017b] Foley, M. M., Magilligan, F. J., Torgersen, C. E., Major, J. J., Anderson, C. W., Connolly, P. J., Wieferich, D., Shafroth, P. B., Evans, J. E., Infante, D., et al. (2017b). Landscape context and the biophysical response of rivers to dam removal in the united states. *PLoS One*, 12(7):e0180107.

[Formann et al., 2014] Formann, E., Egger, G., Hauer, C., and Habersack, H. (2014). Dynamic disturbance regime approach in river restoration: concept development and application. *Landscape and Ecological Engineering*, 10:323–337.

[Garcia de Leaniz et al., 2023] Garcia de Leaniz, C., Wantzen, K. M., Wolter, C., Tharme, R. E., Zalewski, M., and Belletti, B. (2023). Challenges and benefits of restoring river connectivity. *Frontiers in Ecology and Evolution*, 11:1110413.

[Gartner et al., 2015] Gartner, J. D., Magilligan, F. J., and Renshaw, C. E. (2015). Predicting the type, location and magnitude of geomorphic responses to dam removal: Role of hydrologic and geomorphic constraints. *Geomorphology*, 251:20–30.

[GOGOAŞE NISTORAN et al., 2019] GOGOAŞE NISTORAN, D. E., BRAŞOVANU, L., IONESCU, C. S., ARMAŞ, I., and COZMA, A. (2019). Gravelometric image analysis of sediments (prahova river, romania). *GeoPatterns*, 4(1).

[González del Tánago et al., 2012] González del Tánago, M., García de Jalón, D., and Román, M. (2012). River restoration in spain: theoretical and practical approach in the context of the european water framework directive. *Environmental management*, 50:123–139.

[Gough et al., 2018] Gough, P., Garrido, P. F., van Herk, J., and Hands, S. (2018). Dam removal. a viable solution for the future of our european rivers. dam removal europe.

[Gowan and Fausch, 1996] Gowan, C. and Fausch, K. D. (1996). Long-term demographic responses of trout populations to habitat manipulation in six colorado streams. *Ecological Applications*, 6(3):931–946.

[Graham et al., 2005a] Graham, D. J., Reid, I., and Rice, S. P. (2005a). Automated sizing of coarse-grained sediments: image-processing procedures. *Mathematical geology*, 37:1–28.

[Graham et al., 2005b] Graham, D. J., Rice, S. P., and Reid, I. (2005b). A transferable method for the automated grain sizing of river gravels. *Water Resources Research*, 41(7).

[Green, 2023] Green, G. (2023). Dam fine work: record number of barrier removals helps restore rivers across europe. *Guardian*.

[Groll, 2017] Groll, M. (2017). The passive river restoration approach as an efficient tool to improve the hydromorphological diversity of rivers – case study from two river restoration projects in the german lower mountain range. *Geomorphology*, 293:69–83.

[Im et al., 2018] Im, D., Choi, S.-U., and Choi, B. (2018). Physical habitat simulation for a fish community using the anfis method. *Ecological Informatics*, 43:73–83.

[Jähnig et al., 2011] Jähnig, S., Lorenz, A., Hering, D., Antons, C., Sundermann, A., Jedicke, E., and Haase, P. (2011). River restoration success: a question of perception. *Ecological Applications*, 21(6):2007–2015.

[Kellerhals and Bray, 1971] Kellerhals, R. and Bray, D. I. (1971). Sampling procedures for coarse fluvial sediments. *Journal of the Hydraulics Division*, 97(8):1165–1180.

[Kim et al., 2015] Kim, S., Toda, Y., and Tsujimoto, T. (2015). Geomorphological and riparian vegetation responses following a low-head dam removal: a study based on literature review. *International Journal of River Basin Management*, 13(3):315–324.

[Kondolf, 1997] Kondolf, G. M. (1997). Profile: hungry water: effects of dams and gravel mining on river channels. *Environmental management*, 21(4):533–551.

[Konrad et al., 2011] Konrad, C. P., Olden, J. D., Lytle, D. A., Melis, T. S., Schmidt, J. C., Bray, E. N., Freeman, M. C., Gido, K. B., Hemphill, N. P., Kennard, M. J., et al. (2011). Large-scale flow experiments for managing river systems. *BioScience*, 61(12):948–959.

[Kristensen et al., 2018] Kristensen, P., Whalley, C., Zal, F. N. N., Christiansen, T., et al. (2018). European waters assessment of status and pressures 2018. *EEA Report*, (7/2018).

[Lang et al., 2021] Lang, N., Irniger, A., Rozniak, A., Hunziker, R., Wegner, J. D., and Schindler, K. (2021). Grainet: mapping grain size distributions in river beds from uav

images with convolutional neural networks. *Hydrology and Earth System Sciences*, 25(5):2567–2597.

[Löfgren et al., 2009] Löfgren, S., Kahlert, M., Johansson, M., and Bergengren, J. (2009). Classification of two swedish forest streams in accordance with the european union water framework directive. *AMBIO: A Journal of the Human Environment*, 38(7):394–400.

[Magilligan et al., 2016] Magilligan, F. J., Graber, B. E., Nislow, K. H., Chipman, J. W., Sneddon, C. S., and Fox, C. A. (2016). River restoration by dam removal: Enhancing connectivity at watershed scales. *Elementa*, 4:000108.

[Major et al., 2017] Major, J. J., East, A. E., O'Connor, J. E., Grant, G. E., Wilcox, A. C., Magirl, C. S., Collins, M. J., and Tullos, D. D. (2017). Geomorphic responses to dam removal in the united states–a two-decade perspective. *Gravel-bed rivers: Processes and disasters*, pages 355–383.

[Major et al., 2012] Major, J. J., O'Connor, J. E., Podolak, C. J., Keith, M. K., Grant, G. E., Spicer, K. R., Pittman, S., Bragg, H. M., Wallick, J. R., Tanner, D. Q., et al. (2012). *Geomorphic response of the Sandy River, Oregon, to removal of Marmot Dam*. US Geological Survey Reston, VA, USA.

[McKay and Fischenich, 2011] McKay, S. K. and Fischenich, J. C. (2011). Robust prediction of hydraulic roughness.

[Milan and Heritage, 2012] Milan, D. J. and Heritage, G. L. (2012). Lidar and adcp use in gravel-bed rivers: advances since gbr6. *Gravel-bed rivers: Processes, tools, environments*, pages 286–302.

[open river programme, 2023] open river programme (2023). Free trebbia river: catchment development and river restoration through the first dam removals in italy. `https://openrivers.eu/projects/202203366-free-trebbia-river/?highlight=trebbia`. [Accessed 18-11-2023].

[Orr, 2002] Orr, C. H. (2002). *Patterns of removal and ecological response: a study of small dams in Wisconsin*. University of Wisconsin–Madison.

[Otsubo and O'Sullivan, 2018] Otsubo, M. and O'Sullivan, C. (2018). Experimental and dem assessment of the stress-dependency of surface roughness effects on shear modulus. *Soils and foundations*, 58(3):602–614.

[Palmer and Ruhi, 2019] Palmer, M. and Ruhi, A. (2019). Linkages between flow regime, biota, and ecosystem processes: Implications for river restoration, science, 365, eaaw2087.

[Palmer et al., 2010] Palmer, M. A., Menninger, H. L., and Bernhardt, E. (2010). River restoration, habitat heterogeneity and biodiversity: a failure of theory or practice? *Freshwater biology*, 55:205–222.

[Pedersen et al., 2007] Pedersen, M. L., Andersen, J. M., Nielsen, K., and Linnemann, M. (2007). Restoration of skjern river and its valley: project description and general ecological changes in the project area. *Ecological engineering*, 30(2):131–144.

[Peters et al., 2017] Peters, R. J., Liermann, M., McHenry, M. L., Bakke, P., and Pess, G. R. (2017). Changes in streambed composition in salmonid spawning habitat of the elwha river during dam removal. *JAWRA Journal of the American Water Resources Association*, 53(4):871–885.

[PRATICHE et al., 2006] PRATICHE, B., LA GESTIONE, P. L. P. E., DEL RETICOLO IDROGRAFICO, M. N., and NELL'OTTICA, D. R. F. (2006). Fluviale.

[Rice and Church, 2010] Rice, S. P. and Church, M. (2010). Grain-size sorting within river bars in relation to downstream fining along a wandering channel. *Sedimentology*, 57(1):232–251.

[Robinson et al., 2000] Robinson, K. M., Bennett, S. J., Casali, J., and Hanson, G. J. (2000). Processes of headcut growth and migration in rills and gullies. *International Journal of Sediment Research*, 15(1):69–82.

[Rosgen, 2011] Rosgen, D. L. (2011). Natural channel design: fundamental concepts, assumptions, and methods. *Stream restoration in dynamic fluvial systems: scientific approaches, analyses, and tools*, 194:69–93.

[Rüther et al., 2013] Rüther, N., Huber, S., Spiller, S., and Aberle, J. (2013). Verifying a photogrammetric method to quantify grain size distribution of developed armor layers. In *Proceedings of the 35th IAHR Congress, Chengdu, China*, volume 7.

[Salerno et al., 2022] Salerno, L., Moreno-Martínez, Á., Izquierdo-Verdiguier, E., Clinton, N., Siviglia, A., and Camporeale, C. (2022). Satellite analyses unravel the multi-decadal impact of dam management on tropical floodplain vegetation. *Frontiers in Environmental Science*, 10:871530.

[Sawaske and Freyberg, 2012] Sawaske, S. R. and Freyberg, D. L. (2012). A comparison of past small dam removals in highly sediment-impacted systems in the us. *Geomorphology*, 151:50–58.

[Schmitz et al., 2009] Schmitz, D., Blank, M., Ammondt, S., and Patten, D. T. (2009). Using historic aerial photography and paleohydrologic techniques to assess long-term ecological response to two montana dam removals. *Journal of Environmental Management*, 90:S237–S248. Understanding and linking the biophysical, socio economic and geopolitical effects of dams.

[Shields Jr et al., 2011] Shields Jr, F., Knight, S. S., Lizotte Jr, R., and Wren, D. G. (2011). Connectivity and variability: Metrics for riverine floodplain backwater rehabilitation. *Stream Restoration in Dynamic Fluvial Systems: Scientific Approaches, Analyses, and Tools, Geophys. Monogr. Ser*, 194:233–246.

[Sime and Ferguson, 2003] Sime, L. and Ferguson, R. (2003). Information on grain sizes in gravel-bed rivers by automated image analysis. *Journal of Sedimentary Research*, 73(4):630–636.

[Simon, 1989] Simon, A. (1989). A model of channel response in disturbed alluvial channels. *Earth surface processes and landforms*, 14(1):11–26.

[Simon et al., 2013] Simon, A., Bennett, S. J., and Castro, J. M. (2013). *Stream restoration in dynamic fluvial systems: Scientific approaches, analyses, and tools*. John Wiley & Sons.

[Smith et al., 2014] Smith, B., Clifford, N. J., and Mant, J. (2014). The changing nature of river restoration. *Wiley Interdisciplinary Reviews: Water*, 1(3):249–261.

[Stanley and Doyle, 2003] Stanley, E. H. and Doyle, M. W. (2003). Trading off: the ecological effects of dam removal. *Frontiers in Ecology and the Environment*, 1(1):15–22.

[Stanley et al., 2002] Stanley, E. H., Luebke, M. A., Doyle, M. W., and Marshall, D. W. (2002). Short-term changes in channel form and macroinvertebrate communities following low-head dam removal. *Journal of the North American Benthological Society*, 21(1):172–187.

[Surian et al., 2004] Surian, N., Rinaldi, M., et al. (2004). Channel adjustments in response to human alteration of sediment fluxes: examples from italian rivers. *IAHS publication*, 288:276–282.

[Tealdi et al., 2011] Tealdi, S., Camporeale, C., and Ridolfi, L. (2011). Long-term morphological river response to hydrological changes. *Advances in Water Resources*, 34(12):1643–1655.

[Weil, 1986] Weil, J. (1986). The synthesis of cloth objects. *ACM Siggraph Computer Graphics*, 20(4):49–54.

[Wikipedia, 2023] Wikipedia (2023). Grain size — Wikipedia, the free encyclopedia. [Online; accessed 21-December-2023].

[Wikipedia contributors, 2023] Wikipedia contributors (2023). Trebbia — Wikipedia, the free encyclopedia. [Online; accessed 11-December-2023].

[Wilcox et al., 2014] Wilcox, A. C., O'Connor, J. E., and Major, J. J. (2014). Rapid reservoir erosion, hyperconcentrated flow, and downstream deposition triggered by

breaching of 38 m tall condit dam, white salmon river, washington. *Journal of Geophysical Research: Earth Surface*, 119(6):1376–1394.

[Wohl et al., 2005] Wohl, E., Angermeier, P. L., Bledsoe, B., Kondolf, G. M., MacDonnell, L., Merritt, D. M., Palmer, M. A., Poff, N. L., and Tarboton, D. (2005). River restoration. *Water Resources Research*, 41(10).

[Wolman, 1954] Wolman, M. G. (1954). A method of sampling coarse river-bed material. *EOS, Transactions American Geophysical Union*, 35(6):951–956.

[Zinke and Flener, 2013] Zinke, P. and Flener, C. (2013). Experiences from the use of unmanned aerial vehicles (uav) for river bathymetry modelling in norway. *Vann*, 48(3):351–360.